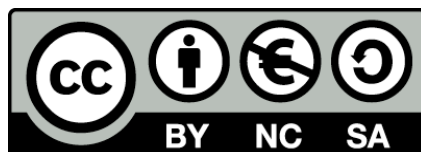




UNIVERSITAT<sub>DE</sub>  
BARCELONA

## Electrochemical Plug-and-Power e-readers for Point-of-Care Applications

Yaiza Montes Cebrián



Aquesta tesi doctoral està subjecta a la llicència **Reconeixement- NoComercial – Compartir Igual 4.0. Espanya de Creative Commons.**

Esta tesis doctoral está sujeta a la licencia **Reconocimiento - NoComercial – Compartir Igual 4.0. España de Creative Commons.**

This doctoral thesis is licensed under the **Creative Commons Attribution-NonCommercial-ShareAlike 4.0. Spain License.**



UNIVERSITAT DE  
BARCELONA

PhD Thesis:

# Electrochemical Plug-and-Power e-readers for Point-of-Care Applications

Author: Yaiza Montes Cebrián

---

Supervised by:

Dr. Pere Lluís Miribel Català  
Dr. Jordi Colomer Farrarons



# Electrochemical Plug-and-Power e-readers for Point-of-Care Applications

Memoria presentada para optar al grado de doctor por la  
Universidad de Barcelona

Programa de doctorado en Ingeniería  
y Ciencias Aplicadas

Autora: Yaiza Montes Cebrián

Directores: Dr. Pere Lluís Mirbel Català  
Dr. Jordi Colomer Farrarons

Tutor: Dr. Pere Lluís Mirbel Català

Departamento de Ingeniería Electrónica y Biomédica  
Facultad de Física, Universidad de Barcelona



UNIVERSITAT DE  
BARCELONA

Una firma manuscrita en tinta negra, que parece ser la del autor o tutor, situada debajo del logotipo de la universidad.



# Aknowledgements

En primer lugar, quiero agradecer al Dr. Pere Miribel Català toda su dedicación y entusiasmo. Han sido muchos años de trabajo donde nunca me ha faltado su apoyo y comprensión. Sus grandes consejos, tanto técnicos como personales, me han ayudado a elaborar este trabajo. Gracias por confiar en mi y acompañarme durante todo el proceso, sin ti esta tesis doctoral no se hubiera hecho realidad.

En segundo lugar, y no por ello menos importante, quiero agradecer al Dr. Jordi Colomer Farrarons toda la ayuda que me ha dado durante estos años, tanto a nivel profesional como personal. Gracias por guiarme y aconsejarme durante todos estos años, tus pautas y consejos han sido fundamentales en la elaboración de esta tesis.

A mi compañero de tesis y amigo, Albert Álvarez Carrulla. Has sido uno de los pilares fundamentales de esta tesis. No tengo palabras para expresar mi agradecimiento por el apoyo que me has dado. Me has ayudado a nivel técnico, pero más aún a nivel personal. Nunca olvidaré los momentos que hemos vivido juntos, las largas horas en el laboratorio, los momentos en el bar, el congreso en Lyon, entre muchos otros.

Agradezco a la Universidad de Barcelona su apoyo económico a través de l'Ajut de Personal Investigador Predoctoral en formació (APIF), que permitió financiar mis tres primeros años de tesis así como mi estancia predoctoral en Dublin.

También quiero agradecer al Ministerio de Economía Español, a la Agencia Estatal de Investigación y al Fondo Europeo de Desarrollo Regional (AEI / FEDER, UE), por financiar esta investigación a través del proyecto Circuitos para la gestión de la recolección de energía para aplicaciones de baja tensión y baja potencia (MINAUTO) - Número de concesión TEC2016-78284-C3-3-R).



*Una manera de hacer Europa*

## Aknowledgements

Prof. Richard Reilly, gracias por haberme dado la oportunidad de realizar mi estancia predoctoral en su laboratorio en el Trinity College of Dublin, y por todo el apoyo que me brindó durante esos meses. No olvidaré su amabilidad ni los detalles que tuvo conmigo. Fue una gran experiencia tanto a nivel profesional como personal.

El mayor de los agradecimientos se lo quiero dar a mi familia, las personas más importantes de mi vida. Gracias a mis padres, Lidia y Juan, por el cariño incondicional y por la educación que me habéis dado. Sois y seréis mi mayor apoyo, gracias por aguantarme y entenderme en los momentos más duros. Mi queridísimo hermano Yeray, gracias por estar siempre a mi lado, dándome cariño y comprensión. Al resto de mi familia, especialmente a mis abuelos Paquita, Fernando y Transi, y a mis tíos Paqui, Ángel, Fernando, Mari y Marcos, quería darles las gracias por preocuparse por mí y darme tanto cariño. También quiero dar las gracias a mi segunda familia, Joaquín, Mari, Cristina y Raquel, por vuestro cariño durante tantos años.

A mis amigas, Laura y Sandra, gracias por haberme dejado compartir con vosotras mis penas y alegrías, y estar ahí siempre que lo he necesitado. Carlos, a ti también, gracias por tus consejos y cariño.

Y a ti David, que eres mi paz y equilibrio. Has sido uno de mis mayores apoyos durante estos años. Me has aguantado y dado el mayor de los cariños. Has estado siempre ahí, compartiendo conmigo los buenos y los malos momentos. Gracias por todo lo que haces por mí, eres lo mejor que me ha pasado.

# Contents

<b>Aknowledgements</b>	<b>i</b>
<b>Contents</b>	<b>iii</b>
<b>1 Introduction</b>	<b>1</b>
1.1 Point-of-Care Diagnostics . . . . .	2
1.1.1 Main elements of Point-of-Care Diagnostics . . . . .	4
1.1.1.1 Biosensors and new materials . . . . .	4
1.1.1.2 Microfluidics . . . . .	6
1.1.1.3 Hardware and software . . . . .	6
1.1.2 Point-of-care diagnostics in low- and middle-income countries . . . . .	8
1.1.2.1 Regulatory and policy guidelines . . . . .	10
1.1.2.2 Infrastructures health system . . . . .	10
1.1.2.3 Point-of-Care diagnostics development . . . . .	11
1.1.2.4 Geographical access . . . . .	11
1.1.2.5 Supply chain . . . . .	11
1.1.3 Investments in Point-of-Care Diagnostics . . . . .	12
1.1.4 Classification of Point-of-Care systems based on biosensing method . . . . .	13
1.1.4.1 Electrochemical biosensors . . . . .	15
1.1.4.2 Optical and mechanical biosensors . . . . .	21
1.2 Architecture of POC technologies . . . . .	26
1.2.1 Front-end: Instrumentation architectures . . . . .	27
1.2.1.1 Potentiostat-based solutions . . . . .	27
1.2.1.2 Current sense amplifier . . . . .	35
1.2.2 Back-end solutions . . . . .	37



## CONTENTS

1.2.2.1	Low-power microcontroller-based platforms . . .	37
1.2.2.2	Smartphone-based POC . . . . .	39
1.2.2.3	Qualitative data obtained with ultra-low-power electronics . . . . .	40
1.2.3	Power Management: battery and self-powered solutions	42
1.2.3.1	Power-free POC devices . . . . .	43
1.2.3.2	Battery-powered POC devices . . . . .	44
1.2.3.3	Self-powered POC devices . . . . .	45
1.3	Objectives . . . . .	48
1.4	Contribution of this thesis . . . . .	50
<b>2</b>	<b>Results</b>	<b>55</b>
2.1	Publication 1 . . . . .	55
2.2	Publication 2 . . . . .	67
2.3	Publication 3 . . . . .	85
<b>3</b>	<b>Summary and discussion of the results</b>	<b>101</b>
<b>4</b>	<b>Conclusions</b>	<b>113</b>
4.1	General conclusions . . . . .	113
4.2	Self-powered portable electronic system for POC applications .	114
4.3	Portable USB-powered potentiostat for POC amperometric detections . . . . .	115
4.4	Future steps towards low-powered devices for biosensing POC applications . . . . .	116
<b>Appendix A</b>	<b>List of publications</b>	<b>119</b>
A.1	Journals . . . . .	119
A.2	Patents . . . . .	120
A.3	Conferences . . . . .	120
<b>Appendix B</b>	<b>Multimodal TDT system for biosensing Dystonia disorder</b>	<b>123</b>
<b>Appendix C</b>	<b>Resumen en castellano</b>	<b>127</b>
<b>References</b>		<b>133</b>

## CONTENTS

<b>Abbreviations</b>	<b>149</b>
<b>List of figures</b>	<b>151</b>
<b>List of tables</b>	<b>155</b>



# Chapter 1

## Introduction

We are living a great technology revolution and along with it, the progress of medicine, an area that has evolved in recent years [1–4]. Technological advances in the medical field can help save lives by providing innovative healthcare solutions for the diagnosis, prevention, monitoring, and treatment of diseases.

The constant innovations in medicine have considerably increased the expectancy and quality of life, as well as health care [5]. Medical technology is present in our daily lives, from the single-use systems to the most sophisticated equipment, such as glucometers, pregnancy tests, and many other technologies and services that have radically improved both the medical practice as the world health [6–10]. Innovation is driving significant changes throughout the health sector and is called to transform health in the coming years. World Health Organization (WHO) defines innovation in health as “new or improved health policies, systems, products and technologies, and services and delivery methods that improve people’s health and well-being” [11]. Moreover, the innovation concept also includes creativity, efficiency, quality, sustainability, safety, and affordability.

Medical devices play a crucial role in proper and successful diagnosis. They can provide accurate and relevant data about the patient, seeking the general welfare of the entire population. The increase in these electronic medical devices is improving patient outcomes and reducing healthcare costs [12].

According to the Medical Device Market Report: Trends, Forecast, and Competitive Analysis: “The global medical device market is expected to

## CHAPTER 1. INTRODUCTION

reach an estimated \$409.5 billion by 2023, and it is forecast to grow at a Compound Annual Growth Rate (CAGR) of 4.5% from 2018 to 2023. The major drivers for the growth of this market are healthcare expenditure, technological development, aging population, and chronic diseases” [13]. The new way of managing health and its data is transforming institutions and medical centers, saving costs, improving their profitability, reducing waiting time and, above all, improving patient care and experience.

Currently, conventional diagnostic methods are still dominant around the world. These diagnostics tests usually are performed in centralized laboratories with accurate and automated equipment, which analyzes numerous samples at an affordable price. Despite the advantages, centralized laboratories, also known as provider-centered healthcare, tend to be slow. Sometimes, centralized tests are not convenient for the patient because they are slow and require more than one visit to the doctor to complete the evaluation process. This process is especially tiresome in people with chronic diseases such as diabetes since they must be regularly monitored [14]. Usually, from the sample collection to the diagnostic result, patients anxiously await several days or even weeks. This waiting time increase in rural areas with deficient infrastructures, which have clinics and centralized laboratories a significant distance away.

The healthcare approach is changing due to economic pressures and the general recognition that care needs to be more patient-centered [15]. Patient-centered healthcare is becoming a global trend since the growth of the population and their aging is increasing health expenditure. This fact makes many countries are reducing the average healthcare spending per person. One way to reduce health spending is to encourage patients to be evaluated and treated in primary care centers. In this way, it is possible to reduce the saturation of hospitals, which are more expensive and slower. The need for self-monitoring the glucose has boosted the growth of the Point-of-Care (POC) diagnostics, which is the largest segment of POC by far.

### 1.1 Point-of-Care Diagnostics

During the latest years, POC devices have arisen as rapid and accurate diagnostic systems centered on the patient. According to the Dimensions.ai website, more than 1.7 million articles and 325 thousand patents about POC Diagnostic Testing have been published during the last 5 years. Most of them

## CHAPTER 1. INTRODUCTION

have comparable accuracy and sensitivity to centralized laboratory systems in order to allow quick diagnostic decisions.

There are many definitions of POC testing and no accepted universal definition. According to the article “International definition of a point-of-care test in family practice: a modified e-Delphi procedure” POC test can be defined as “a test to support clinical decision-making, which is performed by a qualified member of the practice staff nearby the patient and on any part of the patient’s body or its derivatives, during or very close to the time of consultation, to help the patient and physician to decide upon the best-suited approach, and of which the results should be known at the time of the clinical decision-making” [16].

The features of POC devices depend on the application, the final scenario where the POC is going to be used, and the profile of the final user. However, most of these devices have in common some attributes: a) short time-to-result and close to the patient in order to provide a rapid diagnosis and manage clinical decisions in the same clinical encounter; b) simple to use; c) results should be concordant with an established laboratory method and; d) device together with associated reagents and consumables should be safe to use and robust in storage and usage.

POC testing has the potential to improve healthcare. For this reason, developers of such devices must be guided by more specific design criteria to ensure that the technology can address the needs of the user. In response to the need for improved diagnostics tests, the WHO Sexually Transmitted Diseases Diagnostics Initiative established some guidelines to develop POC testing devices for the detection of sexually transmitted infections (STI) in resource-limited countries [17]. These attributes, also known as “ASSURED” criteria, provide a framework for evaluating POC devices in resource-constrained communities (Table 1.1).

A = Affordable	Accessible at a reasonable price for public healthcare systems, as well as for users and patients. The tests should be cheap and should reduce the costs for the patient.
S = Sensitive	Must give few false negatives.
S = Specific	Must give few false positives.
U = User-friendly	Easy to carry out tests and in a few steps by unskilled people after minimal training. The results should be clear and easy to understand.

## CHAPTER 1. INTRODUCTION

R = Robust and rapid	The test must have a short response period without the need for refrigerated storage and must resist transport and, have a long shelf life. In the best cases, they should not even require electricity to work.
E = Equipment-free	The equipment must be compact with easy disposal and sample handling. Reagent handling, analysis, data interpretation, and storing of waste products should limit the intervention of users and their exposure to bio-hazard as much as possible.
D = Deliverable	The tests should be carried out in the field. Consequently, the system must be portable.

Table 1.1: The ASSURED criteria that indicate the attributes that should have a POC device.

### 1.1.1 Main elements of Point-of-Care Diagnostics

The development of POC needs cooperation between different areas of knowledge, and the use of different key enabling technologies (KET) to implement suitable solutions in order to overcome specific needs for the particular scenarios of application [18, 19]. These areas are biosensors and new materials, microfluidics, hardware, and software (Figure 1.1).

#### 1.1.1.1 Biosensors and new materials

Advances in chemistry and materials are improving the performance of POC testing. In-vitro diagnostics require affinity reagents, which are small molecules (such as antibodies, peptides, among others) that specifically binds to a target molecule to identify, quantify, capture, or influence its activity.

Biosensors are integrated analytical diagnostic tools with high potentials in POC applications, which offer a number of benefits in many areas [20, 21]. These small devices use a recognition element, normally a biomolecule, to bind a specific analyte and transduction mechanisms to detect this binding event. The use of electrochemistry in biosensors make these devices more practical, sensitive, accurate, fast, and cheaper [22].

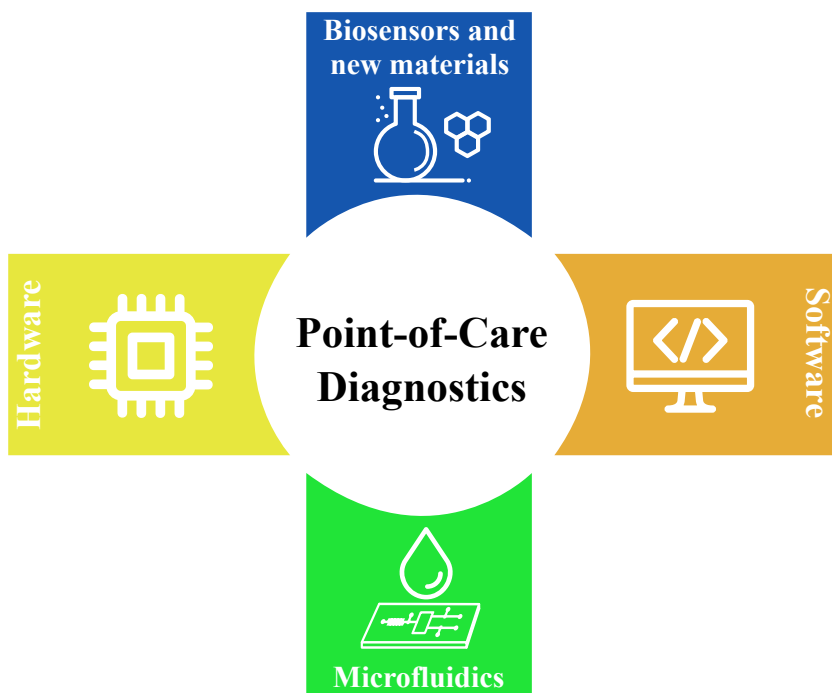


Figure 1.1: Main fields that compose Point-of-Care Diagnostics.

As has been mentioned, POC systems must be sensitive and accurate, as well as practical, low-cost, and portable. Therefore, electrochemical biosensors have the potential to become a key aspect for the development of POC testing.

Moreover, new materials have been introduced to improve the capabilities of POC diagnostics. Paper-based diagnostics has the potential to expand the capabilities of POC testing, due to the paper is an accessible and inexpensive material [23]. It is also able to transport fluids via capillary flow, thus removing the need to use pumps or other external equipment to drive fluid flow [24]. Biosensing systems based on flexible polymers substrates are emerging due to their enhanced physicochemical properties. These innovative systems have the potential to be integrated into wearable devices for personalized health monitoring [25]. Flexible substrates could allow performing minimal or non-invasive diagnostic tests [26] and could be integrated into a wide variety of wearable devices.



## CHAPTER 1. INTRODUCTION

### 1.1.1.2 Microfluidics

Microfluidic lab-on-a-chip (LOC) technologies have been considered as a promising solution to achieve the requirements of the POC diagnostics [27]. They have the potential of miniaturizing and integrate into a small chip most of the functional modules used in centralized laboratories such as micropumps, microvalves, and microseparators, among others [28, 29].

Some of their advantages are its small size, low sample and reagent volume, high capability of integration, and rapid analysis time. It also has the potential to accomplish complex diagnostic assays, usually performed in a centralized laboratory, into a single microfluidic chip. All the integrated modules that compose a microfluidic LOC performs the steps of a diagnostic assay, including fluid handling, sample pre-treatment, sample separation, signal amplification, washings, and signal detection.

Furthermore, this technology enables POC diagnostic devices accessible to non-specialized users due to these devices are self-contained, automated, easy-to-use, and rapid. Current research efforts toward POC testing based on microfluidics' LOC technologies are focused on developing methods to detect different types of analytes such as proteins, cells, nucleic acids, and other biological substances [30].

### 1.1.1.3 Hardware and software

Portable electronic medical devices are emerging to revolutionize health care systems that will enable people to be monitored by themselves improving surveillance thanks to the early detection of diseases. Moreover, these advances could mean more efficient and effective health care personalized and centered on patients who take greater responsibility for their health [31, 32].

The miniaturization and the integration of the electronic components enable the development of novel and compact devices to prevent and monitoring health parameters. These innovations include smart devices, customized wearable platforms, and wireless Internet-of-Things (IoT) systems, among others.

Devices based on IoT technologies are of great interest [33]. This technology interconnects digitally everyday objects with the Internet using Bluetooth Low Energy (BLE) or Wi-Fi modules, among other communication resources. These modules use standard protocols, which allow sending and

## CHAPTER 1. INTRODUCTION

storing information in large capacity databases for later analysis [34].

Moreover, these electronic systems also can be used in primary healthcare centers, where can provide a rapid diagnosis and allow take clinical decisions in the same visit with the medical consultant.

These innovative portable devices are adapting to new technologies creating novel systems with small size and low cost that allow performing the most common clinical tests anywhere (such as immunoassays, molecular diagnostics, and enzymatic assays). An example is hand-held glucometers, the most widespread type of POC, which are widely used in the home setting by diabetic patients who need a constant control of their blood glucose level.

The use of smartphones has facilitated the progress of imaging, sensing, and diagnostic tools. Furthermore, they are enhancing the measurement capabilities of researchers, educators as well as citizen, opening the door to new opportunities and developments [35]. It is increasing the use of smartphones to monitor some health parameters such as body temperature, and galvanic skin response, among others [35]. These devices, attached to external accessories, are capable of making diagnostic imaging or sensing physical parameters. There are several types of fitness monitoring sensors, which are used for tracking movement and heart rate as well as pulse oximeters used to measure blood oxygen as an indicator for lung disease [36]. Furthermore, the camera lens of smartphones can be used to perform a rapid blood analysis as it was demonstrated in [37]. In this work, the authors developed an imaging cytometry platform installed on a cellphone for the measurement of the density of red and white blood cells and the hemoglobin concentration in human blood samples.

Science, technology, and innovation are evolving rapidly, but the autonomy of electronic devices is still a big problem [38]. Although the current batteries are increasing the capacity, they are still limited and very polluting. Many studies are focused on the use of fuel cells as a power sources. Fuel cells (FC) are electrochemical cells that convert the chemical energy of a fuel and an oxidizing agent into electricity through reduction-oxidation reactions. They can produce electrical energy continuously for as long as fuel and oxidant are supplied, creating infinite and non-polluting energy sources. However, the use of FC to power biomedical devices is still limited since their safety, durability, and cost must be improved [39].

Usually, the data collected (whether by mobile applications, Internet, or social media platforms) are stored in large databases for analysis. These data

## CHAPTER 1. INTRODUCTION

are useful in medical disease research, although it is important to analyze and validate the results to avoid data misinterpreting and protect patient confidentiality. Recently, the European Union approved the General Data Protection Regulation (GDPR). This regulation affects almost all industries, but in health, the GDPR gives patients more control over the personal data collected and provides more information about how these data are used [40].

### 1.1.2 Point-of-care diagnostics in low- and middle-income countries

The developing world and low-resource settings face barriers to accessing health services, where health care infrastructures are weak, and access to medical services is a challenge [41].

According to a new United Nations report published in 2019, the world population will increase 2 billion over the next 30 years, from 7.7 billion people to 9.7 billion in 2050 [42]. Population statistics indicate that nine countries will represent more than half of the world's population growth between now and 2050, in descending order of the expected increase: India, Nigeria, Pakistan, the Democratic Republic of the Congo, Ethiopia, United Republic of Tanzania, Indonesia, Egypt and the United States of America. India is expected to become the most populous country in the world in approximately 2027, displacing China. In addition, the data predict that the population of Sub-Saharan Africa will grow by 99 %, doubling in 2050 [42]. The life expectancy of developing countries is 7.4 years below the world average in 2019, due to the high levels of childhood mortality, violence, and the impact of the Human Immunodeficiency Virus (HIV) epidemic.

Poverty and diseases are still one of the most significant challenges in the developing world where infectious diseases cause significant mortality. In lower-income countries, most diseases are entirely avoidable or treatable with a quick diagnosis. The so-called '10-90 GAP' says that only 10% of global health research is devoted to conditions that account for 90 % of the global disease burden [43]. Infectious diseases, such as malaria, HIV, tuberculosis, and pediatric acute respiratory infections (ARIs), cause 95 % of deaths all over the world [44].

Numerous efforts are focused on developing technological innovations, although effective diagnostic testing has been difficult to achieve in these places. POC diagnostic is a valuable tool to improve the management of

## CHAPTER 1. INTRODUCTION

infectious diseases in an earlier stage that could kill millions of people. These tests offer rapid results, and they can be simple enough to be used at the primary care level in remote places with a lack of laboratory infrastructures. POC testing can help patients to self-test in the privacy of their homes, especially for stigmatizes diseases such as HIV.

An example is the study published by Mashamba-Thompson et al. [45], in which the impact of HIV POC diagnostics in HIV-infected women was demonstrated. The review study showed that the HIV POC test is significantly associated with decreased mother-to-child transmission of HIV, increased linkage to antiretroviral treatments, and HIV care for infected women.

Another example is syphilis, a curable infection transmitted sexually or during pregnancy from the mother to the fetus. Due to syphilis causes genital ulcers, it can increase the risk of transmission and acquisition of HIV. Most of the people with syphilis are not diagnosed and can transmit the infection to their sexual contacts or the fetus. In the case of not receiving treatment, 25 % of pregnant women with syphilis will give birth to a dead baby, and 33 % will be born a baby with low weight and more likely to die in the first month of life [46]. In most countries, within the processes of pregnancy monitoring, pregnant women are evaluated for syphilis. However, in sub-Saharan Africa, less than 50 % of pregnant women are undertaken to the syphilis test [47]. The studies demonstrate that these POC tests can increase syphilis' pregnancy detection in developing countries [48]. Available POC tests for syphilis are sensitive, specific, and do not require complex equipment. Moreover, these tests are inexpensive (cost less than \$1), rapid (provide a result in 15 minutes), and only requires a drop of blood. POC tests for syphilis must accomplish the ASSURED criteria and could make syphilis tests accessible to all women anywhere. Furthermore, dual POC tests for diagnosing HIV and syphilis could prevent HIV transmission from mother to children, and prevent adverse pregnancy outcomes due to syphilis, reducing the 300,000 cases reported annually.

A key point is to identify the barriers for POC diagnostics in the low- and middle- income countries. The fact of having available POC diagnostics does not ensure its success. If these devices are not widely used, and the correct intervention process is not followed, they do not have a significant impact on the society. Despite the increase in the investment in POC diagnostics for the developing world, there are numerous barriers to overcome. These challenges may depend on different factors: the country, sector (public or private), area

(urban and rural settings), among others [49]. Some barriers that must be overcome to achieve the success of POC devices are listing below (Figure 1.2).

## Barriers in developing countries

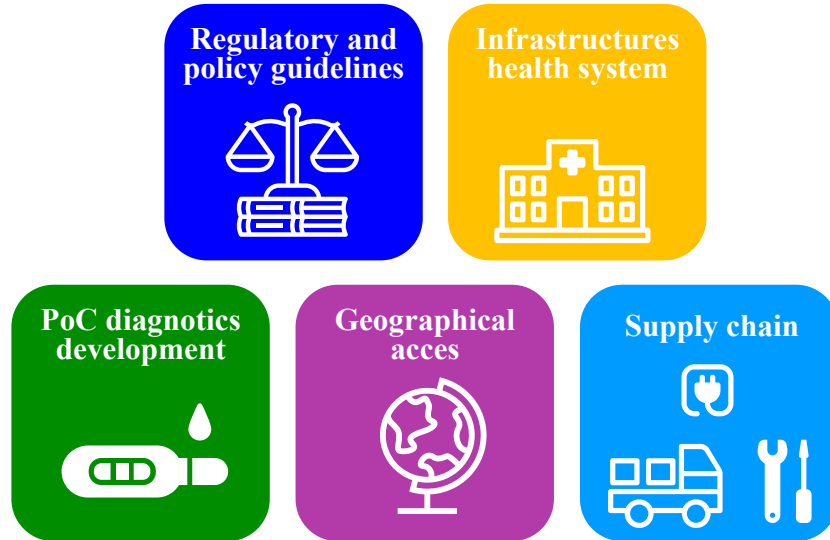


Figure 1.2: Challenges to overcome for implementing POC diagnostic devices in developing countries.

### 1.1.2.1 Regulatory and policy guidelines

Unclear or cumbersome processes and the lack of adequate guides make POC devices difficult to trademark [18, 32]. Some studies showed that weak regulations on POC testing are more challenging compared to drugs and vaccines [18]. The distribution of POC devices is a logistical challenge. Another obstacle is funding from multinational organizations for assistance and non-governmental organizations (NGOs), which makes countries dependent on these partners [18, 32].

### 1.1.2.2 Infrastructures health system

Health systems with weak infrastructures and lack of knowledge of the end-user are a challenge in low-income countries [18, 49]. In other to implement successful POC platforms, it is necessary to take into account sev-

## CHAPTER 1. INTRODUCTION

eral topics: adaptable diagnostic technologies; quality backup infrastructure; trained personnel; and the active participation of developers, suppliers, health professionals, and local health authorities [18]. However, developing countries have a lack of trained health professionals, and the few trained health workers are overloaded with a large number of patients [18, 49].

Sometimes, implement some POC testing is difficult due to primary healthcare clinics in rural areas often lack basic infrastructures, such as constant electricity supply, refrigerators, waste disposal units, and temperature control [49]. Moreover, professionals in hospitals and large healthcare centers are often opposed to rapid tests performed outside the laboratory, due to fear of losing their job or the control over the tests [18, 49].

### **1.1.2.3 Point-of-Care diagnostics development**

Traditionally, technologies have been developed to meet the needs of developed countries that have funded and regulated high-quality laboratories. However, this approach does not cover the needs of healthcare centers without necessary infrastructures [18, 32]. Besides different design criteria must be taken into account to develop POC testing devices for environments with limited resources [18, 50, 51].

### **1.1.2.4 Geographical access**

Geographical access is a significant barrier for POC testing. In low-income countries, the majority of the population lives in the countryside, so access to health facilities means to walk or travel by public transport over long distances [52]. The study presented by Gething et al. shows that 33 % of women in Ghana take two hours to arrive at health centers that provide emergency obstetric and neonatal care [53]. Other studies also showed that the access to POC tests and treatment for HIV disease in sub-Saharan Africa is compromised by distance to health centers [52].

### **1.1.2.5 Supply chain**

The supply chain is one of the greatest barriers in accessibility to POC tests in environments with limited resources [18, 48, 54]. The main factors which cause problems are: irregular supply; limited reagents; inappropriate

## CHAPTER 1. INTRODUCTION

diagnostic systems; confusing acquisition systems; distribution delays; and poor maintenance [18].

Proper distribution processes are necessary for the success of the implementation of POC systems due to the reagents have a limited shelf life and often require proper management of the cold chain [18,32,49]. It is also important to maintain the quality of the processes, a challenge due to the lack of experience or training of health workers in these developing countries [18,32].

Deficiencies in the supply chain generate poor quality POC tests, discrediting the reliability of POC diagnostics [49]. An example is a study presented by Biza et al., which identified a poor supply chain in the implementation of prenatal care packages in different health facilities in Mozambique [55].

### 1.1.3 Investments in Point-of-Care Diagnostics

The healthcare, and increasingly patients, demand more technical advances in medical diagnostics. There are many studies focused on the development of POC devices, although there has not been significant progress in the market in recent years. However, the pandemic caused by the 2019-novel Coronavirus (2019-nCoV) has increased the demand and the rapid development of POC diagnostic tests. The manifestation of the virus infection is highly nonspecific, for this reason, POC devices are crucial to confirm suspected cases, screen patients, and conduct virus surveillance to control the outbreak [56–58].

The POC diagnostics market can be divided into two blocks: the so-called “non-professional” products (glucometers and pregnancy tests), and the “professional” products, which includes all other tests (infectious disease, cardiac markers, lipids, coagulation, hematology, among others) [59]. Glucometers are the most widespread product followed by pregnancy tests, while infectious disease tests are the fastest-growing product. According to the 8th edition report of the International Diabetes Federation (2017) [60], approximately 425 million adults, between 20-79 years, had diabetes in 2017-18 and it is expected to rise to 629 million by 2045. POC glucometers are one of the most useful tools to manage this disease since it can control the glycemic levels in diabetic patients.

There are several reports available to document the growth of the POC test markets. According to the study “Point of Care Diagnostics/Testing

## CHAPTER 1. INTRODUCTION

market size, share & trends analysis report by product (glucose, blood gas / electrolytes, cancer marker), by end-use (clinic, hospital), and segment forecasts, 2019 - 2025” [61], the POC diagnostics market was valued at USD 18.09 billion in 2018 and is expected to increase the CAGR 3.3 %. The growth will be produced thanks to the improvements in the laboratory automation techniques, and the new cost-effective and high-quality medical solutions.

Bill & Melinda Gates Foundation and Grand Challenges Canada announced grants over USD 31 million to develop innovative POC diagnostics test for the developing world [62]. Some factors which boost the POC diagnostics market growth are the increase of chronic diseases and life expectancy. These issues make it look for new solutions like the POC testing, which increasingly patients and clinicians are open to using.

### 1.1.4 Classification of Point-of-Care systems based on biosensing method

POC devices can be classified in different ways. They can be categorized into small portable devices (such as urine albumin tests, blood glucose, and coagulation, among others) and as large bench-top systems (for example, blood gas and electrolyte systems) [63]. Small handheld devices are developed using microfabrication techniques and can show a qualitative or quantitative measurement of a wide range of analytes. Although they seem straightforward at first sight, internally are complex. These handheld systems can perform various tasks such as separating cells from plasma, adding reagents and reading color or other endpoints. On the other side, POC bench-top systems are a reduced version of the central laboratory equipment (such as Afinion<sup>TM</sup>CRP, Alere<sup>TM</sup>q, Pima<sup>TM</sup>CD4, and Cholestech LDX<sup>TM</sup> from Abbott company [64–67]). In these smaller and less-complexity versions, some steps have been automated, such as automatic sample washing, calibration, and quality control, for not depend on vulnerable operators.

It is also possible to classify POC devices according to the biosensor used. A biosensor is a measurement system that detects the presence or concentration of specific biomolecules, microorganisms, or other biological analytes through a physicochemical detector. The detection takes place in three steps. First, the analyte binds to a recognition element, also so-called bioreceptor. The biological binding event is translated into a signal using a transducer. This signal is processed and translated into the concentration of the analyte, among others [22].



## CHAPTER 1. INTRODUCTION

These devices are composed of two fundamental elements: a biological receptor (microorganism, immobilized enzymes, deoxyribonucleic acid or DNA, cells, among others) prepared to detect a substance taking advantage of the specificity of biomolecular interactions and a transducer, which interprets the reaction of biological recognition produced by the receptor and translates the binding event into a quantifiable signal [21, 68] (Figure 1.3).

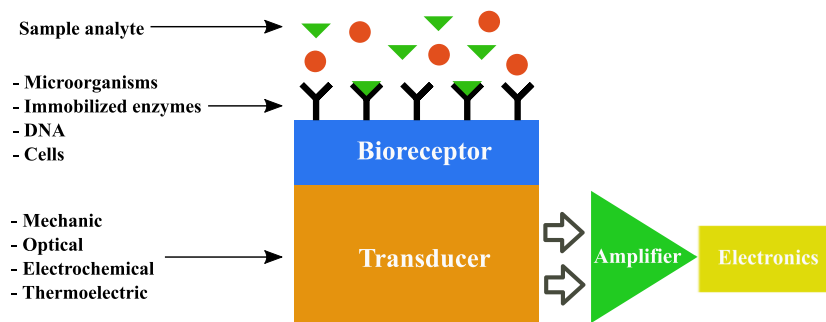


Figure 1.3: Block diagram of the structure of a biosensor.

There are two main methods for biomarker detection: label-based and label-free detection (Figure 1.4).

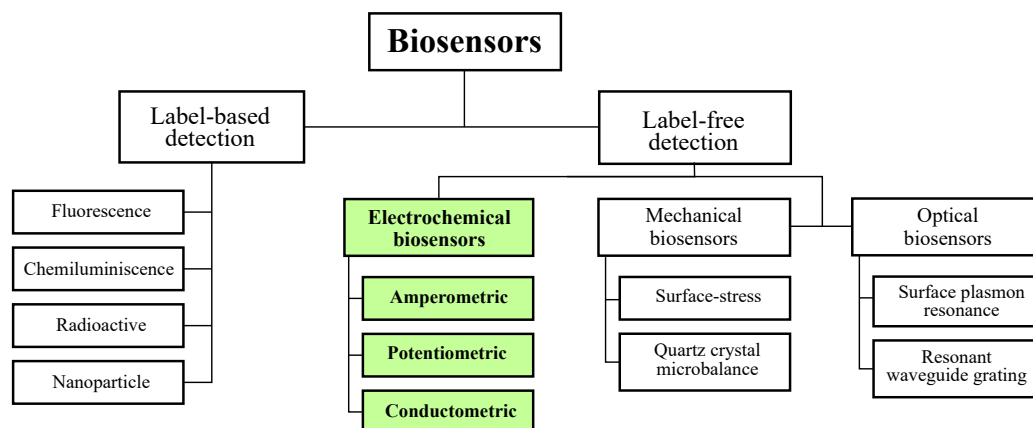


Figure 1.4: Classification of biosensors based on the detection method [22].

Label-based techniques tag query molecules with fluorescent dyes, isotopes, nanoparticles, among others [69]. The molecule of interest is chemically or temporarily linked to an external molecule to detect molecular presence or activity, which can modify its intrinsic properties. The enzyme-linked immune-absorbent assay (ELISA) is one of the most used label-based clinical tests for the detection of protein markers, together with the Frequency Resonance Energy Transfer (FRET) transduction method. However, these

## CHAPTER 1. INTRODUCTION

techniques can modify the characteristics of the query molecules. Besides, these labeling procedures are complex and may become prolonged over time, making labeling techniques non-practical for use in POC applications [69,70].

Detection methods without labels measure inherent properties, such as mass or dielectric properties. Label-free techniques are more suitable for POC diagnosis because they do not interfere with marker molecules [69,71]. Advances in POC devices based on biosensors depend on the improvement of biosensor techniques to rapid and multiple biomarker detection with high selectivity and sensitivity.

Next, different types of label-free sensors are explained by classifying them according to the method of signal transduction. This doctoral dissertation describes the development of full-custom platforms for electrochemical detections. For this reason, it is paid special attention to electrochemical biosensors. Besides, optical and mechanical biosensors are roughly described, although they do not form part of the study of this thesis.

### 1.1.4.1 Electrochemical biosensors

Electrochemical biosensors are of great interest since they enable a practical, rapid, and low-cost analysis of species with high specificity, sensitivity, and selectivity. These kind of sensors convert the biological recognition event into an electrical signal proportional to the analyte concentration [72].

The electrodes that make up these sensors are inexpensive and can be integrated into portable, miniaturized, and easy-to-use electronic systems capable of performing rapid measurements [73]. These systems allow determining the concentration of an analyte within a complex sample next to the patient and in near real-time, making them very interesting for medical diagnosis and environmental monitoring applications. One of the most relevant characteristics of electrochemical biosensors is the possibility of detecting analytes without damage the material [74].

In particular, amperometric biosensors are widely used for determining blood glucose levels in people with diabetes. They provide the result in minutes using a drop of blood. Currently, these systems have been improved and enable continuous glucose monitoring [75].

They are also used in industrial and environmental analysis applications [76]. Thanks to them, food manufacturing processes are controlled,

## CHAPTER 1. INTRODUCTION

evaluating their quality, and monitoring organic pollutants. An example is the use of electrochemical biosensors to detect *Salmonella* and *E. coli* O157:H7 [74]. Recently, the use of nanotechnology focused on the development of biosensors has increased, which allows reducing the dimensions of the electrochemical sensor elements and increasing the signal-to-noise ratio [73].

Electrochemical biosensors can be based on two- or more-electrode configuration. The conventional electrochemical cell contains three separate electrodes: the working electrode (WE), the auxiliary or counter electrode (CE) and the reference electrode (RE). The detection capacity depends on the materials, the surface modification, and the dimensions of the electrodes.

The RE has a stable and well-defined electrochemical potential, besides no current flows through it. This electrode is essential to establish and know the exact potential without variations. The RE is kept at a certain distance from the place where the electrochemical reaction occurs in order to maintain stable potential [20].

The current is applied or measured through the CE and the WE. The CE establishes a connection with the electrolytic solution, providing a flow of electrons between both electrodes [20]. On the other hand, the WE act as a transduction element in the biochemical reaction. The WE can be called cathodic (when reduction occurs) or anodic (when oxidation occurs). It can be made of different materials, creating a wide variety of electrode types (screen printed electrode, Pt electrode, gold electrode, silver electrode, carbon paste electrode, carbon nanotube paste electrode, among others).

To ensure the half-reaction is fast enough and to avoid the kinetic limit of the process, CE often has a larger surface area than WE. Furthermore, both electrodes must be conductive and chemically stable.

Screen-printed electrodes are widely used electrochemical sensors, which are fabricated by depositing thin films of inks on the substrate of the electrode (glass, plastic or ceramic) [77]. They are usually used to develop amperometric biosensors since they are cheap and allow a large-scale fabrication. Typically, these biosensors are disposable, reducing pollution and loss of sensitivity. An example of this type of electrodes is depicted in Figure 1.5.

### **Electrochemical biosensors classification**

They can be classified depending on their signal transduction method. These methods include: a) amperometric detections, which rely on measuring the electrochemical oxidation or reduction current that is related directly

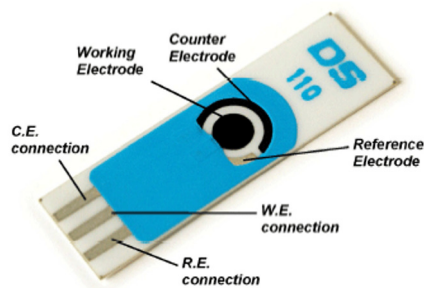


Figure 1.5: Electrochemical biosensor based on screen-printed electrode [78]. Reprinted from Metrohm-DropSens website.

to the concentration of the electroactive species; b) potentiometric detection that measures potential changes at the working electrode concerning the reference electrode, under conditions of constant current flow (usually zero); and c) conductometric detections, which are based on changes of electric conductivity of biolayer at the electrode surface, whose conductivity is affected by the analyte present [20].

a. **Amperometric biosensors**

Amperometric biosensors are integrated devices that measure currents resulting from the oxidation or reduction of a biochemical reaction for the quantification of an analyte. The simplicity of the transducer enables its use on low-cost portable systems suitable for a wide range of applications [20, 73].

In order to perform the detection, the product must be electroactive and undergoes a redox process. Many biological compounds (glucose, cholesterol, etc.) are not electroactive, so it is necessary to combine reactions to produce an electroactive element.

b. **Potentiometric biosensors**

Potentiometric sensors are devices comprised of a biological sensor element connected to a physicochemical transducer. The transducer generates an electrical potential signal when the target analyte binds to the bioreceptor, which is proportional to the logarithm of the concentration of active substances produced or consumed in the reaction [79]. They measure the accumulation of a charge potential

## CHAPTER 1. INTRODUCTION

at the WE concerning the RE, under conditions of constant current flow (usually zero) [72].

The potential difference, measured between the RE and the WE, depends on the activity of the ions of the sample to be analyzed. The principle of potentiometric detection is based on the Nernst equation [80], which relates the potential difference to the activities of the species responsible for the response.

### c. **Conductometric biosensors**

In conductometric biosensors, the biorecognition event causes a change in the ionic species concentration, which leads to a change in the electrical conductivity that can be measured. These biosensors are based on the measurement of the variations of the conductance with the use in an AC signal at a fixed operating frequency [68].

Some advantages of conductometric biosensors are: a) they can be miniaturized and integrated using a thin-film technology; b) they use an inexpensive technology, enabling the large scale production; c) they do not require a RE; d) transducers are not light-sensitive; and e) they operate at low-amplitude AC signal, preventing Faraday processes on electrodes [81].

## **Electrochemical detection techniques**

Three of the most commonly used techniques in electrochemistry are cyclic voltammetry, chronoamperometry, and electrochemical impedance spectroscopy.

### a. **Cyclic voltammetry (CV)**

In this potentiodynamic electrochemical measurement technique, a variable potential is applied to the electrochemical cell while the current that provides this electrochemical cell is measured (Figure 1.6). The WE potential is varied over time until it reaches an established potential value, then it changes direction. This process is repeated an established number of cycles. The result is plotted in a cyclic voltammogram, which represents the current through WE against the voltage applied to an electrochemical cell.

CV is a technique widely used to study the electrochemical properties of an analyte in a solution. Electroactive surfaces are typical in electrochemical devices, such as energy extraction devices (batteries

## CHAPTER 1. INTRODUCTION

and fuel cells), as well as electrochemical sensors (glucometers, among others). The great advantage of the CV is the diversity of information it gives since a single scan provides a large amount of information about the chemical and physical behavior of a system. It shows the relationship between the speed of electrolysis on the electrode surface and the transport speed of the chemical species that react to that surface by diffusion. Different physical phenomena can be observed performing voltammetry at different scan rates, modifying the rate of change of voltage over time.

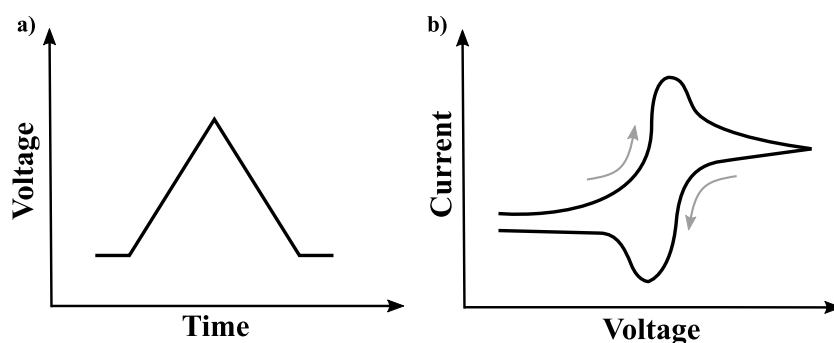


Figure 1.6: Typical cyclic voltammetry input (a) and output (b) waveforms.

### b. Chronoamperometry (CA)

It is a specific electrochemical technique in which chemical species (known as electroactive substances) produced redox reactions at inert metal electrodes [82]. CA is a time-dependent technique that drives the WE at a constant potential. In this technique, the electrode current is measured against the time (Figure 1.7).

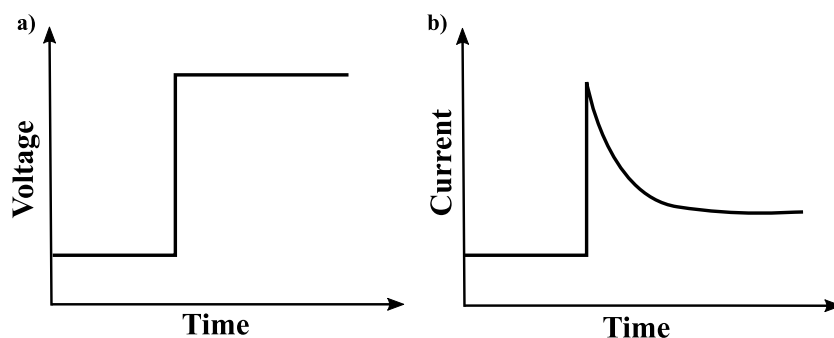


Figure 1.7: Typical chronoamperometry input (a) and output waveforms (b).

In this technique, the current varies according to the diffusion of an analyte from the bulk solution to the sensor surface. CA measures

## CHAPTER 1. INTRODUCTION

the dependence between the current and time of a diffusion-controlled process that varies with the analyte concentration. This sensitive technique does not require analyte or bioreceptor labeling.

The procedure is as follows. Before beginning the experiment, the electrode is maintained at a potential in which no faradaic process occurs. Then, the potential rises to a value at which a redox reaction occurs. For reactions under diffusion control, the current decreases  $t^{1/2}$ , following the Cottrell equation, Equation (1.1). The Cottrell equation defines the current-time dependence for linear diffusion control at an electrode.

$$I = nFAc_0\sqrt{\frac{D}{\pi t}} \quad (1.1)$$

where,

I: current,

F: Faraday's constant,

N: number of transferred electrons for each molecule,

A: electrode area,

$c_0$ : analyte concentration,

D: diffusion coefficient,

T: time.

### c. **Electrochemical Impedance Spectroscopy (EIS)**

Electrical resistance is the ability of a circuit element to resist the flow of electrical current. Ohm's law, Equation (1.2), defines resistance (R) as the ratio between voltage (V) and current (I).

$$R = \frac{V}{I} \quad (1.2)$$

This well-known relationship is limited to the ideal resistor. The real world contains circuit components with more complex behavior, such as the impedance. Like resistance, impedance measures the ability of a circuit to resist the flow of an electrical current. However, the impedance is frequency-dependent, so it is necessary to apply an AC potential to the electrochemical cell and then measure the current through the cell.

The response to a sinusoidal potential signal is a sinusoidal current signal, which can be considered as a sum of sinusoidal functions (a

## CHAPTER 1. INTRODUCTION

Fourier series). The impedance ( $Z$ ) is calculated by setting the input potential ( $V$ ) and measuring the induced current ( $I$ ) (Equation (1.3)).

$$Z = V \cdot I \quad (1.3)$$

In an EIS, an AC potential is applied to the sample under test, normally a small amplitude sinusoidal signal. Then, the inducted AC current through the sample is measured (Figure 1.8a). An EIS measures the impedance, a complex quantity with a magnitude and phase that represents the resistive and capacitive effects. The resistance forms the real part of the complex impedance, in-phase with the applied signal, while capacitance forms the imaginary part of the complex impedance, out-of-phase with the applied signal. A Nyquist diagram is often used to represent the impedance (Figure 1.8.b). This diagram plots the imaginary component against the real component of the impedance as a function of the frequency.

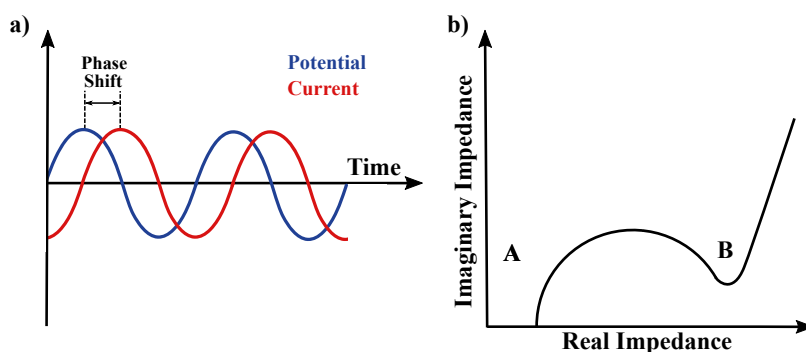


Figure 1.8: a) An oscillating perturbation in the cell produces an oscillating current response. b) Schematic of a Nyquist plot. Top-right points are at lower frequencies, while bottom-left points are at higher frequencies.

EIS is a powerful technique used in a broad range of applications, such as a corrosion monitoring processes [83], food physiological status [84], human body analysis [85], among others.

### 1.1.4.2 Optical and mechanical biosensors

#### Optical biosensors

Optical sensors use light to detect the binding of a target molecule. They are composed of a biorecognition element and an optical transduction sys-



## CHAPTER 1. INTRODUCTION

tem. The biorecognition elements can be enzymes, antibodies, antigens, nucleic acids, cells, among others. Two examples of optical biosensors are Surface Plasmon Resonance (SPR) and Resonant Waveguide Grating (RWG) biosensors. Both use an evanescent field to detect the interaction between the biorecognition element and the analyte.

### a. Surface Plasmon resonance biosensors

SPR biosensors are optical sensors that detect changes in the refractive index due to the binding of molecules to a sample. The SPR phenomenon allows direct measurement, without labels, recognizing the concentration of immobilized biomolecules in the SPR sensor [86].

Polarized light with a particular angle excites a specific mode of the electromagnetic field-surface plasmon. This generates surface plasmons and the reduction of the intensity of the reflected light at a specific angle, so-called resonance angle. The surface plasmon propagates along with a thin film of metal (or other conductive materials) and its field probes the medium adjacent to the metal (usually glass and liquid) [87]. The index of refraction in the proximity of the metal surface alters the speed of the surface plasmon, which can be detected analyzing changes in the light wave coupled to the surface plasmon. This effect is proportional to the surface mass, so, if specific biorecognition elements are immobilized on the metal surface when a sample is contacted with the sensor surface, the analyte molecules are captured by these biorecognition molecules. This union produces changes in the index of the refraction of the surface of the sensor, which can be measured by the optical detector [86, 87].

SPR is a potential optical biosensing technology since it allows real-time, label-free, and noninvasive measurements. Some researchers have published reports presenting SPR biosensors for studying various kinds of biological reactions. Firdous et al. developed a SPR biosensor as an approach to early-stage detection of viral and malignant diseases, such as cancer tumors [88]. The developed instrument captured and detected a biomarker in vitro for cancer diagnostics. In another study, Dorin Harpaz et al. developed a functionalized gold SPR chip to detect NT-proBNP and S100  $\beta$  stroke biomarkers [89]. The biomolecular interaction was detected through the refractive-index shift measured with a camera. Both biomarkers were detected in the typical range of stroke concentrations, which ranges from 0.25 ng/mL to 10 ng/mL, demonstrating a limit-of-detection lower than ng/mL.

## CHAPTER 1. INTRODUCTION

There are several advantages of SPR biosensor technology. Due to its versatility, they can detect a wide variety of analytes, which does not have any particular property (such as fluorescence or absorption). Also, it is possible to perform real-time analysis, providing a quick and flexible response. However, they also have some limitations. The specificity of detection is based on the ability of biomolecular recognition elements to recognize and capture analytes. Therefore, if biomolecular recognition elements are sensitive to non-target molecules but structurally similar, it can hide a specific response. Moreover, interferences can produce variations in the refractive index, such as variations in the background refractive index (due to the temperature of the sample or composition variations) [90].

### b. **Resonant waveguide grating biosensors**

This optical sensor combines the optical methods of evanescent field detection and optical phase difference measurement. The technique is also known as Optical waveguide interferometric [91].

An RWG biosensor probes the grating sensor area with an evanescent field, as depicts Figure 1.9. The biological area changes when biorecognition molecules capture analyte molecules. This produces a variation in the refractive index of the area, and a phase shift of the guided mode concerning the reference field. The interfering fields of these modes produce a signal at the sensor output, proportional to the change in the refractive index and the analyte concentration. [91]. This technique can be used to perform measurements of cellular responses under microfluidics [92] or to detect of avian influenza virus [93].

## **Mechanical biosensors**

Advances in micro and nanofabrication technologies enable the development of mechanical biosensors with moving parts of nanometric size. Microelectromechanical systems (MEMS) and nanoelectromechanical systems (NEMS) provide high mass resolution. The uniform reduction of its dimensions increases its ability to be displaced or deformed, converting the applied force into a measurable displacement. These capabilities open up new opportunities to measure small forces present in biological interactions. There are different types of mechanical biosensors, such as surface-stress sensors and quartz crystal microbalances, among others.

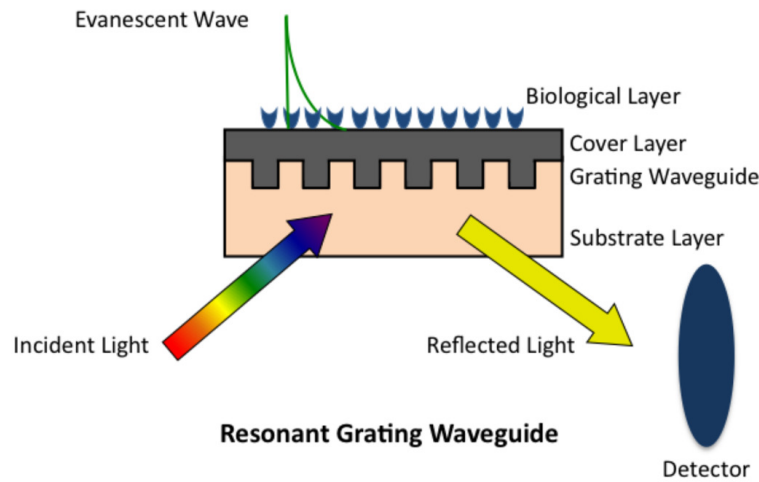


Figure 1.9: Schematic of a resonant grating waveguide biosensor. Reprinted from [94] with permission.

a. **Surface-stress mechanical biosensors**

Nanomechanical biosensors usually have a cantilever-shaped which is sensitive to the biomolecule of interest. These devices measure the deviation of a miniature mechanical device. When biomolecules bind, it is developed a surface tension, which produces the deviation of the mechanical element due to electrostatic repulsion or attraction, steric interactions, hydration, and entropic effects (Figure 1.10).

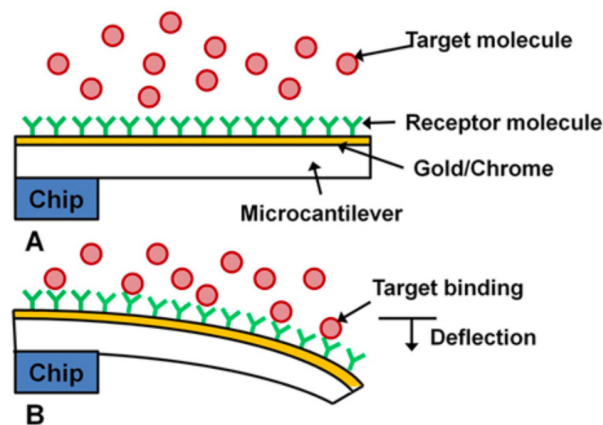


Figure 1.10: Schematic of cantilever biosensors response: (A) initial state and (B) sensing state. Reprinted from [95] with permission.

The displacement of the cantilever can be detected through the piezoresistive method. Piezoresistive materials vary their resistiv-

## CHAPTER 1. INTRODUCTION

ity when their surface suffer stress. The resistance of the cantilever changes when it is bent, which is measured through a Wheatstone bridge. The main advantage of this technique is that both the sensor and the detection circuit can be easily integrated into a chip. In the study presented by Marie et al., they developed a piezoresistive cantilever system capable of detecting DNA hybridization [96]. Electrical (piezoresistive) readout has also been employed to measure the binding of proteins [97] and DNA [98]. Due to this technique requires electrical circuits, it is necessary to protect the system in the case of carried out experiments in liquids. This protection produces heat dissipation and thermal deviations that can cause parasitic deviations of the cantilever.

### b. **Quartz crystal microbalances (QCM)**

These label-free biosensors are centimeter-scale mechanical resonators extremely sensitive to mass, which allows the detection of the binding event between analytes and bioreceptors on their surface. QCM provides a rapid detection of pathogens and toxins because of its simplicity in concept, sensitivity, ease-of-use, low cost, shorter analysis time, and their easy production.

The main component of QCM biosensors is a quartz crystal wafer sandwiched between two metal electrodes, in which an oscillating electric field produces an acoustic wave (Figure 1.11). The resonant frequency of these biosensors is dependent on the mass change at the crystal surface. Analyte concentration can be sensed by combining QCM devices, and highly specific biomolecules immobilized on the surface. Many researchers applied QCM based biosensor as the transducer to the detection microorganisms, such as *E.coli* bacteria [99] and metastatic breast cancer [100].

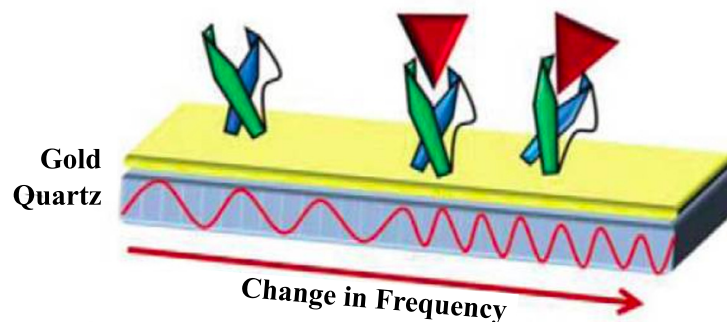


Figure 1.11: Schematic of quartz crystal microbalance biosensor: when analyte binding occurs, the resonance frequency varies. Reprinted from [101] with permission.

## 1.2 Architecture of POC technologies

The integration of electronic technologies and biosensors enables the development of biomedical platforms to detect specific biomarkers in health and environmental fields.

This thesis is focused on the development of full-custom low-power electronic platforms for POC applications oriented to work with electrochemical biosensors. The doctoral dissertation was focused on this type of biosensors because of the wide range of possibilities and advantages that they present. Some key benefits of electrochemical biosensors are their robustness, easy integration, and good detection limits [20]. Furthermore, they enable to develop low-cost, miniaturized, and easy-to-use devices for a wide range of applications.

The main modules that involve the development of electronic systems for electrochemical detections generally are the Front-end module, the Back-end module, and the Power Management module (Figure 1.12).

The Front-end module contains the instrumentation electronics which carry out the measurement. These circuits bias the signal to drive the electrochemical sensor and conditioning the signal provided. Then, the measurement signal is sent to the Back-end module, in which it is processed and translated to produce a readable signal, easy to represent. The Power Management module controls, regulates, and distributes power to the modules that comprise the system.

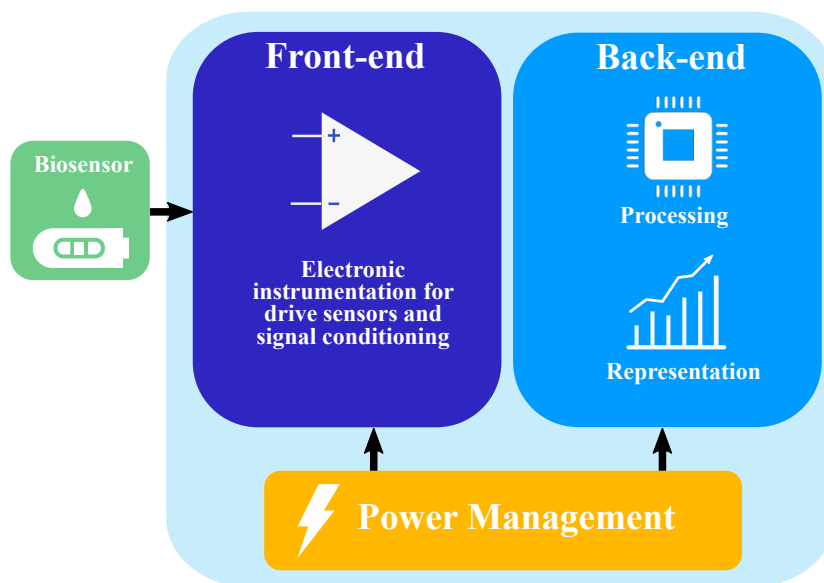


Figure 1.12: Block diagram of an electronic system to make electrochemical measurements.

## 1.2.1 Front-end: Instrumentation architectures

### 1.2.1.1 Potentiostat-based solutions

One of the key elements of electrochemical instrumentation is the potentiostat, an electrochemical equipment widely used in both research and industry [102]. It is used for many purposes, ranging from the study of biosensors for detecting cancer cells [103] to the sensing of harmful sub-substances in the food and chemical industry [104].

The main tasks of a potentiostat amplifier are: a) driving the electrodes of the electrochemical cell to the desired input signal,  $V_{IN}$ , ensuring an invariant voltage at the RE by adjusting the current in the auxiliary electrode or CE, and b) obtaining an output voltage signal proportional to the value of the measured analyte.

As is stated in the previous section, Electrochemical biosensors can be based on two- or more-electrode configuration.

The two-electrode configuration consists of a RE, which fixes a constant potential reference, and a WE wherein the chemical reaction of interest occurs. The current is applied or measured through the RE and the WE, as it

## CHAPTER 1. INTRODUCTION

is depicted in the Figure 1.13a. The RE carries out two tasks: a) it allows a charge flow through the cell, and b) maintains a constant interfacial potential, regardless of current. However, in this configuration is difficult to accurately fulfill both tasks since the flow of current through the electrode can cause a voltage drop. Besides, the current present in the RE generates a variation of the voltage interface [102]. This fact leads to poor control of the WE potential, causing the electrode potential does not remain at a constant value. These problems occurs in large-scale electrolysis or rapid-voltammetric analysis methods in organic solvents. A solution is to use biosensors with large RE and a small WE, although it may not always be feasible to do [102]. This topology is typically used with energy conversion or storage devices, like fuel cells or batteries [105].

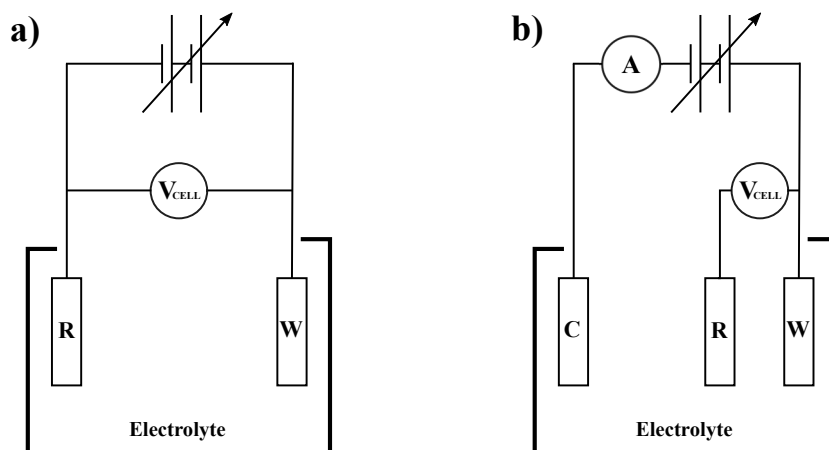


Figure 1.13: Basic schematic of (a) two-electrode and (b) three-electrode configuration.

The three-electrode set-up solves many of the problems of the two-electrode configuration. In this topology (Figure 1.13b), the RE has a stable and well-defined electrochemical potential, avoiding any flow of current between the RE and the WE. Due to the current flow through the RE is negligible, the voltage drop between the RE and WE is small. Thus, the potential at RE is more stable, and there is compensation for the voltage drop across the solution that allows more control over the WE potential. In this set-up, the role of the CE is to inject all the current needed to balance the current at the WE.

A potentiostat is based on a feedback circuit made up of advanced electronic components that control with precision the potential to drive sensors and obtain reliable information at the output. There are numerous topologies, but it usually consists of two modules: the Control Amplifier, and the

## CHAPTER 1. INTRODUCTION

Current-to-Voltage converter (Figure 1.14).

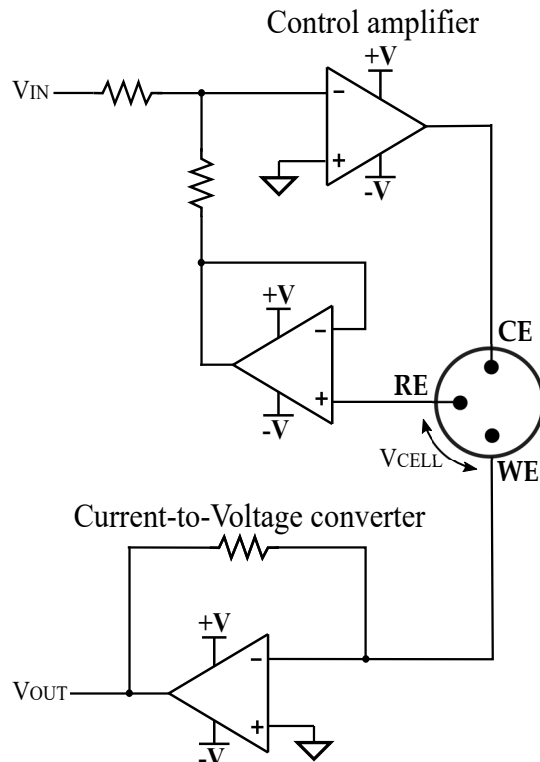


Figure 1.14: Example of a potentiostat circuit comprised of the Control Amplifier, and the Current-to-Voltage Converter.

The Control Amplifier performs three main functions: it acts as a feedback element, measures the voltage of the cell, and forces  $V_{CELL}$  and  $V_{IN}$  to be equal. This module compares the actual cell voltage ( $V_{CELL}$ ) to the desired cell voltage ( $V_{IN}$ ), and drives current into or from the CE, forcing these voltages to be the same. The  $V_{IN}$  is usually generated by means of a Digital-to-Analog Converter (DAC), which can generate constant voltages, voltage ramps, and even sine waves.

It is mainly composed of operational amplifiers. An ideal operational amplifier has infinite input impedance, avoiding a flow of current through its inputs. Real operational amplifiers have an input bias current that can vary its operation. However, operational amplifiers used in potentiostats have small input currents, of the order of picoamps, which reduce, and even eliminate this effect. Another relevant parameter of the operational amplifier is the bandwidth, which characterizes the maximum frequency that the circuit can measure. The input capacitance of the operational amplifier along



## CHAPTER 1. INTRODUCTION

with the resistance of the reference electrode forms an RC filter. If the time constant of this filter is large, the filter can limit the bandwidth and cause system instabilities. When the input capacitance is small, the operation of the circuit is more stable, and it can tolerate reference electrodes of higher impedance.

The basic implementation of the Control Amplifier is depicted in Figure 1.15a. As it shows, the WE is connected to ground, and an operational amplifier controls the cell current,  $I_{CELL}$ , matching the cell potential,  $V_{CELL}$ , to the desired potential,  $V_{IN}$ .

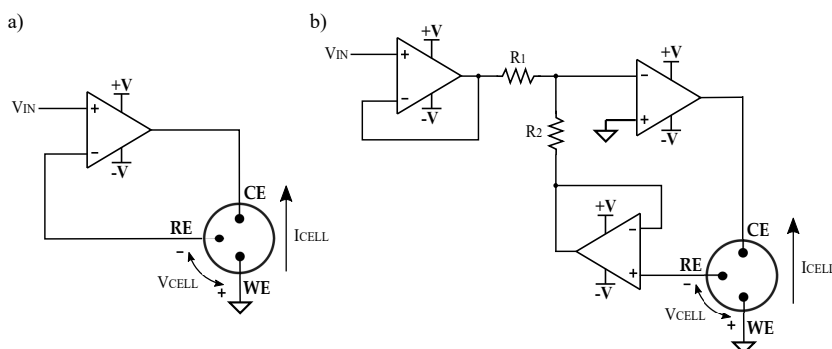


Figure 1.15: Schematic of a) a basic control amplifier circuit; and b) a Control Amplifier circuit using voltage followers to isolate it and the RE.

Another possible implementation is depicted in Figure 1.15b, which uses operational amplifiers as a voltage follower to isolate the Control Amplifier and the RE [106]. In this case, the cell potential,  $V_{CELL}$  is proportional to  $V_{IN}$  and depends on the value of  $R_1$  and  $R_2$  resistors (Equation (1.4)).

$$V_{CELL} = V_{IN} \cdot \frac{R_1}{R_2} \quad (1.4)$$

The Current-to-Voltage Converter circuit measures the current of the cell and translates it into voltage. For this purpose, an Instrumentation Amplifier, a Transimpedance Amplifier, or a Switching Capacitors circuit can be used.

The Instrumentation Amplifier (IA) measures the voltage difference in a resistor placed on the CE (Figure 1.16). In this configuration, the current through the resistance  $R_{IA}$  is the same as the current generated by the electrochemical reaction ( $I_{CELL}$ ). Besides, the polarization voltage ( $V_{CELL}$ ) is very stable due to the direct connection of the WE to the ground.

## CHAPTER 1. INTRODUCTION

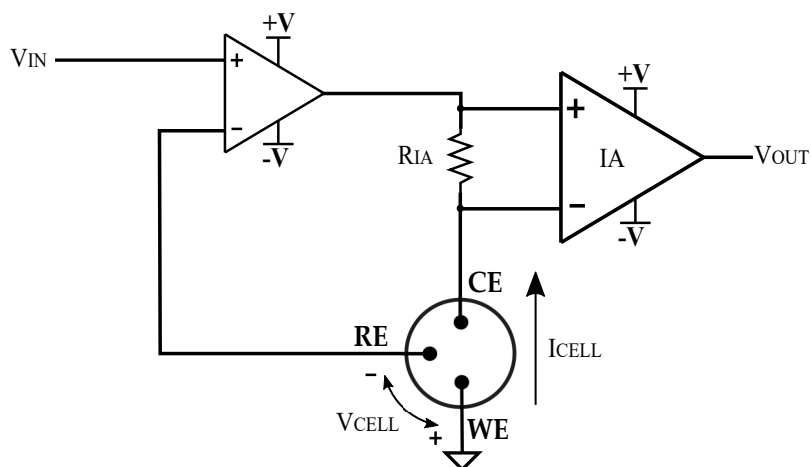


Figure 1.16: Potentiostat circuit formed by a basic Control Amplifier configuration with an Instrumentation Amplifier as a Current-to-Voltage converter.

The transfer function that relates the current through WE and output voltage,  $V_{OUT}$ , is theoretically described by the Equation (1.5).

$$V_{OUT} = A \cdot I_{CELL} \cdot R_{IA} \quad (1.5)$$

where,

$V_{OUT}$  is the IA's output voltage,

$A$  is the amplifier's gain,

$I_{CELL}$  is the current generated by the electrochemical reaction,

and  $R_{IA}$  is the resistance located in the input terminals of the IA.

Another Current-to-Voltage Converter circuit widely used in potentiostats circuits is the Transimpedance Amplifier (TIA). In this circuit, a feedback resistor ( $R_{TIA}$ ) placed between the positive input and the output of an operational amplifier converts current generated by the reaction ( $I_{CELL}$ ) into a voltage ( $V_{OUT}$ ) using Ohm's law, as shows Figure 1.17 and Equation (1.6). In this configuration, the feedback of the operational amplifier maintains the WE at virtual ground. As it is stated previously, the input bias current of the TIA should be small, and the input impedance large in order to minimize current losses.

$$V_{OUT} = -I_{CELL} \cdot R_{TIA} \quad (1.6)$$

The Switching Capacitors solution is based on a TIA circuit in which

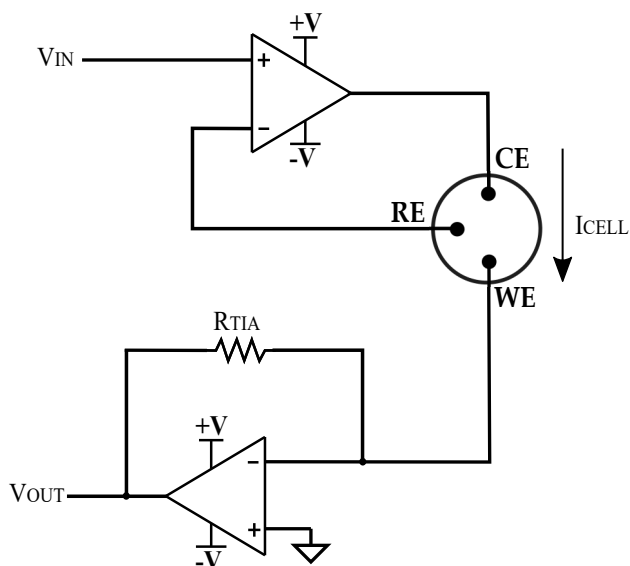


Figure 1.17: Potentiostat circuit which combines a basic Control Amplifier configuration with a Transimpedance Amplifier as a Current-to-Voltage converter.

the resistor is replaced by a switch. The schematic of this architecture is depicted in Figure 1.18. This solution requires a clock control signal, which can be generated by a microcontroller that also can process the signal and transmits the data.

The system works as follows: on the first semi-cycle of the clock, the switch is closed, and the current of the electrochemical cell ( $I_{CELL}$ ) charges the capacitor ( $C_{SC}$ ) to the output voltage ( $V_{OUT}$ ). On the second semi-cycle, the switch is opened, and  $V_{OUT}$  is connected to the ground discharging the capacitor. The capacitor and the value of the clock cycle can be adjusted in order to have a wide measurement range. The Equation (1.7) shows the expression that relates the circuit parameters with the output voltage.

$$V_{OUT} = \frac{-I_{CELL} \cdot T_{CLK}}{2C_{SC}} \quad (1.7)$$

As the solution based on the TIA circuit, the WE is referenced to ground through the virtual ground. Consequently, to minimize current losses, the amplifier input bias current should be small, and input impedance large. Besides, the capacitance of the electrochemical cell must be some orders of magnitude higher than the capacitor  $C_{SC}$  to avoid that the charge injection being larger than desirable.

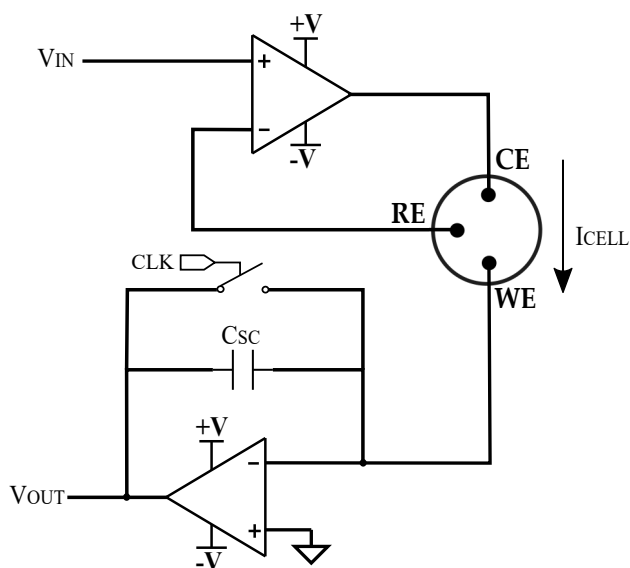


Figure 1.18: Potentiostat circuit composed of a basic Control Amplifier configuration with a Switching Capacitor as a Current-to-Voltage converter.

The Switching Capacitor configuration is commonly used in ASIC (Application-Specific Integrated Circuit) developments due to its difficulty to fabricate resistors of the large values, and easy to integrate low-capacitance values, making possible to create multichannel sensor systems [107, 108].

Different potentiostat architectures with their advantages and disadvantages are shown in Table 1.2. The choice of the most appropriate front-end instrumentation depends on a variety of factors such as area, power consumption, minimum current detection, the operation frequency, among others.

## CHAPTER 1. INTRODUCTION

Potentiostat architectures	Advantages	Disadvantages
Instrumentation amplifier	<ul style="list-style-type: none"> <li>- The WE is directly connected to the ground terminal when the IA is connected between the CE and the Control Amplifier.</li> <li>- The current path does not have active components.</li> </ul>	<ul style="list-style-type: none"> <li>- The resistors increase the flicker and thermal noise.</li> <li>- Difficult to integrate.</li> </ul>
Transimpedance amplifier	<ul style="list-style-type: none"> <li>- Simple.</li> </ul>	<ul style="list-style-type: none"> <li>- The WE is virtually connected to the ground terminal.</li> <li>- The current path has active components.</li> <li>- The input current bias of the amplifier causes current measurement losses.</li> </ul>
Switching capacitor circuit	<ul style="list-style-type: none"> <li>- Easy to integrate.</li> </ul>	<ul style="list-style-type: none"> <li>- The WE is virtually connected to the ground terminal.</li> <li>- The current path has active components.</li> <li>- It depends on electrode morphology and parasitic capacitors.</li> </ul>

Table 1.2: Summary of front-end solutions based on potentiostat architecture [109].

Several POC systems based on potentiostats are presented in the literature, and the vast majority are based on a TIA [110–112]. An example is the potentiostat developed by Sun et al. [113], which used an integrator and a pulse width modulation hardware to generate the signal to drive the sensor and a resistive feedback to measure the current output signal. Another example is the smartphone-based electrochemical device presented in [114]. Punter et al. also described a portable POC device for early detection of anemia based on direct hematocrit measurement from whole blood samples through impedance analysis [111]. The electronic instrumentation combined a Wien bridge oscillator and potentiostat based on TIA. The device was validated through 24 blood samples, obtaining an accuracy error of 2.83 % and a mean coefficient of variation of 2.57 %.

## CHAPTER 1. INTRODUCTION

It is also proposed potentiostats based on IA. An example is the low-current, high sensitivity, and high linearity biosensor dedicated to neurotransmitter detection based on IA presented in [115], which included an error cancellation loop composed of high gain and rejection ratio amplifiers. The proposed potentiostat had 0.1 % accuracy and 10 nA current sensitivity.

As is stated above, switching capacitor-based techniques are commonly used in integrated systems. In [107], the authors developed a miniaturized biosensing platform for amperometric electrochemical sensing in 0.35  $\mu\text{m}$  CMOS technology. The system was composed of a fully integrated current readout circuit that measured currents in the range of  $\pm 20 \mu\text{A}$  with an input noise of 0.47 pA and an input leakage current of 2.1 nA. Another example is presented in [108], in which a current readout circuit based on a switching capacitor technique is described for interfacing with electrochemical biosensors for POC Bovine Viral Diarrhea diagnostics.

### 1.2.1.2 Current sense amplifier

One of the key aspects of this thesis is to develop different electronic systems able to detect the current provided by the electrochemical cell.

Sensing current flow is a frequent requirement in electronic systems, and there are a wide variety of techniques for this purpose.

A commonly used technique is current sense resistors also called shunt resistors. Typically, this current sensing technique is used in high-voltage applications such as battery chargers or overcurrent protection circuits. However, the increase of portable devices has risen the demand for dedicated current monitors in a small package and with a low quiescent current.

This doctoral dissertation has explored the use of the current sense amplifier to measure the low-current signals provided by fuel cells due to its low-complexity that enables easy-integration on self-powered systems or even flexible substrates.

This architectures can be classified into low-side current sensing and high-side current sensing (Figure 1.19).

In low-side current configurations, the sense resistor is placed between the active load and ground [116]. This technique is more simple to implement because the sense voltage is ground referenced. However, low-side current

## CHAPTER 1. INTRODUCTION

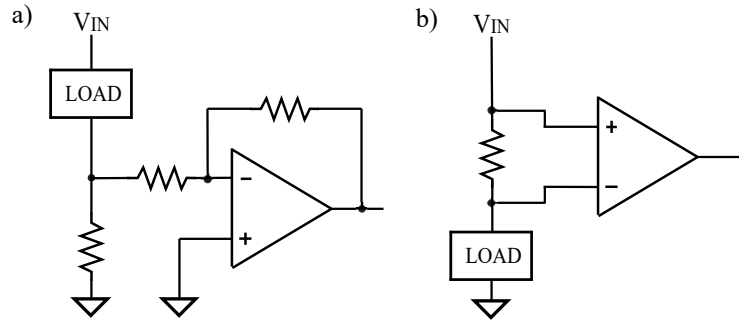


Figure 1.19: Principle of a) low-side current configuration, and b) high-side current configuration.

configurations have some disadvantages: the load is not ground referenced, and leakage currents cannot be sensed.

High-side current configurations place the current sense resistor between the power source and the active load. The two advantages of this configuration concerning low-side configuration are: it detects downstream failures with the option to trigger appropriate corrective action, and it avoids ground disturbances because the shunt resistor is not connected directly to the ground. These benefits make the high-side current sensing configuration more used.

Figure 1.20 depicted a high-side current sense amplifier, which can be configured with a gain to amplify the output signal. It is composed of generic components such as operational amplifiers, resistors, and p-channel Metal-Oxide-Semiconductor Field-Effect Transistor (MOSFET).

The negative feedback of the amplifier forces the voltage in  $R_2$  upon gain resistor  $R_1$  [117], while the current through  $R_1$  flows through p-channel MOSFET to resistor  $R_4$ , developing a ground-referenced output voltage. This voltage can be used to drive an ADC without additional buffering. This circuit amplifies the voltage across a small value sense resistor by the ratio of resistors ( $R_4/R_1$ ) [116].

Resistor tolerances determine the gain accuracy, and the offset voltage ( $V_{OS}$ ) of operational amplifier introduces an error of  $V_{OS}/R_4$ . The total gain of this solution is depicted in Equation (1.8).

$$V_{OUT} = I_{LOAD} \cdot R_2 \cdot \frac{R_4}{R_1} \quad (1.8)$$

## CHAPTER 1. INTRODUCTION

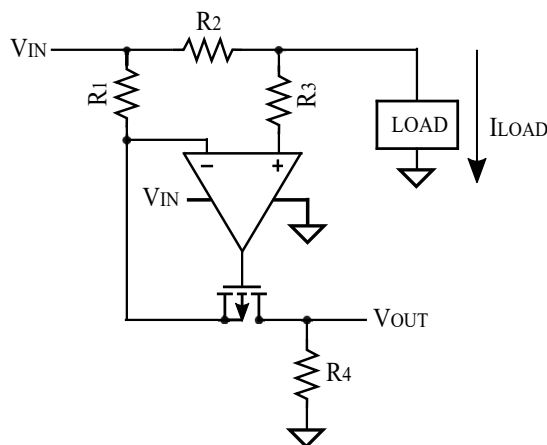


Figure 1.20: High-side current monitoring amplifier

Current-sense amplifiers solutions are less common in POC devices. The author of this thesis proposed a self-powered solution able to provide a qualitative measurement of the analyte concentration by measuring the current generated by a Biological Fuel Cell (BFC) [118] with a current-sense amplifier solution able to be efficiently integrated into POC diagnosis systems. The proposed architecture can be applied to different types of BFC and opens the door to be implemented on flexible and printable plastic substrates.

### 1.2.2 Back-end solutions

#### 1.2.2.1 Low-power microcontroller-based platforms

Most of the POC devices available in the market do not offer quantitative outcomes. Obtaining quantitative results is often a challenge because requires complex and expensive electronic sensors and equipment. One of the possibilities for these challenges is the use of microcontrollers.

In the last two decades, applications of microcontrollers have increased, and today it is one of the most widely used integrated circuits. They can make easier the design and implementation of POC devices for handling samples and detecting health parameters.

There are a wide variety of microcontrollers available in the market that have extraordinary capabilities with powerful tools of computing, communication, and networking. This combined with an active online community,



## CHAPTER 1. INTRODUCTION

which helps with difficulties in writing codes and shares knowledge, could potentially help in the successful spread of POC devices. Furthermore, in recent years, these have reduced their cost and opened new opportunities thanks to the emergence of open-source platforms that provide easy-to-use development environments [119–121].

Microcontroller-based systems allow obtaining more accurate data thanks to its powerful signal processing and graphic interfaces. These systems can display the data on a laptop, on a Thin Film Transistor (TFT) screen integrated into the device, or send the data through wireless communications such as Wi-Fi or Bluetooth to smartphones.

Some examples of microcontrollers-based platforms for POC applications are described below.

A paper-based POC device to detect the Zika virus was described by Pardee et al. [122]. The device was powered by a rechargeable lithium-ion battery and had a 4 GB memory that allowed to perform the tests without the need for a laptop, although it was used later to dump data. They used an Arduino platform to control a LED array and electronic sensors, with a total cost of under USD 250. Gahan et al. proposed a portable analysis platform to detect kidney disease in the urine [123]. The POC device was based on the Arduino board, a color sensor, and a urine strip. The authors showed how the sensor detected the change in color on the strip, produced for the presence of albumin in the urine.

Other published works did not need the use of a laptop to analyze or display the signals obtained. An example is the portable and real-time optical detector to measure the fluorescence intensity of the tagged bio-samples described in [124]. In this work, the authors presented an optical detection matrix that excited the sample by an LED and sensed the light emitted from the sample. An Arduino microcontroller controlled the LED, amplified the detected signal, and display the measurement data on a screen. The system was validated measuring the concentration of food poisoning protein.

Another example of a POC system is MySignals, developed by the Spanish electronics manufacturer Libelium. It is a physiological monitoring platform for biometric and medical applications based on Atmega 2560 microcontroller [125]. It allows connecting more than fifteen off-the-shelf sensors such as body temperature, electromyography, electrocardiography, galvanic skin response, glucometer, spirometer, among others. The platform includes Wi-Fi and Bluetooth Low Energy communication module, and a complete

## CHAPTER 1. INTRODUCTION

graphic system with a TFT touchscreen that allows showing the data in real-time.

The author of this thesis developed a biosensing device based on a microcontroller with the collaboration of the members of Reilly lab, within the framework of a predoctoral stay at the Trinity Center for Biomedical Engineering and Trinity College Institute of Neuroscience of the Trinity College Dublin (Ireland) [126]. During this stay, the author developed an electronic system to investigate the Dystonia disorder. This platform are described in detail in the Appendix section.

### 1.2.2.2 Smartphone-based POC

Biosensing platforms based on the smartphone are an emerging technique for POC diagnostics that is rapidly gaining recognition in the market [127, 128]. Biomedical parameters can be measured using smartphones thanks to the embedded sensors, apps, wired and wireless connection methods. One of the advantages of POC smartphone-based devices is that the results can be saved on secure cloud servers or can be shared with the specialists to give a diagnostic.

Several research works proposed smartphones as biomedical analyzers. An example is the device proposed by Guo [129]. He presented a miniaturized POC electrochemical analyzer based on a smartphone that used an electrochemical test strip for measuring uric acid in whole blood. The disposable test strip is placed into a slot placed at the edge of the phone, which connected the sensor with the amperometric module embedded into the smartphone. A picture of the proposed device is depicted in Figure 1.21.

Ji and his group also developed an electrochemical detection system based on a smartphone to perform CVs [114]. The system combines three electrodes, an electrochemical detector, and a smartphone (Figure 1.22). It had a potentiostat that generated the stimuli signals and performed the CV measurements. A Bluetooth module transmitted the result and the commands to control the device between the detector and the smartphone. Besides, an application controlled the system and displayed the data.

It is envisaged smartphone-based sensing devices will be a powerful tool for the next-generation technology for detecting and monitoring cancer biomarkers at early stages. An example is described by Oana Hosu et al. They designed a smartphone-based colorimetric immunosensor for the detection of

## CHAPTER 1. INTRODUCTION

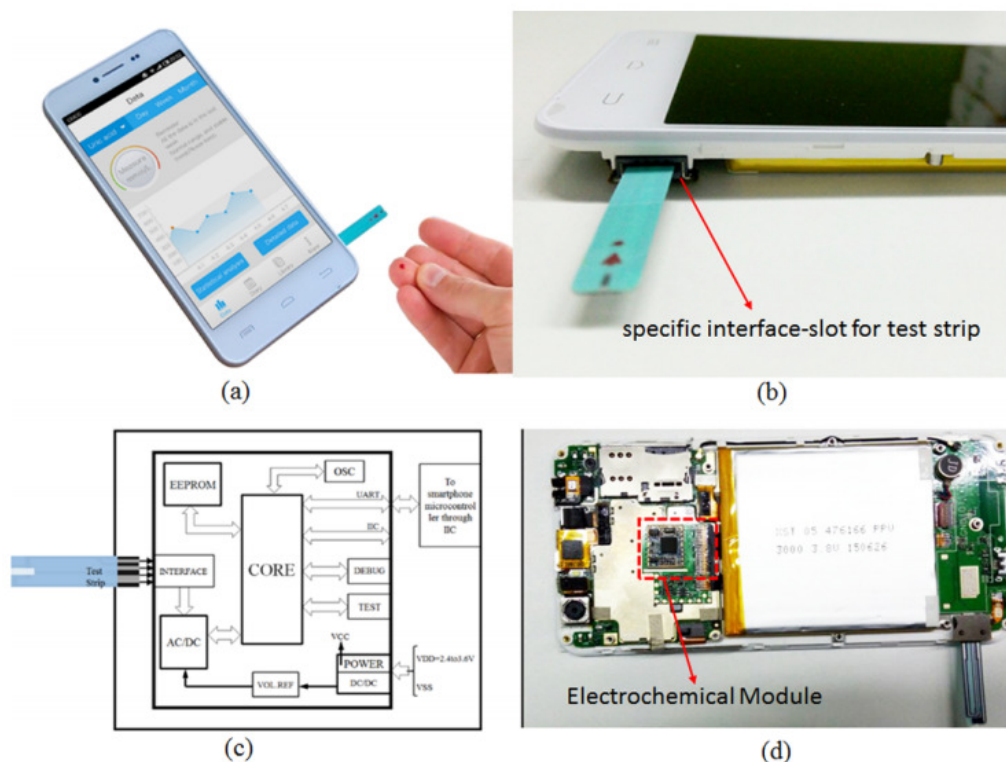


Figure 1.21: a) Photograph of the proposed device; b) Smartphone with the sensor pre-buried; c) Diagram of the electrometer; d) Capture of the electrochemical module integrated into the PCB of the smartphone. Reproduced from [129] with permission from American Chemical Society.

cancer antigen 125 [130]. In this work, the smartphone camera was integrated into a custom dark box and used as a transducer of color image acquisition and data handling. Im et al. also proposed a novel approach to molecular and cellular diagnostics based on molecular-specific microbeads that generated unique diffraction patterns imaged by smartphones [131]. The platform was used to monitor precancerous or cancerous cells in cervical specimens and also to detect human papillomavirus DNA.

### 1.2.2.3 Qualitative data obtained with ultra-low-power electronics

In most cases, FCs or other types of energy harvesting devices do not provide enough energy to supply low-power integrated circuits. For this reason, it is commonly used ultra-low consumption circuits. Most of these systems

## CHAPTER 1. INTRODUCTION

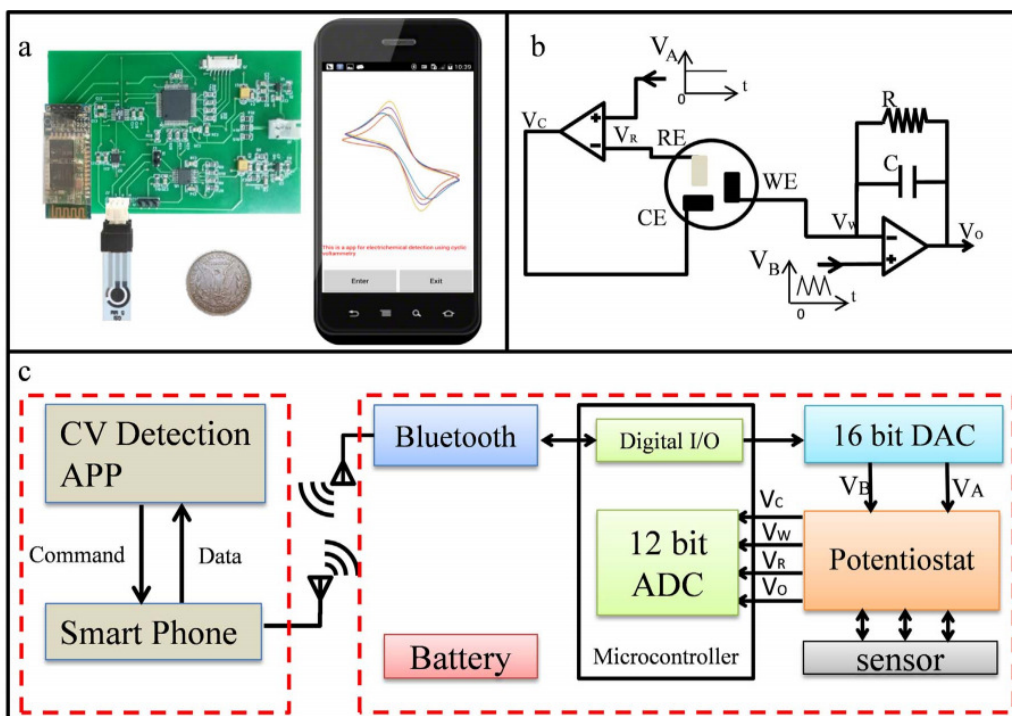


Figure 1.22: a) Photograph of the hand-held detector. b) Schematic of the potentiostat based on a transimpedance amplifier. c) Block diagram of the smartphone-based CV system. Reproduced from Ref. [114] with permission from Biosensors and Bioelectronics Journal.

use passive components, such as resistors and capacitors, and semiconductors such as MOSFETs and diodes, to process the signal and display a qualitative result.

An example of a device with a qualitative representation is described in [132]. The authors proposed a patch composed of a paper battery whose output was fully dependent on the conductivity of the liquid sample, in this case sweat, enabling a sensor and battery to be merged in a single element. They used a very simple circuit to discern between two states, a healthy condition, and a non-healthy condition. The circuit combined discrete electronic components and two electrochromic displays to show the result, one for test and another for control. The control display ensured that the device worked properly, while the test display was only activated when the battery reached a voltage that is equal to or above a determined threshold. This display was controlled by an n-channel MOS transistor that acted as a switch when a voltage higher than 1.2 V was applied to its gate. Also, two diodes

## CHAPTER 1. INTRODUCTION

prevented the power discharge when the battery ceases to operate.

The authors of this thesis proposed a self-powered event detection platform to monitor biological agents in which a BFC is used as a power source and a sensor [118]. The self-powered system used the energy provided by the BFC to monitor the concentration of the sample and to supply the low-power electronics unit. A discrete high-side current sensing circuit monitored the current proportional to the sample concentration and provided to its output a voltage proportional to this current. An event detector circuit was used to display the level concentration. It combined three comparators based on operational amplifier, and a voltage reference integrated circuit to set the voltage threshold of the comparator. Moreover, a resistor network was used to adjust the three concentration levels to detect. The comparator output changes to a high level when the reference voltage reaches a voltage determined by the resistors network. Furthermore, LEDs or an electrochromic display could be connected at the output of the comparator to show the concentration's level of the sample. Electrochromic displays are composed of organic or inorganic substances that change color when charged with electricity and are activated with voltages below 1 V. Due to its ultra-low-power consumption and simplicity, they are used in different types of applications [133].

### 1.2.3 Power Management: battery and self-powered solutions

A key issue of the design of POC systems is how to power the system. Most of the POC diagnostics systems require a fluid manipulation that can be controlled by microfluidic components, such as micropumps, microvalves, and microseparators, among others [28, 29]. These microfluidic components require significant external energy to apply external forces. For example, close or open a valve can demand power from tens of milliwatts to several Watts, demanding high voltages and currents (around 150 V and 1A) [134]. Therefore, these platforms require domestic electric power, only available in developed countries. For this reason, passive actuation techniques are more suitable for POC diagnostics because no external energy is required, although they must generate more stable external forces [135, 136].

Optical techniques are widespread in POC fields due to their low-power consumption. On one side, colorimetric approaches do not require external power systems for operation [137]. While, laser and light-emitting diode (LED) light sources are commonly used in POC diagnostics devices because

## CHAPTER 1. INTRODUCTION

of their capability of integration into small-scale POC devices, operating into a wide range of wavelengths with power consumption in the order of milliwatts [138, 139].

Electrochemical detection techniques have traditionally received the most attention in POC testing due to the possibility to develop portable readers with low-cost and low-power [113, 140].

An ideal POC device must work independently and self-sustainable in challenging field conditions. There have proposed POC devices with external or integrated power, in which the power was obtained by the electrical grid or commercial batteries. These solutions are suitable for developed countries. Besides, innovative power supply approaches have been proposed that suggest a path to more ideal POC diagnostics whose power sources are appropriate even in resource-limited settings.

POC testing devices can be classified into three categories based on the employed power technique: (a) power-free, (b) self-powered, and (c) battery-powered POC diagnostics systems.

### 1.2.3.1 Power-free POC devices

Power-free solutions are usually colorimetric systems, which do not need an electronic circuit to read the test result. These systems are cheap, although many times their results are qualitative or do not provide numerical data and can lead to errors on the measure.

Recently, Song et al. have proposed an assay for the rapid detection of the Zika virus without the need for an external power source [141]. They used an easy-to-use POC disposable cassette that carries out all the unit operations from sample introduction to detection (Figure 1.23a).

They performed the molecular detection using a colorimetric transduction technique. The system is suitable for resource-poor settings, where there is a lack of centralized laboratory facilities and trained personnel. Castro and her group created an inexpensive and portable device for detecting anti-T.cruzi antibodies in whole blood solutions using magnetic levitating microbeads that do not require electricity [143]. In addition, they also developed a machine-vision algorithm to automatically interpret the results of the tests from a digital image, providing a rapid, accurate, and user-friendly POC devices for Chagas disease that can be used in resource-limited settings.

## CHAPTER 1. INTRODUCTION

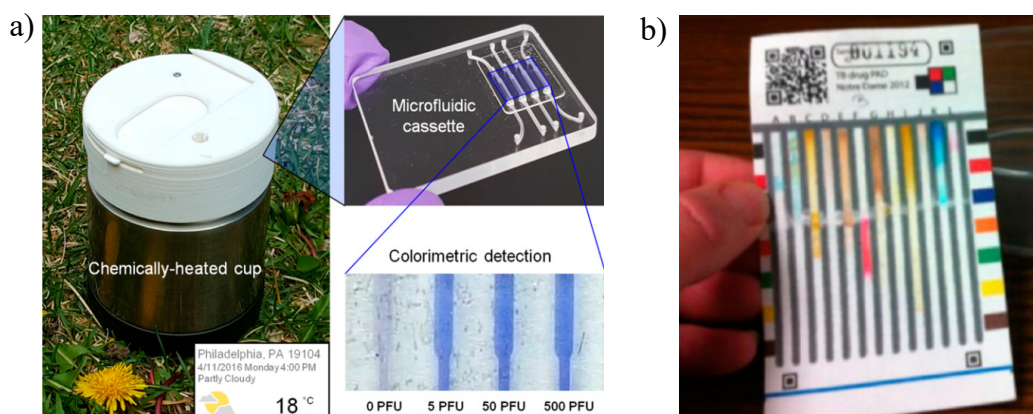


Figure 1.23: a) Capture of the chemically heated cup for POC diagnostics of the Zika virus and microfluidic cassette for nucleic acid extraction. b) Capture of the PAD colorimetric testing in which the sample was “swiped” to deposit material for analysis in several lanes. Reprinted from [141] and [142] with all permissions.

Innovative paper-based techniques for power-free POC testing have also been proposed. Weaver et al. described a test-card assay formed with different reagents deposited on each lane, separated by hydrophobic barriers [142]. The reactions in each lane on the paper leaves a “color bar code” dependent on the concentration, which can be visually analyzed for detecting active pharmaceutical substances, such as HIV DNA or blood hemoglobin (Figure 1.23b).

### 1.2.3.2 Battery-powered POC devices

Power-free POC diagnostics systems can flow liquids through capillary forces with no need power sources or moving parts. However, highly-sensitive and accurate sensors, such as chemical or biomolecular diagnostic, require external readout instrumentation for display a numerical and quantitative result [144, 145]. These applications need external power sources that must be miniaturized and integrated for developing handheld and portable devices [146].

In the state-of-art, there were proposed some POC platforms powered by commercial batteries. Ahrberg and his group reported a portable battery-powered system able to perform real-time polymerase chain reaction (PCR) [147]. It was powered by an external 12-V battery, and it was able to measure four PCRs simultaneously in less than 35 minutes. The system was validated with the Ebola virus [148], performing quantitative analysis to de-

## CHAPTER 1. INTRODUCTION

termine viral load and the effectiveness of the Ebola treatment. Dou et al. developed an analytical POC platform composed of a spectrophotometric system and a microfluidic chip, which was powered by a 9 V-battery [149]. The system was validated using methylene blue as a model analyte and compared with a commercial spectrophotometric system. Another example of a battery-powered POC device was proposed by Shu and his group [150]. They developed a portable flow genetic analysis system for real-time quantification of nucleic acids. The handheld molecular diagnostic platform, powered by lithium batteries, enabled a visual detection of more than 10 DNA copies in 15 minutes and allowed an accurate DNA quantification.

### 1.2.3.3 Self-powered POC devices

POC diagnostic devices are focused for low-resource settings in which the use of commercial batteries is a solution. However, these power sources have several drawbacks, such as cost and recycling issues [151, 152].

An innovative solution to replace batteries is the use of self-powered sources that harvest energy. These technologies have been applied successfully in POC devices in which energy was harvested from the heat, chemical reactions, and vibration, among others [132, 153–155].

At present, the fast development and the improvement of low power devices allow harvesting environmental energy to power electronic devices. It is envisaged that the future of diagnostics and health monitoring will have smartphone-based systems or portable readers supplied by saliva or blood and thus, continuously monitoring human health.

Fuel cells (FCs) are electrochemical devices that continuously converts chemical energy into electricity for as long as fuel and oxidant are supplied to it. Power generation through biological fuel cells (BFC) is similar to that through conventional FC since both involve reduction-oxidation reactions. The main difference is that BFCs use organic products as fuel for power generation. Moreover, these devices can work as a power source and as a sensor because their output current is directly correlated with the concentration of fuel.

One of the primary sources of energy of the human body is glucose. Several studies have demonstrated the feasibility of glucose BFCs, a type of BFC that generates energy oxidizing glucose at the anode, and reducing oxygen at the cathode [156, 157].



## CHAPTER 1. INTRODUCTION

Furthermore, innovative self-powered FC-based systems are proposed based on glucose BFCs [158–160]. Qumrul et al. [161] developed a low-cost device able to operate with no need for external power sources. They proposed a simple electronic device that extracted the glucose level from the sample obtaining an instantaneous measurement using a digital multi-meter for signal readout. Another example is the system proposed in [156], in which the performance of a glucose BFC powering a small electronic device was demonstrated (Figure 1.24). The BFC was capable of providing open-circuit voltages of 0.735 V, and a power density of  $46.31 \mu\text{Wcm}_2$  in a glucose concentration of 3 mM, and  $169.41 \mu\text{Wcm}_2$  and 0.971 V in 20 mM concentration. The authors amplified the voltage to 1.8 V through a circuit composed of a charge pump, among other active and passive components, and energy storage elements. In order to validate the feasibility of the system, they powered a LED continuously for 14 days.

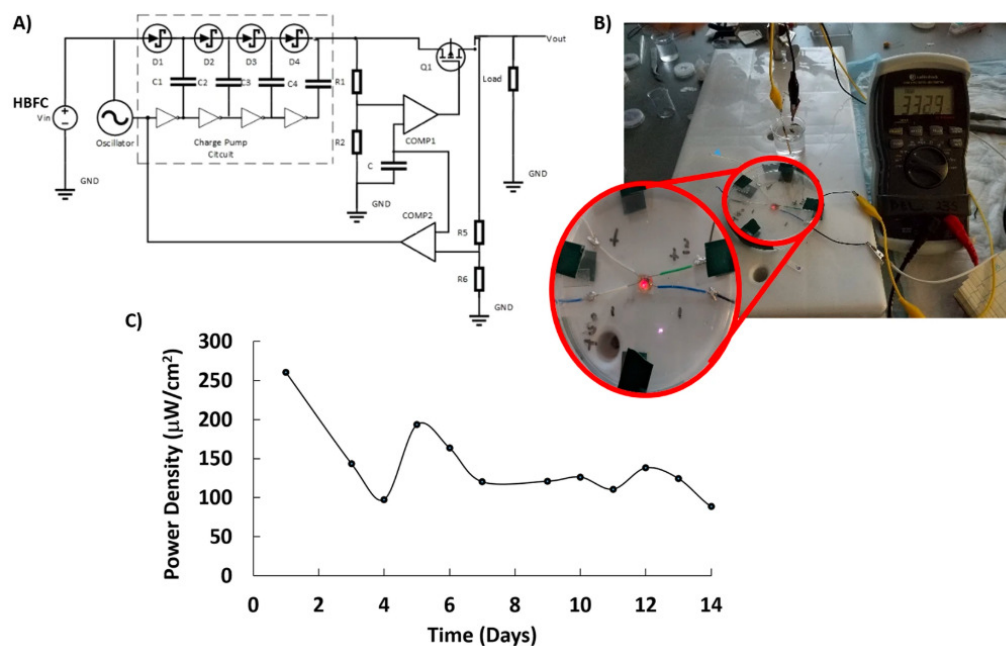


Figure 1.24: A) Schematic of the circuit formed by a charge pump based on an amplifier circuit, B) capture of the system, and (C) power curve of glucose BFC. Reprinted from [156] with permission.

The main disadvantage of *in vitro* testing based on BFCs is that it requires invasive draws. For this reason, several recent studies are focused on the design of devices based on BFC for non-invasive and wearable applications.

Recently, a paper-based self-powered sensor patch was proposed for non-

## CHAPTER 1. INTRODUCTION

invasive detection of glucose in human sweat [162]. The disposable glucose sensing device did not require external power sources nor sophisticated external transducers. However, as is depicted in Figure 1.25.a, the device needed laboratory instruments to show the glucose concentration. Another example of wearable BFC is presented in [153]. The authors designed a stretchable and flexible lactate BFC which provided an open circuit voltage of 0.74 V and a power density of  $520 \mu\text{Wcm}^2$ . The BFC voltage was boosted with a DC-DC converter to power an LED operating in pulse mode to demonstrate the potential of the system (Figure 1.25b). Ortega et al. [132] presented a self-powered skin patch used for the measurement of sweat conductivity that allows screening cystic fibrosis. The patch, composed of a sensor and a battery merged in a single element, operated with a simple electronic circuit that provides a qualitative result that can be read in an electrochromic display. The platform consisted of two output indicators, control, and test, which indicated a healthy condition and a non-healthy condition.

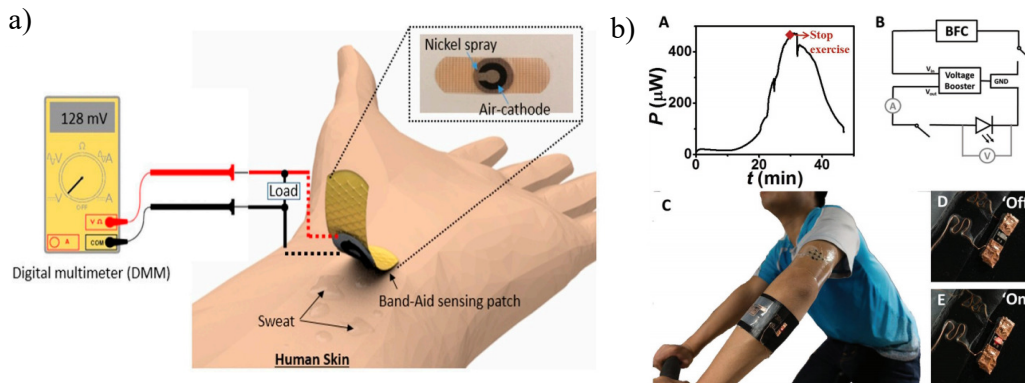


Figure 1.25: a) Diagram of the self-powered, wearable, and disposable patch for monitoring glucose in sweat to detect hypoglycemia-related to the exercise. b) Power output profile during an on-body experiment, schematics used by the authors to power an LED with the BFC, capture of experiment setup, and the LED switched on and off. Reprinted from [162] and [153] with permission.

## 1.3 Objectives

Point-of-Care (POC) testing is an emerging technology applicable to an immense variety of applications, which demands constant technology improvement. It is of great importance to developing POC systems capable of operating in biomedical environments in order to be able to perform rapid tests on the patient's side, thus increasing early diagnosis. This fact raises the need to research and develop compact and low-power consumption electronic circuits, with acceptable levels of sensitivity and accuracy that can be integrated into portable and low-cost devices.

Typically, POC portable systems use batteries as an electrical power source that must be periodically replaced or recharged and have limited autonomy. This is a simple task in developed regions, although it is challenging in low-resource settings, which is where these portable diagnostic devices are most needed. Biological fuel cells (FC) are electrochemical devices that convert chemical energy into electricity, using organic products as fuel. These devices generate an electric current proportional to the concentration of the organic product used. This electric current can be used both to detect the concentration of the organic product used and to power electronic systems.

This doctoral dissertation presents the development of Plug-and-Power electronic readers (e-readers) for electrochemical detections with intelligence for displaying quantitative results, and the demonstration of their possibilities in POC biomedical applications. The research looks for developing miniaturized, portable, and low-power consumption electronic POC solutions capable of being powered from a battery or a USB port or being self-powered devices by using alternatives power sources such as fuel cells.

The main objectives of this doctoral dissertation consist of:

- Design electronic instrumentation circuits able to trigger the electrochemical reaction and measure the sensor response. These low-power electronic systems must be able to adapt to different situations and acquire a wide range of current values.
- Design low-power electronic circuits for measuring low-current signals and extracting the energy provided by biological FCs. The circuits must extract the power of the FC at the same time as they measured the concentration of the biological product.

## CHAPTER 1. INTRODUCTION

- Design electronic circuits to acquire and process the sensor signals and provide a qualitative result.
- Design electronic solutions of different levels of complexity that enable display analytical results in a clear and reliable way.
- Develop smart, easy-to-use, and plug-and-play electronic systems that require minimal user interaction.
- Develop easy-friendly graphical user interfaces that can be used by individuals with minimal prior training.
- Integrate electronics modules, both hardware and software level, into compact and portable devices applicable to POC environments.

## 1.4 Contribution of this thesis

Diagnostic tests are conventionally analyzed with large bench-top analyzers at central laboratories. Usually, this involves that patients must wait over long periods before receiving their results. This situation is compounded in rural areas and developing countries, where there is a shortage of trained personnel and basic diagnostic equipment [41, 48].

POC testing allows monitoring health conditions and obtain rapid results near the patient. They allow reducing medical costs and controlling infectious outbreaks without the need for dedicated laboratory equipment. Moreover, POC diagnostics removes the constraints of requiring large healthcare infrastructures, complex medical equipment, and well-trained technicians. This emerging technology is applicable to a wide variety of applications [63]. Like other technology, POCs are constantly improving thanks to different advances in electronics technologies, and the development of new applications.

In recent years, the interest to develop POC testing devices has increased, as has been pointed out in the Introduction chapter of this thesis. According to the Dimensions.ai website, over the past 5 years, more than 1.7 million articles, and more than 325,000 patents on POC testing have been published. There is a growing need to develop low-cost, portable, easy-to-use POC devices to diagnose diseases at an early stage.

The pandemic caused by the 2019-novel Coronavirus also showed the importance of POC devices. POC tests were crucial due to the manifestation of the virus infection was highly nonspecific. These diagnostics systems helped to confirm suspected cases, screen patients, and conduct virus surveillance to control the outbreak [56–58].

The blood glucose detector is the quintessential POC device, which is based on the concept of lateral flow immunoassay [24]. This device detects the presence of a certain analyte, in this case, glucose. However, lateral flow is not always a valid technique. There is a multitude of analytes that require other methods based on more complex electronic systems capable of supplying the necessary energy to trigger a reaction, detect the sensor response, and show the result to the user. For this reason, it is needed high-performance and miniaturized electronic circuits integrable into POC systems.

Usually, portable POC systems use batteries as a source of electrical power, which must be replaced or recharged periodically and have limited

## CHAPTER 1. INTRODUCTION

autonomy. This simple task is a challenge in low-resource settings, that is where these systems are most needed.

The main objective of this doctoral dissertation is the development of Plug-and-Power electronic readers (e-readers) for electrochemical detections and the demonstration of their possibilities in biomedical studies as POC testing. These systems can be powered from a USB port or battery or must be self-powered systems, which extracts the energy from alternatives power sources such as fuel cells.

Electrochemical detection approaches proposed in this thesis can acquire low-current signals, process them, and display a quantitative result, consuming minimum power. Thanks to their reduced energy consumption, it was possible to develop self-powered platforms able to operate only with the energy extracted from the biological sample. Proposed platforms can also be powered through external devices, such as USB ports and rechargeable or disposable batteries. These devices are easy-to-use and plug-and-play, and allow those unskilled individuals to carry out tests after minimal training. Due to their user-friendly interface, results are clear and easy to understand. The solutions proposed in this doctoral dissertation enhance POC testing, whose premises are laboratory decentralization, personalized medicine, rapid diagnosis, and patient care improvement [16].

The introductory chapter of this thesis analyzes the state-of-the art of POC diagnostics with the aim to study their strengths and weakness and determine the necessary improvements. An overview of the impact of POC testing on healthcare in low- and middle-income countries is given, focusing on barriers in regulatory and policy guidelines, the geographical location, characteristics of health infrastructure system, and supply chain management. Furthermore, a classification of POC diagnostic testing is done according to the biosensor used, highlighting sensors and detection techniques based on electrochemical sensors. The development of technologies and devices is entailed to the integration of electronic technologies and biosensors. Furthermore, the introductory chapter provides an overview of possible architectures to develop low-power and portable POC technologies for electrochemical detections, analyzing the state-of-the-art and, describing different solutions.

The third chapter shows the results of this doctoral dissertation, which is presented as an article compendium. According to the Dimensions.ai website, in the last 5 years, more than 13,000 articles and 4,000 patents have been published about low-power and portable POC systems for electrochemical detections.

## CHAPTER 1. INTRODUCTION

The publications are presented in the thesis in chronological order. However, the studies were carried out in reverse sequence to the publication of the investigations. The first developments were discrete USB- and battery-powered electronics. These complex electronic systems led to simplified devices that prompted the development of self-powered platforms. Although, due to the strategic interests of the research groups, the publications were published in reverse chronological order.

The publication entitled “‘Plug-and-Power’ Point-of-Care diagnostics: A novel approach for self-powered electronic reader-based portable analytical devices” was published in the *Biosensors and bioelectronics* journal of the Elsevier editorial. All categories of the journal are ranked at first quartile (Q1). Moreover, it has a CiteScore of 17.6 and an Impact Factor of 10.257 in 2019. The other two publications that make up this thesis were published in the *Sensors* journal (MDPI editorial). *Sensors* is an Open Source journal ranked at first quartile (Q1) in the Instrumentation category. It has a CiteScore of 5.0 and an Impact Factor of 3.275 in 2019. The manuscript entitled “Self-Powered Portable Electronic Reader for Point-of-Care Amperometric Measurements” has more than 775 abstract-views and 750 full-text views, and the article “Competitive USB-Powered Hand-Held Potentiostat for POC Applications: An HRP Detection Case” has more than 600 abstract-views and 785 full-text views.

One of the challenges of this thesis is to develop self-powered and easy-to-use electrochemical detection systems capable of displaying qualitative data and measuring wide current ranges with high resolution. The article entitled “‘Plug-and-Power’ Point-of-Care diagnostics: A novel approach for self-powered electronic reader-based portable analytical devices” described an innovative portable POC device able to provide a quantitative result of glucose concentration of a sample. The proposed system combines a plug-and-play reader and a disposable paper sensor. The battery-less electronic reader extracts the energy from the disposable unit, acquires the signal, processes it, and shows the glucose concentration on a display. Due to the low-power consumption of the instrumentation and processing circuits, the whole electronic system can operate only with the energy extracted from the disposable element, based on two elements that acts as a sensor and the power source. Furthermore, the process of energy collection, measurement, and data processing is done by the device, without the need for any external action. The smart device minimizes the user interaction, which only must deposit the sample on the strip and wait a few seconds to see the test result. Moreover, the high-performance device provides accurate and high-resolution

## CHAPTER 1. INTRODUCTION

results. It can measure currents of up to  $30 \mu\text{A}$  and have a resolution of 13 nA with an error lower than 1.8 %.

The second publication entitled “Self-Powered Portable Electronic Reader for Point-of-Care Amperometric Measurements” presents in detail the conception, design, implementation, and characterization of the electronic circuits that composed the battery-less electronic reader. This versatile concept detects amperometrically a wide variety of analytes, process, and display the results without the need for commercial batteries since the energy to carry out the test is extracted from a Fuel Cell (FC). The e-reader was validated following different approaches, using FCs as a power element and as a dual powering and sensing element. The device was tested with glucose, urine, methanol, and ethanol FCs and sensors in order to show the adaptability of the system to different scenarios, validating the possibility of extrapolated the system to a wide variety of fields beyond clinical diagnostics, such as veterinary or environmental fields.

The third article presents the study entitled ”Competitive USB-Powered Hand-Held Potentiostat for POC Applications: An HRP Detection Case”, in which the AmpStat system was developed. It is a low-cost, miniaturized, and customizable USB-powered potentiostat for amperometric detections. The portable device combines a connector that houses the disposable amperometric sensor, a full-custom electronic board for signal acquisition, and software called AmpView, which represents and saves the results. The customizable device was designed to measured currents up to  $11.2 \mu\text{A}$ , although it can be easily adapted to detect currents up to 3 mA. The efficacy of the AmpStat prototype was evaluated by measuring amperometrically horseradish peroxidase in a concentration range from  $0.01 \text{ ng}\cdot\text{mL}^{-1}$  to  $1 \mu\text{g}\cdot\text{mL}^{-1}$ . In this study, the performance of the device was compared against three commercial potentiostats. They were tested in parallel with the proposed device, obtaining the limit of detection, the limit of quantification, and the sensitivity of the four equipment. The developed potentiostat provided a reasonably accurate detection with results comparable to those obtained using three commercial systems, which were significantly more expensive. As proof of concept, the system was validated by detecting horseradish peroxidase samples, although it could be easily extended its scope and measure other types of analytes or biological matrices. It has been powered externally through the USB port. However, in the future, the device will be upgraded and adapted to be self-powered and send the data through a wireless module to a computer or smartphone.



## CHAPTER 1. INTRODUCTION

In the context of this thesis, it has been carried out other researches, whose results are presented in the Annexes section.

Some of these studies have been presented in conferences, such as ultra-low-power instrumentation circuits applicable to self-powered systems, and electronic instrumentation circuits for different biosensing applications.

Within the framework of this thesis, I have also participated in the design of the electronic instrumentation of the patent EP19382604.7 entitled “Self-powered system and method for power extraction and measurement of energy-generator units”.

Furthermore, a portable biosensing system was developed to investigate Dystonia disorder with the collaboration of the members of Reilly lab, within the framework of a predoctoral stay at the Trinity Center for Biomedical Engineering and Trinity College Institute of Neuroscience of the Trinity College of Dublin (Ireland). Dystonia is a neurological movement disorder that causes involuntary muscle contractions that produce abnormal movements or postures, sometimes painful. Temporal discrimination is the shortest time interval at which a subject can discriminate two sequential stimuli as being asynchronous. Some studies associate cervical dystonia with abnormal temporal discrimination. During the stay in Dublin, it was developed a multimodal electronic platform and custom software for measuring temporal discrimination intervals through visual and tactile stimuli, and a combination of both. This portable device is powered through a USB port, and it is connected to an Android smartphone through Bluetooth Low Energy communication module. With the custom App developed for this device, the user can control the stimuli, register the data, and send them via email, with the advantage that it can be used by unskilled people after minimal training thanks to its user-friendly interface.

Finally, in the fifth and sixth chapters, it is summarized the results, and it is presented the researches conclusions, recommending future developments to create the next generation of low-power and self-powered POC devices.

# Chapter 2

## Results

### 2.1 Publication 1

#### **‘Plug-and-Power’ Point-of-Care diagnostics: A novel approach for self-powered electronic reader-based portable analytical devices**

*By*

**‘Yaiza Montes-Cebrián<sup>a\*</sup>**, Lorena del Torno-de Román<sup>b</sup>, Albert Álvarez-Carulla<sup>a</sup>, Jordi Colomer-Farrarons<sup>a</sup>, Shelley D. Minter<sup>c</sup>, Neus Sabaté<sup>b,d,e</sup>, Pere Ll. Miribel-Catalá<sup>a</sup>, Juan Pablo Esquivel<sup>b</sup>.

<sup>a</sup> *Discrete-to-Integrated (D2In) Research Group, Department of Electronic and Biomedical Engineering, Faculty of Physics, University of Barcelona (UB), 1st Martí i Franqués St., 08028 Barcelona, Spain*

<sup>b</sup> *Instituto de Microelectrónica de Barcelona IMB-CNM (CSIC), C/ del Tilers, Campus Universitat Autònoma de Barcelona (UAB), 08193 Bellaterra, Barcelona, Spain*

<sup>c</sup> *Department of Chemistry, University of Utah, 315 S 1400 E Room 2020, Salt Lake City, UT 84112, USA*

<sup>d</sup> *Catalan Institution for Research and Advanced Studies (ICREA), Passeig Lluís Companys 23, 08010 Barcelona, Spain*

<sup>e</sup> *Fuelium, Av. De Can Domenech – Edifici Eureka, Campus de la UAB, 08193 Bellaterra, Barcelona, Spain*

*Published in*

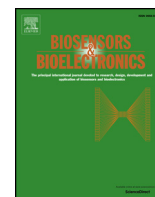
**‘Biosensors and Bioelectronics 118 (2018) 88-96**





Contents lists available at ScienceDirect

## Biosensors and Bioelectronics

journal homepage: [www.elsevier.com/locate/bios](http://www.elsevier.com/locate/bios)

## ‘Plug-and-Power’ Point-of-Care diagnostics: A novel approach for self-powered electronic reader-based portable analytical devices

Yaiza Montes-Cebrián<sup>a,\*</sup>, Lorena del Torno-de Román<sup>b</sup>, Albert Álvarez-Carulla<sup>a</sup>,  
Jordi Colomer-Farrarons<sup>a</sup>, Shelley D. Minteer<sup>c</sup>, Neus Sabatè<sup>b,d,e</sup>, Pere Ll. Miribel-Català<sup>a</sup>,  
Juan Pablo Esquivel<sup>b</sup>

<sup>a</sup> Discrete-to-Integrated (D2In) Research Group, Department of Electronic and Biomedical Engineering, Faculty of Physics, University of Barcelona (UB), 1st Martí i Franquès St., 08028 Barcelona, Spain

<sup>b</sup> Institut de Microelectrònica de Barcelona IMB-CNM (CSIC), C/ del Tíllers, Campus Universitat Autònoma de Barcelona (UAB), 08193 Bellaterra, Barcelona, Spain

<sup>c</sup> Department of Chemistry, University of Utah, 315 S 1400 E Room 2020, Salt Lake City, UT 84112, USA

<sup>d</sup> Catalan Institution for Research and Advanced Studies (ICREA), Passeig Luís Companys 23, 08010 Barcelona, Spain

<sup>e</sup> Fuelium, Av. De Can Domenech – Edifici Eureka, Campus de la UAB, 08193 Bellaterra, Barcelona, Spain



## ARTICLE INFO

## Keywords:

Plug-and-Power  
Self-powered  
Paper-based  
Glucometer  
Low-power electronics

## ABSTRACT

This paper presents an innovative approach in the portable Point-of-Care diagnostics field, the Plug-and-Power concept. In this new disposable sensor and plug-and-play reader paradigm, the energy required to perform a measurement is always available within the disposable test component. The reader unit contains all the required electronic modules to run the test, process data and display the result, but does not include any battery or power source. Instead, the disposable part acts as both the sensor and the power source. Additionally, this approach provides environmental benefits related to battery usage and disposal, as the paper-based power source has non-toxic redox chemistry that makes it eco-friendly and safe to follow the same waste stream as disposable test strips. The feasibility of this Plug-and-Power approach is demonstrated in this work with the development of a self-powered portable glucometer consisting of two parts: a test strip including a paper-based power source and a paper-based biofuel cell as a glucose sensor; and an application-specific battery-less electronic reader designed to extract the energy from the test strip, process the signal provided and show the glucose concentration on a display. The device was tested with human serum samples with glucose concentrations between 5 and 30 mM, providing quantitative results in good agreement with commercial measuring instruments. The advantages of the present approach can be extended to any kind of biosensors measuring different analytes and biological matrices, and in this way, strengthen the goals of Point-of-Care diagnostics towards laboratory decentralization, personalized medicine and improving patient compliance.

## 1. Introduction

Point of Care (POC) diagnostics have been proving their benefits in public global health over centralized laboratory diagnostics as they remove the constraints of requiring large healthcare infrastructures, complex medical equipment and well-trained technicians. POC devices allow monitoring of health conditions, reducing medical costs, as well as controlling infectious outbreaks, without the need of dedicated laboratory equipment. In addition, these devices offer the advantages of rapid results and patient proximity (Chan et al., 2017; Choi, 2016;

Drain et al., 2014; Wang et al., 2016a; Zarei, 2017; Yager et al., 2006). The development of portable POC diagnostics pursues the characteristics defined by the World Health Organization in the acronym ASSURED (affordable, sensitive, specific, user-friendly, rapid and robust, equipment free, and deliverable to users) to provide suitable solutions to even the lowest-resource global health settings (Fu et al., 2011). Despite the many advances in the field, equipment-free POC diagnostic devices still face important challenges related to reliability. The use of an electronic reader allows overcoming this aspect, as it provides an unambiguous qualitative/quantitative result of an assay and can

\* Corresponding author.

E-mail addresses: [ymontes@ub.edu](mailto:ymontes@ub.edu) (Y. Montes-Cebrián), [lorena.deltorno@imb-cnm.csic.es](mailto:lorena.deltorno@imb-cnm.csic.es) (L. del Torno-de Román), [albertalvarez@ub.edu](mailto:albertalvarez@ub.edu) (A. Álvarez-Carulla), [jcolomerf@ub.edu](mailto:jcolomerf@ub.edu) (J. Colomer-Farrarons), [minteer@chem.utah.edu](mailto:minteer@chem.utah.edu) (S.D. Minteer), [nsabate@fuelium.tech](mailto:nsabate@fuelium.tech) (N. Sabatè), [peremiribelcatala@ub.edu](mailto:peremiribelcatala@ub.edu) (P.L. Miribel-Català), [juanpablo.esquivel@csic.es](mailto:juanpablo.esquivel@csic.es) (J.P. Esquivel).

<https://doi.org/10.1016/j.bios.2018.07.034>

Received 3 May 2018; Received in revised form 13 July 2018; Accepted 16 July 2018

Available online 18 July 2018

0956-5663/ © 2018 Elsevier B.V. All rights reserved.

improve the sensitivity and the limit of detection.

The reader-disposable approach is predominantly used in the POC devices commercially available, and it is still the one mostly followed by initiatives undergoing research and development phases (Chin et al., 2012; Gervais et al., 2011; Zarei, 2017). These devices consist on a reusable electronic reader unit and a disposable part in the form of a strip, cartridge or card. The disposable test strip is used to collect the sample and transport it to the biosensor where the measurement is performed. After a single use, this strip is discarded avoiding cross-contamination. Depending on the detection principle and sample matrix to be detected, portable readers may also perform a variety of functions including for example sample pretreatment, hydraulic controls, heating, timing, light sources, photodetectors, electrochemical instrumentation, Radio frequency communications and, in most cases, displays as the interface between the device and the user to set up the test and show the result.

An example is the system presented by (Cruz et al., 2014). The authors present an approach capable of performing cyclic voltammetry for electrochemical immunosensing of cortisol. In contrast to the device presented here, the reported approach is not self-powered and, moreover, it does not have a custom-made design for the application since it uses a commercial miniaturized potentiostat on an evaluation board. However, the developed prototype is low-cost, portable and the analog front-end is based on a transimpedance amplifier (TIA).

To perform these functions, portable readers require a source of electrical power. This need has been fulfilled with either primary or secondary batteries. Regardless of their autonomy, batteries must be replaced or recharged periodically to maintain the device operation. This may seem a simple task in developed regions with reliable electric power grids and ubiquitous battery supplies. However, it can be quite challenging in low-resource settings, which is precisely where this kind of portable diagnostic devices are needed the most. Additionally, uncontrolled disposal of used batteries is becoming a severe problem in such regions of the world, as there is not only a lack of environmental regulations but also proper recycling facilities (Widmer et al., 2005; Larcher and Tarascon, 2015; Ongondo et al., 2011).

This paper presents a novel solution to the power requirements in the portable diagnostics field, the Plug-and-Power concept. We propose a plug-and-play reader-disposable device in which the energy required to perform a single test is always available within the disposable test component. In this case, the reader unit contains all the required electronic systems to run the test, including a display to visualize the result, but does not include any battery or power source. Instead, the disposable part acts as both the sensor and the power source. Additionally, this approach provides environmental benefits related to battery usage and disposal. The paper-based power source used for this approach has non-toxic redox chemistry that makes it eco-friendly and safe to follow the same waste stream as the disposable test strip or cartridge, including incineration, a typical outcome of those components that have been in contact with biological samples. The operation of this device, from the user perspective, is the same as for a conventional device, with the added advantage of not worrying about recharging it or where to recycle the used batteries. This approach strengthens the goals of Point-of-Care diagnostics towards laboratory decentralization, personalized medicine and improving patient compliance.

The applicability of this novel approach is demonstrated with the development of a self-powered portable blood glucometer, one of the Point-Of-Care applications that is already well-established in the market. Although many methods of glucose monitoring have been proposed (Fischer et al., 2016; Kulkarni and Slaughter, 2017; Lee et al., 2017; Narvaez Villarrubia et al., 2016; Slaughter and Kulkarni, 2016), the most widely used by both patients and healthcare professionals are the portable blood glucometers, as they are small, inexpensive, rapid and user-friendly (Wang et al., 2016a; Wang et al., 2016b; Zarei, 2017). These advantages are maintained in the presented Plug-and-Power

prototype, which consists of two parts: a test strip including a paper-based power source and a paper-based bio-fuel cell as the glucose sensor; and an application-specific battery-less electronic reader designed to extract the energy from the test strip, sample and process the signal provided by it and display the glucose concentration in the sample on a digital display.

## 2. Device concept and operation

The design and operation of the presented device resembles that of a typical commercial handheld glucometer, consisting of two parts: a disposable test strip and an electronic reader. However, this device introduces a new approach based on two main features: 1) the disposable test strip generates the electrical power used by the electronic reader to perform a measurement, and 2) the glucose concentration is measured by the reader from the output signal of a bio fuel cell, rather than using a classical solution based on a three-electrode configuration electrochemical cell.

The whole system is compact, lightweight and portable. The battery-less electronic reader has a size of  $85.0 \times 42.0 \times 21.0$  mm, while the disposable test strip has a size of  $20.0 \times 25.0 \times 1.8$  mm. From a user point of view, the device is easy to operate, as shown in Fig. 1. First, the strip is introduced in the reader. Then, the user adds the sample to the inlet of the test strip. Finally, the user can read the result of the test in the display of the smart electronic reader. After the measurement, the test strip can be safely discarded, while the electronic reader can be reused indefinitely for subsequent measurements.

The internal operation of the device can also be seen in Fig. 1. Once the liquid sample is added to the test strip, it flows by capillary action through a piece of paper. The sample diverges towards both ends of the paper, reaching on one side the power source, and on the other side, the sensor. The liquid activates the power source and the produced energy wakes up the electronic circuit in the reader. Then, the electronics regulate the power to a suitable working voltage of up to 3V for the instrumentation. Afterwards, the circuit performs an amperometric glucose measurement using the sensor. The signal measured from the sensor is converted and processed to, finally, show on a display the quantitative result of glucose concentration contained in the sample.

### 2.1. Paper-based test strip

The disposable test strip is composed by two main components, a paper-based power source and a paper-based bio fuel cell acting as a glucose sensor. The components share a single paper strip of  $5 \times 20$  mm that receives the sample in its middle zone and diverges it towards both ends. Fig. 2a shows a picture of the disposable test strip and Fig. 2b depicts an exploded view of its main components.

The paper-based power source has been customized by Fuelium Company for this application based on one of their batteries models LF55. This paper-based power source is composed of a paper membrane placed in contact with two electrodes. The proprietary electrode technology contains no heavy metals nor other toxic components, so it does not require special disposal considerations after its use. The batteries are only activated upon addition of an aqueous sample and provide a steady power output after being activated by either deionized water (D.I.) water or any physiological fluid such as plasma, serum, saliva, sweat or urine. Since these batteries only start their operation after activation with the liquid sample, they do not suffer from self-discharge during storage so their shelf life complies with the requirements of diagnostics test kits. For this application, the electrodes have been placed on top and bottom sides of a paper strip and the power source has been adjusted to provide an output voltage of 1.5 V and a minimum power of 10 mW for at least 20 min after being activated with a serum sample with a minimum volume of 12.5  $\mu$ L.

Instead of using a sensor based on a typical three-electrode configuration electrochemical cell, the glucose concentration is measured

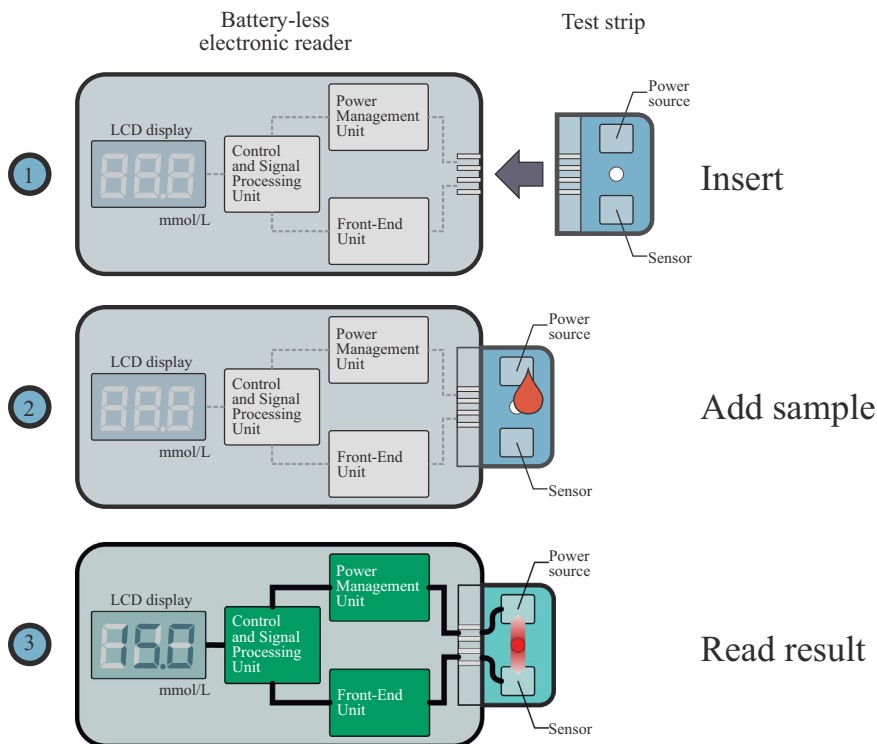


Fig. 1. Operation of Plug-and-Power Point-of-Care diagnostics device.

from the output signal of a paper-based enzymatic fuel cell. The device is composed of a glucose dehydrogenase (GDH) anode and a bilirubin oxidase (BOX) cathode placed on both sides of the paper strip. The fuel cell provides a response in power output that is proportional to the glucose concentration in the sample. This sensing method based in fuel cells response is used, for example, in many commercial breath alcoholmeters, known as breathalysers. It is a well-established and proven technique that is endorsed by industry and law-enforcement agencies worldwide (Leonard, 2012; Noordzij, 1975). In this case, the device performs a chronoamperometric measurement, subjecting the fuel cell to a fixed voltage while recording the produced current. All the electrodes are connected to silver tracks ink-jet printed on a plastic film.

The disposable strip components are assembled on top of an acrylic substrate to provide mechanical robustness.

2.2. Battery-less electronic reader

The electronic reader was conceived considering the particular features of this application. It was designed to operate with the voltage and power ranges provided by the paper-based power source and ensures robustness and portability. The block diagram of the electronic reader is depicted in Fig. 3. The disposable test strip provides the power that must be managed by the reader, and the signal to generate the glucose measurement.

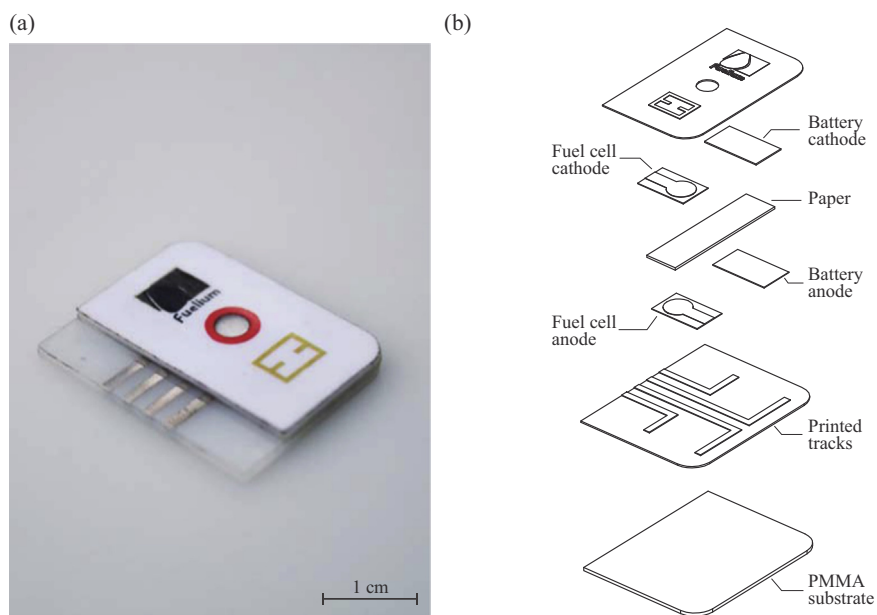


Fig. 2. a) Picture of paper-based test strip. b) Exploded view of its main components.

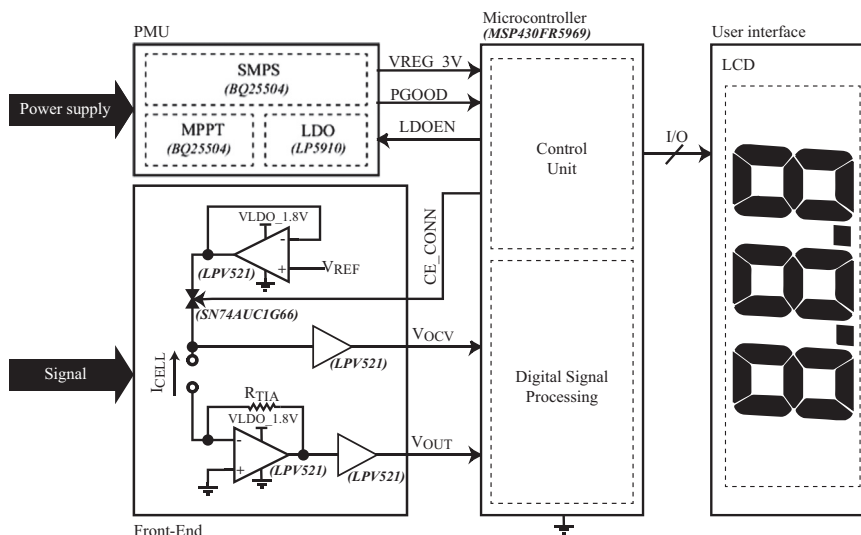


Fig. 3. Circuit of the battery-less electronic reader system.

The power supplied by the test strip goes to the Power Management Unit (PMU), where it is managed, and the control signals and voltage supplies of the system are generated. Meanwhile, the measurement signal, proportional to the concentration of glucose, is sent to the Front-End (FE) where the measurement is performed. Finally, the Control and Processing Unit (CPU), converts and processes the received information and sends it to a display, where the measurement result is shown.

### 2.2.1. Power management unit

The PMU is responsible for extracting and managing the available energy from the power source and offering a regulated output voltage in order to supply the different modules in the system. The PMU has been designed to work with the power provided by the disposable paper-based power source. In order to provide the necessary voltage to supply the components, a boost DC/DC converter in a cascade with a Low-Dropout (LDO) linear regulator are used. The first one boosts the voltage provided by the power source to 3.0 V (VREG\_3V) to supply power to both the control and processing unit and the screen used to display the result. Meanwhile, the LDO provides a very stable 1.8 V (VLD0\_1.8 V) regulated voltage with high noise rejection (Fig. 3). The 1.8 V is used to supply the analog block composed by the front-end module, which needs a very stable and well-regulated voltage supply with high noise rejection to avoid the effect of the inherent switching noise at the output of the boost converter and the effect of transient voltage variations at the power supply. The regulated voltage levels were selected in order to be able to supply common Components off-the-shelf (COTS) parts, where 3.0 V is a typical voltage supply for digital parts (as microcontrollers or Analog-to-Digital Converters (ADC)) and 1.8 V, for low-voltage analog COTS parts (as Operational Amplifiers (OpAmp) or bandgap references).

Furthermore, the PMU has a Maximum Power Point Tracking (MPPT) module, which ensures that the energy is extracted efficiently from the power source, i.e. when the system demands energy from the power source, it extracts the maximum power that the power source is able to deliver at that moment. Thus, the solution can attend punctual high-power requirements coming from the different modules and shorten the required start-up time. To achieve that, the MPPT modulates the input impedance of the boost converter and sets the power source operating point to that with output voltage of 0.7 V, where the power source is able to provide the maximum power.

This module also provides some additional features that enable the system to perform a smart power management carried out by the microcontroller. The boost converter outputs a signal called *PGOOD*. This is a low-level signal by default that changes to a high voltage level, as a

flag, when the voltage outputted by the boost converter reaches a voltage of 2.9 V. When regulated voltage drops under 2.4 V, the signal goes to low voltage level. This way, the microcontroller, able to operate with a minimum voltage supply of 1.8 V, can (dis)enable the LDO through a *LDOEN* signal or manage its different Ultra-Low-Power Modes (LPMs) to adapt the system operation to the available energy.

### 2.2.2. Front-end

In order to measure the current provided by the sensor, which is proportional to the glucose concentration, a potentiostat amplifier has been implemented. The potentiostat circuit can be divided into two stages. The first stage is responsible for setting the working voltage of the sensor. Based on the fuel cell characterization, it was obtained the working voltage where the sensor has the highest sensitivity to discriminate between glucose concentrations. During operation, this working voltage is generated using a voltage divider and a buffer amplifier. The second stage performs the current readout and translates this current into voltage using a transimpedance amplifier (TIA) stage. The TIA translates the current signal provided by the sensor ( $I_{CELL}$ ) into a voltage signal by means of a resistor ( $R_{TIA}$ ). The output signal ( $V_{OUT}$ ) obtained at the output of the amplifier is proportional to the current provided by the strip. The equation that relates the output voltage and the current proportional to the glucose concentration is shown in the following equation:

$$V_{OUT} = R_{TIA} \cdot I_{CELL} \quad (1)$$

### 2.2.3. Control and Processing Unit

The system is managed through the CPU. It has been chosen an ultra-low-power microcontroller that needs only 1.8 V as minimum voltage to operate. This device has different operating modes: one active mode and seven software-selectable low-power modes. An interruption event wakes up the microcontroller from low-power mode. Then, the relevant tasks or operations are performed, and finally the microcontroller restores back to the low-power mode on return from the interrupt program. The microcontroller has been selected, because it presents an ultra-low-power system architecture that increases performance at lowered energy budgets, and an ultra-low-power 16-bit control processing unit and intelligent peripherals to extend the autonomy of the system.

For this application two ADC have been used to capture two analog signals. One is the open-circuit voltage of the fuel cell (OCV), which allows to know if the sensor is ready to perform the measurement. The other one is the measurement signal ( $V_{OUT}$ ) related to the current across

the fuel cell ( $I_{\text{CELL}}$ ), which is proportional to the glucose concentration. Some General Purpose Input/Output (GPIO) pins have been used in order to manage and control the PMU module and the display interface.

The conversion of the measured current to a glucose concentration has been carried out by means of a Lookup Table (LUT) (Bengtsson, 2012).

To manage the system, the microcontroller has been programmed to perform the next tasks. Initially, when the voltage supply provided by the boost converter reaches the 1.8 V needed to start its operation, it configures a GPIO pin connected to *PGOOD*. This pin will monitor the state of the regulated voltage supply. Meanwhile, the LDO is disabled using the *LDOEN* signal and the microcontroller goes to LPM to minimize power consumption. When *PGOOD* goes high, meaning that the regulated voltage supply has reached the 2.9 V, and enough energy is harvested to start the application operation, the microcontroller exits the Low-Power Mode (LPM) and starts to configure the different peripherals that are used.

Once the system is initialized, the microcontroller monitors the OCV of the fuel cell to check if the sample is available and start the measurement. If that is the case, it enables the LDO and starts the chronoamperometry, connecting the counter electrode through the *CE\_CONN* signal. During this time, the microcontroller remains in LPM. After the selected time, the microcontroller exits the LPM, outputs the concentration measurement to the display and returns to LPM.

#### 2.2.4. Display output

A commercial 7-Segments Liquid Crystal Display (LCD) has been used to show glucose concentration result due to its low power consumption. The numeric LCD used can display up to 3 digits. In order to facilitate connection and control of the LCD, an integrated circuit has been used, which reduces the number of control signals needed to control the display. The total consumption of this module is 0.33  $\mu\text{A}$  at 3 V.

### 2.3. System integration and assembly

A scheme and picture of the whole system are shown in Fig. 4. The exploded view shows the placement of the different electronic blocks comprising the system, the connector for the disposable test strip, and the 3D printed casing. A Printed Circuit Board (PCB) with dimensions of 77 mm  $\times$  32 mm was designed and implemented.

## 3. Material and methods

### 3.1. Chemicals and materials

All chemicals and biochemicals were, unless otherwise stated, purchased from Sigma-Aldrich. Human serum (H4522, Lot # SLBQ9160V) from human male AB plasma, USA origin, sterile-filtered, was used to validate the operation of the device. Phosphate buffer at pH 7.4 was utilized in preliminary validation studies. It was prepared by the combination of sodium phosphate monobasic dihydrate ( $\text{NaH}_2\text{PO}_4 \cdot 2\text{H}_2\text{O}$ ), sodium phosphate dibasic dihydrate ( $\text{Na}_2\text{HPO}_4 \cdot 2\text{H}_2\text{O}$ ) and potassium chloride (KCl) for a final 100 mM concentration. Glucose solutions were allowed to mutarotate for 24 h and were kept refrigerated at 4 °C until use. Tetrabutylammonium bromide (TBAB)-modified Nafion was prepared as previously reported. (Klotzbach et al., 2006) Flavin adenine dinucleotide-dependent glucose dehydrogenase (FAD-GDH, E.C. 1.1.99.10, GLDE-70-1192, *Aspergillus* sp.) was purchased from Sekisui Diagnostics (Lexington, MA, USA) and used as received. Bilirubin oxidase (BOX, E.C. 1.3.3.5, *Myrothecium* sp., BO-3) was obtained from Amano Enzyme Inc. (Japan) and used as received. Glucose oxidase from *Aspergillus niger* (EC 1.1.3.4, Type X-S, 175 units/mg of solid, 75% protein) and 5% by wt. Nafion EW1100 suspension were purchased from Sigma-Aldrich and used as received. Carboxylated MWCNT and hydroxylated MWCNTs were purchased

from cheaptubes.com.

Standard 14 papers were purchased from GE Healthcare, Pittsburgh, PA, USA. The main structure of the test strip was constructed from pressure sensitive adhesives (PSA) (Adhesives Research) and poly(methylmethacrylate) (PMMA) (Plexiglas, Evonik Performance Materials GmbH, Harmstadt, Germany).

Silver ink (LOCTITE ECI 1011, Henkel, Dusseldorf, Germany) and carbon ink (C2030519P4, Gwent Electronic Materials Ltd., Pontypool, Wales) were used to print the base electrodes for the fuel cell onto a polyethylene terephthalate (PET) substrate. The test strip conducting tracks were ink-jet printed using silver ink (PE410, DuPont, Bristol, UK) on a 125  $\mu\text{m}$  polyethylene naphthalate (PEN) sheet (Teonex, DuPont, Chester, VA, USA). Paper-based power source electrodes were provided by Fuelium (Barcelona, Spain). All electronics components used for the electronic reader were purchased from Farnell (Madrid, Spain).

### 3.2. Device fabrication

The test strip structural components were designed with CorelDraw software (Corel, Ottawa, ON, Canada). Paper, PSA sheets and PMMA were cut with a  $\text{CO}_2$  laser cutter (Mini 24, Epilog Laser, Golden, CO, USA).

The fuel cell configuration was adapted from the one reported in (del Torno-de Román et al., 2018). The fuel cell base electrodes were prepared by screen-printing onto a PET substrate. Initially, a track of silver ink was printed to improve conductivity. Following this, a carbon ink was screen printed on top of the silver layer in order to produce a rounded working electrode surface of 4-mm diameter. The screen-printed substrate was cut in segments of 5 mm  $\times$  9 mm, each containing a single electrode. The active area of the screen-printed electrodes was then functionalized with the corresponding enzymatic ink for anode and cathode. The fuel cell anodes were prepared by adding 1.5 mg of FAD-GDH (30 mg  $\text{mL}^{-1}$ ) enzyme to 75  $\mu\text{L}$  of a 0.2 M citrate/phosphate buffer in ultrapure water. The crosslinker ethylene glycol diglycidyl ether (EGDGE) is diluted in ultrapure water to a concentration of 10% v/v. COOH-MWCNTs are added to isopropanol at a concentration of 5 mg  $\text{mL}^{-1}$  and sonicated for 1 h. Naphthoquinone-Linear poly(ethyleneimine) (NQ-LPEI) was prepared as described in (Milton, 2017) and diluted at a concentration of 10 mg  $\text{mL}^{-1}$  in ultrapure water. In an Eppendorf tube, 67% v/v of the NQ-LPEI solution, 30% v/v of the enzyme and 3% v/v of the cross-linker solution (EGDGE) are combined. 8.5  $\mu\text{L}$  of the combined mixture is deposited on the surface of the electrode and left to dry overnight at room temperature. The fuel cell cathodes were modified by suspending 1.5 mg of BOX in 75  $\mu\text{L}$  of 0.2 M citrate/phosphate buffer. 75  $\mu\text{L}$  of the solution is added to 7.5 mg of Ac-MWCNTs as described in (Meredith et al., 2011; Milton et al., 2015). The solution is vortex mixed for 1 min, followed by 15 s of sonication: this procedure is repeated a total of 4 times. To this mixture, 25  $\mu\text{L}$  of TBAB-Nafion suspension is added, followed by another vortex/sonication step. 33  $\mu\text{L}$  of the mixture is then drop coated onto the surface of the screen-printed electrode and left to dry under a fan for 1.5–2 h. Both anodes and cathodes are stored at 4 °C when not in use.

A modified version of LF55 paper-based power source from Fuelium was adapted to the test strip. The anode and cathode power source electrodes were customized for this application considering the sample type, volume and power requirements. Each electrode had dimensions of 5 mm  $\times$  9 mm, with a projected electroactive surface of 5 mm  $\times$  5 mm. The conducting tracks of the test strip were ink-jet printed using Ag ink on a PEN sheet with a Cera Printer X-serie (Ceradrop, Limoges, France). Silver conducting paste was used for interconnection of fuel cell and power source electrodes to the conducting tracks. All the test strip components were manually assembled layer by layer using an acrylic alignment holder.

The electronic circuit of the battery-less reader was first simulated using Multisim software (National Instruments, Austin, Texas, United States). Ultiboard program (National Instruments, Austin, Texas, United



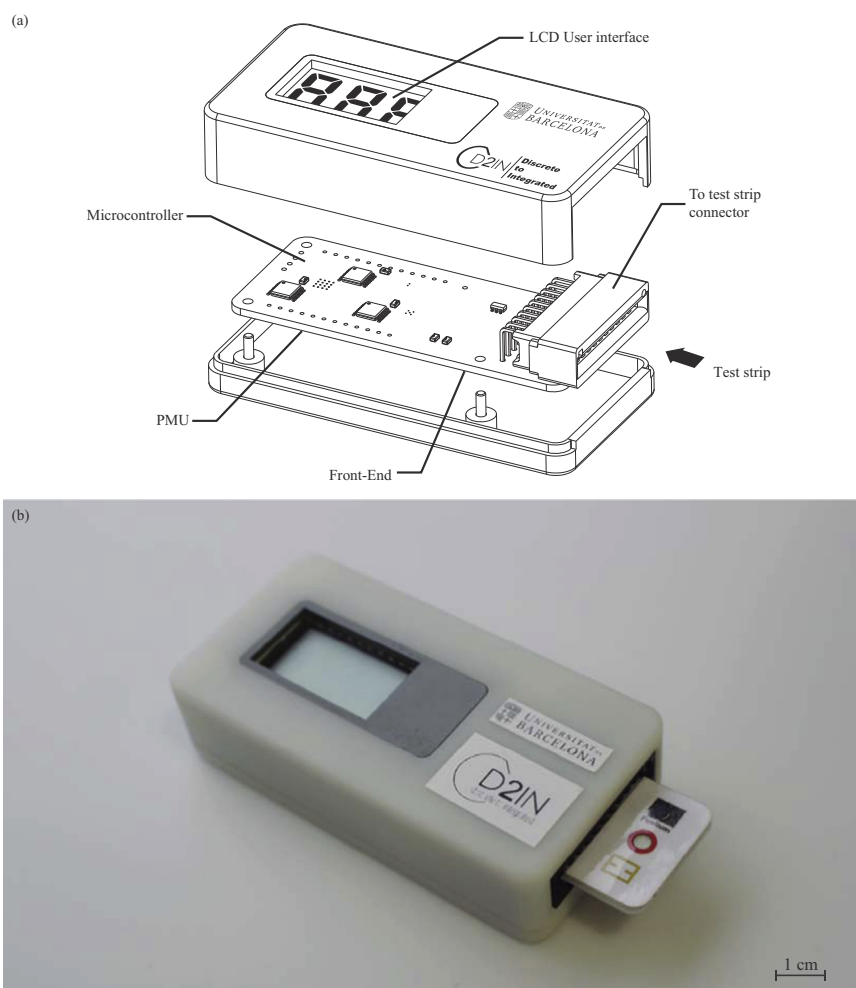


Fig. 4. a) Schematic of the system assembly. b) Photograph of the system.

States) was used to design the printed circuit board. The reader casing was designed using DesignSpark Mechanical.

### 3.3. Electronic and electrochemical characterization and validation

All electrochemical experiments were carried out with an Autolab PGSTAT204 (Metrohm, NL). For fuel cell and power source characterization, the open-circuit voltage of the fuel cell (OCV) of each cell was measured before polarization. Polarization curves were performed in potentiodynamic mode at a scan rate of  $5 \text{ mV s}^{-1}$ . Chronoamperometric curves of fuel cells were measured at  $0.45 \text{ V}$  for each glucose concentration.

The electronic validation and characterization were performed with a Source Measurement Unit (SMU) B2962A by Keysight Technology (USA) and an Agilent Technologies oscilloscope MSO-X 3034A (USA). Initial electronic characterization was carried out simulating the electrical behavior of the test strip via the SMU. The output voltage of the potentiostat was captured for different current curves corresponding to different glucose concentrations.

## 4. Results and discussion

### 4.1. Test strip characterization

The power source polarization curve was obtained after depositing  $50 \mu\text{L}$  of serum at the inlet pad of the consumable test strip. In order to see its performance in time, discharge curves at  $1$  and  $10 \text{ mA}$  were also recorded. Fig. 5a and b show the obtained results. The power source

shows its capability of delivering  $1 \text{ mA}$  for at least  $40 \text{ min}$  (far beyond the typical operating time of point-of-care devices) whereas at  $10 \text{ mA}$  it sustained a voltage above  $1.25 \text{ V}$  for at least  $5 \text{ min}$ .

Bioelectrocatalysis of fuel cell electrodes was validated with half-cell voltammetric characterization. Figs. S1, S2 show representative voltammograms of bioanode and biocathode, respectively. Next, the glucose fuel cell of the test strip was characterized with human serum at different glucose concentrations. Serum as-purchased had a glucose concentration of  $4.8 \text{ mM}$ . A solution of  $1 \text{ M}$  glucose in  $100 \text{ mM}$  PBS buffer was prepared and spiked into the serum sample in order to increase glucose concentration while minimizing dilution of the original biological sample. Fig. 5c shows the polarization curves obtained at different glucose concentrations. From these I-V curves, it could be seen that the highest sensitivity is obtained between  $0.35$  and  $0.50 \text{ V}$ . Therefore, it was decided to polarize the fuel cell at  $0.45 \text{ V}$  to obtain the chronoamperometry curves of the fuel cell and sense glucose concentration. The currents generated by the fuel cell biased at  $0.45 \text{ V}$  were measured for  $80 \text{ s}$ , recording a variability below  $15\%$  for each of the glucose concentrations in serum. Mean chronoamperometric curves are depicted in Fig. 5d.

### 4.2. Battery-less electronic reader validation and characterization

All electronic modules introduced in Section 2.2 were fully characterized and validated individually as a prior step to the total integration of the system shown in Fig. 4. This individual characterization of the full-custom electronics was carried out following a two-phase testing procedure: Phase 1) an initial step using a SMU (section 3.3) to

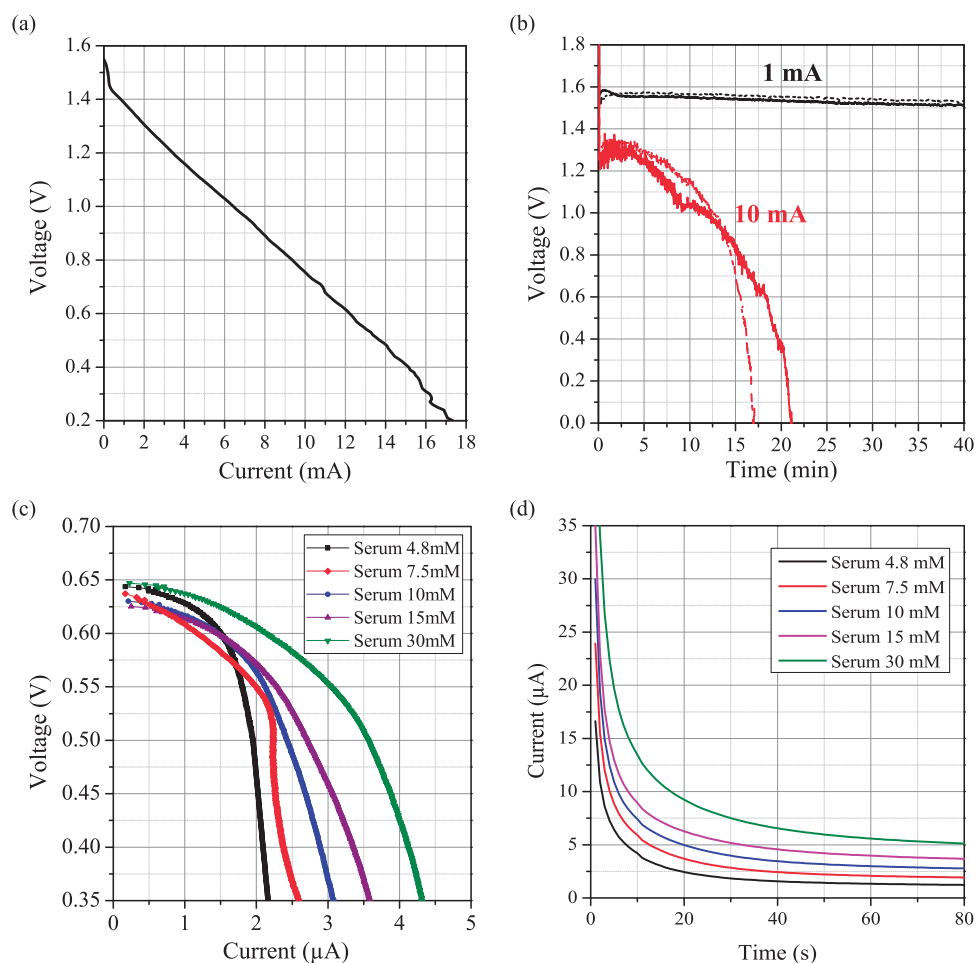


**Fig. 5.** Characterization of the Fuelium LF55 paper-based power source activated with serum samples. a) I-V paper-based power source characteristic. b) Paper-based power source discharge curves at 1 and 10 mA. Characterization of glucose fuel cell integrated in the test strip with different glucose concentrations in serum. c) Fuel cell polarization curves. d) Fuel cell chronoamperometry curves at 0.45 V.

simulate the electrical response/behavior of the test strip; and Phase 2) a second phase using real test strips. Upon successful completion of these two phases, the implementation, integration and validation of the full system (Fig. 4) was done. In such a way, the final assembly was programmed, calibrated to work with the given sensor and validated with real test strips in the final test procedure (Phase 3).

It is important to underline the accurate design of the front-end module to reduce the deviation error of the measurement through it. This error was derived as the difference between the injected current and the current measured through the full-custom electronic module. The electronic system was validated and a final error lower than 1% was verified in test phase 1 with a test strip simulated current produced by the SMU unit and in phase 2 using test strips.

From calibration phase (Phase 3), it was obtained that the electronic reader is able to measure currents up to 30  $\mu\text{A}$  with a resolution of 13 nA. Fig. 6a shows the accuracy of the electronic reader. The electronic reader error is lower than 1.8%. This error depends on the ADC quantification error and the passive component tolerances.

The main effort was to settle the appropriate time to extract the measurement. This point was defined in terms of device resolution and the uncertainty related to the electronics. In this sense, the reader was programmed to measure the current corresponding to a given glucose concentration. In order to characterize the whole system and determine the precise time to extract the measurement, the consumable test strip was connected to the reader and fed with 50  $\mu\text{L}$  of serum at different glucose concentrations between 5 and 30 mmol/L (same considerations as section 4.1).

The currents generated by the glucose fuel cell biased at 0.45 V were measured and recorded by the reader for 80 s. As seen in Fig. 6b, the current measured by the reader ( $I_{\text{CELL}}$ ) virtually match with the chronoamperometry curves presented in Fig. 5d obtained with a commercial potentiostat (Autolab PGSTAT2014). These results allow to validate the operation of the reader and disposable strip system. As expected, the main difference between the curves measured by both instruments was identified for currents larger than 30  $\mu\text{A}$  where the full-custom reader presents a maximum current detection limit, saturating for any higher value.

The chronoamperometric curves shown in Fig. 6b were used to define three operation regions (A, B and C) based on two criteria: the device resolution and the uncertainty in the time of measurement. These regions were used to determine the time to perform the measurement of current after submitting the fuel cell to the bias voltage.

The first criterion, device resolution, depends mainly on the sensor sensitivity and the electronic reader resolution. Based on the data from Fig. 6b, the sensor presents a higher sensitivity in region A whereas the lowest sensitivity is obtained in region C due to its decrease rate over time. On the other side, the electronic reader resolution is defined by the ADC resolution with a time-invariant value of 13 nA, negligible compared to the sensor sensitivity. According to this analysis, region C was ruled out to settle the time to extract the measurement.

The next step was the study of the measurement uncertainty to accurately define the time of the measurement. As it is shown in Fig. 6b, the chronoamperometry has a decreasing exponential response. This response excludes region A to carry out the measurement. In this

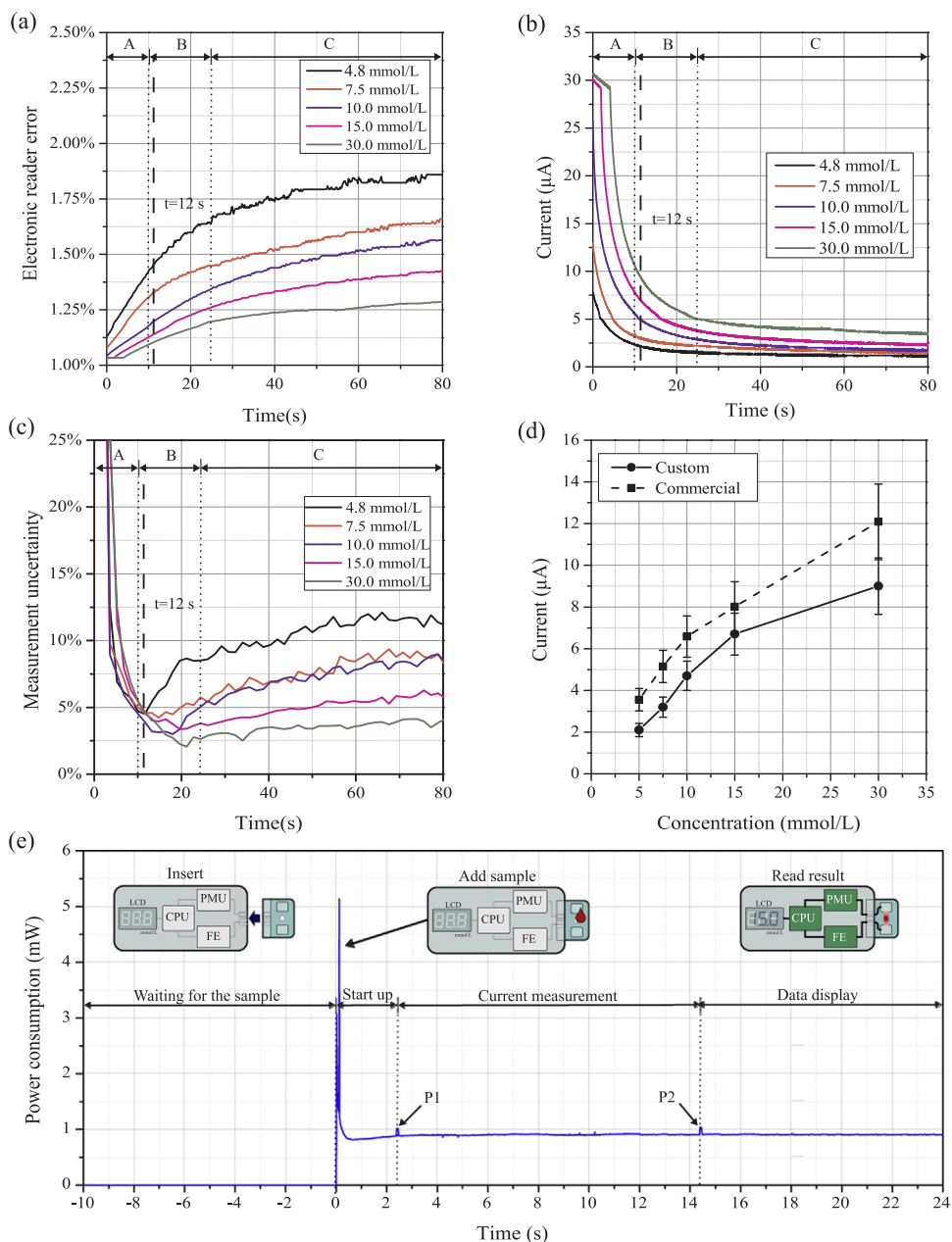


**Fig. 6.** a) Electronic reader current error. b) Chronoamperometry curves done with the battery-less electronic reader. c) Uncertainty in current measurement produced by the electronic reader. d) Transfer function that relates the current captured by the electronic reader with the glucose concentration and comparison against a commercial potentiostat (Autolab PGSTAT204). f) Temporal evolution of the electronic reader power consumption.

region, a small instability in the measurement time instant causes an important uncertainty in current measurement. Therefore, region B is the best region to perform the measurement. At this point, the current uncertainty in time was calculated (Fig. 6c) to establish the best time to extract the measurement within region B. The uncertainty is based on a 0.5 s range defined by the measurement sampling period of the processing unit. It was obtained that the best time to carry out the measurement is at 12 s, because it presents an electronics' uncertainty lower than 5% for the lowest glucose concentration.

A Lookup Table (LUT) (Bengtsson, 2012) based technique was used to translate the current value into the glucose concentration. Fig. 6d shows the transfer function that relates the current captured by the electronic reader with the glucose concentration and compares it against the one measured with the commercial potentiostat (Autolab PGSTAT204). Error bars in both curves account for the variability of the glucose sensor. As it can be seen, the data are proportional and only a

slight shift between the curves is presented. This is caused by the initial current saturation peak but, due to its systematic behavior, it is adjusted by a LUT in the postprocessing at the control unit.

Finally, Fig. 6e shows the operation phases of the system and the temporal evolution of the power consumption. The electronic reader is switched on when the serum sample is introduced into the disposable test strip, defining the start-up of the system. At this moment ( $t = 0$  s), the typical inrush current peak takes place, reaching a value of up to 5 mW. Then, the reader enters into a low power mode, consuming just 900  $\mu$ W. It should be noted that the total electronics power consumption is much lower than the maximum power that the paper-based power source is able to supply, above the 10 mW. During this phase, the system waits in the low power mode of operation until the voltage provided by the disposable is stable. Then, the front-end module is switched on, the measurement is started and maintained during 12 s, which is labeled as the Current measurement phase. Finally, in the Data

display phase, the reader returns to the low power mode and the numerical result is displayed. Two small current peaks take place during the device operation. The first peak (P1) occurs when the front-end module is activated and the second (P2) when the measurement data is acquired and displayed. The result of the glucose concentration measurement is displayed on the screen until the disposable component is removed or it runs out of power after a few hours.

Significant research efforts have been made to develop systems which generate energy while monitor the glucose of a sample (Lee et al., 2017; Slaughter and Kulkarni, 2017). Nevertheless, the proposed systems do not have any electronics module to display the result, and it is necessary an external system to show it. Furthermore, accurate commercial glucometers are available, which just need a small sample volume to perform the measurement (Rajendran and Rayman, 2014). However, they require batteries which become hazardous waste and pose threats to health and the environment if improperly disposed. The novel battery-less system presented in this paper provides quantitative data, besides having a reusable reader and a disposable test-strip, acting as sensor and a power source, which does not contain any toxic material, so it can be safely disposed of after its use without the need of recycling.

## 5. Conclusions

This work presents the Plug-and-Power concept, a novel approach of powering portable Point-Of-Care devices that offers several advantages. In this case, the disposable test strip provides the energy needed to run an electronic reader and perform the test, defining a self-powered plug-and-play POC.

In this case, the developed system is able to monitor glucose and process and display the data without the need to either recharge or replace the batteries, as the energy to run a measurement is always available within the test strip. Additionally, this approach provides environmental benefits related to battery usage and disposal, as uncontrolled battery disposal leads to severe environmental pollution. The paper-based power source used for the present approach does not contain any toxic material, so it can be safely disposed of after its use without the need of recycling. Therefore, this eco-friendly power source can follow the same waste stream as a test strip that has been in contact with biological samples.

The results show that the battery-less reader is able to operate and manage the power provided by the paper-based power source integrated in the consumable test strip. In addition, the electronic reader performs an electrochemical detection, process the output signal of the sensor and express the result on a display. The electronic reader designed is able to measure currents up to 30  $\mu\text{A}$  with a resolution of 13 nA and an error below 1.8%. Due to the low power design of the reader that consumes only 900  $\mu\text{W}$  in low power mode, it is possible to perform the measurement with the power provided by the test strip, which is above the 10 mW. This shows that the self-powered device could be further improved to include additional functionalities for sample preparation or a wireless communications module to visualize the results on a laptop or even on a smartphone. A big challenge would be to integrate the electronic system into a single chip, making possible develop a flexible and totally disposable system.

The advantages of this approach were here demonstrated with the development of a portable glucometer, but this concept can be extended to other kinds of electrochemical sensors measuring other analytes and/or other biological matrices (Chin et al., 2012; da Silva et al., 2017; Kaushik et al., 2018; Wan et al., 2013). Moreover, this can also benefit

portable electronic analytical devices beyond clinical diagnostics, as for example the veterinary or environmental fields.

## Acknowledgements

We would like to acknowledge I. González-Valls from Fuelium, S.L. for guidance in paper-battery handling and operation. Also, the authors would like to thank the support of the MINAUTO Project (TEC2016-78284-C3-3-R and TEC2016-78284-C3-1-R), Ministerio de Economía, Industria y Competitividad – Agencia Estatal de Investigación, and Fondo Europeo de Desarrollo Regional (AEI/FEDER, UE). N. Sabaté would like to thank the financial support received from ERC Consolidator Grant (SUPERCCELL - GA.648518). S.D. Minter would like to thank the financial support of the United States Department of Agriculture NIFA program (11322204).

## Appendix A. Supporting information

Supplementary data associated with this article can be found in the online version at doi:10.1016/j.bios.2018.07.034.

## References

- Bengtsson, L.E., 2012. *J. Sens. Technol.* 02, 177–184.
- Chan, H.N., Tan, M.J.A., Wu, H., 2017. *Lab Chip* 17, 2713–2739.
- Chin, C.D., Linder, V., Sia, S.K., 2012. *Lab Chip* 12, 2118.
- Choi, S., 2016. *Biotechnol. Adv.* 34, 321–330.
- Cruz, A.F.D., Norena, N., Kaushik, A., Bhansali, S., 2014. *Biosens. Bioelectron.* 62, 249–254.
- Drain, P.K., Hyle, E.P., Noubary, F., Freedberg, K.A., Wilson, D., Bishai, W.R., Rodriguez, W., Bassett, I.V., 2014. *Lancet Infect. Dis.* 14, 239–249.
- Fischer, C., Fraiwan, A., Choi, S., 2016. *Biosens. Bioelectron.* 79, 193–197.
- Fu, E., Yager, P., Floriano, P.N., Christodoulides, N., McDevitt, J.T., 2011. *IEEE Pulse* 2, 40–50.
- Gervais, L., de Rooij, N., Delamarque, E., 2011. *Adv. Mater.* 23, H151–H176.
- Kaushik, A., Yndart, A., Kumar, S., Jayant, R.D., Vashist, A., Brown, A.N., Li, C.-Z., Nair, M., 2018. *Nat. Chem.* 8, 9700.
- Klotzbach, T., Watt, M., Ansari, Y., Minter, S.D., 2006. *J. Membr. Sci.* 282, 276–283.
- Kulkarni, T., Slaughter, G., 2017. *Proc. IEEE Sens.*
- Larcher, D., Tarascon, J.-M., 2015. *Nat. Chem.* 7, 19–29.
- Lee, I., Sode, T., Loew, N., Tsugawa, W., Lowe, C.R., Sode, K., 2017. *Biosens. Bioelectron.* 93, 335–339.
- Leonard, R.J., 2012. *J. Forensic Sci.* 57, 1614–1620.
- Meredith, M.T., Minson, M., Hickey, D., Artyushkova, K., Glatzhofer, D.T., Minter, S.D., 2011. *ACS Catal.* 1, 1683–1690.
- Milton, R.D., Lim, K., Hickey, D.P., Minter, S.D., 2015. *Bioelectrochemistry* 106, 56–63.
- Milton, R.D., 2015. FAD-Dependent glucose dehydrogenase immobilization and mediation within a naphthoquinone redox polymer. In: Minter, S. (Ed.), *Enzyme stabilization and immobilization. Methods in molecular biology* 1504 Humana Press, New York, NY. [https://doi.org/10.1007/978-1-4939-6499-4\\_15](https://doi.org/10.1007/978-1-4939-6499-4_15).
- Narvaez Villarrubia, C.W., Soavi, F., Santoro, C., Arbizzani, C., Serov, A., Rojas-Carbonell, S., Gupta, G., Atanassov, P., 2016. *Biosens. Bioelectron.* 86, 459–465.
- Noordzij, P.C., 1975. *Alcohol Drugs Traffic Saf.* 553–560.
- Ongondo, F.O., Williams, I.D., Cherrett, T.J., 2011. *Waste Manag.* 31, 714–730.
- Rajendran, R., Rayman, G., 2014. *J. Diabetes Sci. Technol.* 8, 1081–1090.
- da Silva, E.T.S.G., Souto, D.E.P., Barragan, J.T.C., de F. Giarola, J., de Moraes, A.C.M., Kubota, L.T., 2017. *ChemElectroChem* 4, 778–794.
- Slaughter, G., Kulkarni, T., 2016. *Biosens. Bioelectron.* 78, 45–50.
- Slaughter, G., Kulkarni, T., 2017. *Sci. Rep.* 7, 1471.
- del Torno-de Román, L., Navarro, M., Hughes, G., Esquivel, J.P., Milton, R.D., Minter, S.D., Sabaté, N., 2018. *Electrochim. Acta* 282, 336–342.
- Wan, Y., Su, Y., Zhu, X., Liu, G., Fan, C., 2013. *Biosens. Bioelectron.* 47, 1–11.
- Wang, S., Lifson, M.A., Inci, F., Liang, L.-G., Sheng, Y.-F., Demirci, U., 2016a. *Expert Rev. Mol. Diagn.* 16, 449–459.
- Wang, S.Q., Chinnasamy, T., Lifson, M.A., Inci, F., Demirci, U., 2016b. *Trends Biotechnol.*
- Widmer, R., Oswald-Krapf, H., Sinha-Khetriwal, D., Schnellmann, M., Böni, H., 2005. *Environ. Impact Assess. Rev.* 25, 436–458.
- Yager, P., Edwards, T., Fu, E., Helton, K., Nelson, K., Tam, M.R., Weigl, B.H., 2006. *Nature-Lond.* 442, 412.
- Zarei, M., 2017. *TrAC - Trends Anal. Chem.*



## 2.2 Publication 2

### Self-Powered Portable Electronic Reader for Point-of-Care Amperometric Measurements

*By*

**‘Yaiza Montes-Cebrián**, Albert Álvarez-Carulla, Jordi  
Colomer-Farrarons, Manel Puig-Vidal and, Pere Ll. Miribel-Catalá.

*Department of Electronic and Biomedical Engineering, Faculty of Physics, Uni-  
versity of Barcelona (UB), 1st Martí i Franqués St., 08028 Barcelona, Spain*





*Published in*

**Sensors** 2019, 19, 3715; doi:10.3390/s19173715



Article

# Self-Powered Portable Electronic Reader for Point-of-Care Amperometric Measurements

Yaiza Montes-Cebrián \*, Albert Álvarez-Carulla, Jordi Colomer-Farrarons, Manel Puig-Vidal and Pere Ll. Miribel-Català

Department of Electronics and Biomedical Engineering, Faculty of Physics, University of Barcelona, Martí i Franquès 1, 08028 Barcelona, Spain

\* Correspondence: ymontes@ub.edu; Tel.: +34-93-4020-876

Received: 1 August 2019; Accepted: 25 August 2019; Published: 27 August 2019



**Abstract:** In this work, we present a self-powered electronic reader (e-reader) for point-of-care diagnostics based on the use of a fuel cell (FC) which works as a power source and as a sensor. The self-powered e-reader extracts the energy from the FC to supply the electronic components concomitantly, while performing the detection of the fuel concentration. The designed electronics rely on straightforward standards for low power consumption, resulting in a robust and low power device without needing an external power source. Besides, the custom electronic instrumentation platform can process and display fuel concentration without requiring any type of laboratory equipment. In this study, we present the electronics system in detail and describe all modules that make up the system. Furthermore, we validate the device's operation with different emulated FCs and sensors presented in the literature. The e-reader can be adjusted to numerous current ranges up to 3 mA, with a 13 nA resolution and an uncertainty of 1.8%. Besides, it only consumes 900  $\mu$ W in the low power mode of operation, and it can operate with a minimum voltage of 330 mV. This concept can be extended to a wide range of fields, from biomedical to environmental applications.

**Keywords:** self-powered; point-of-care diagnostics; low power electronics; smart electronics; portable; amperometric measurements

## 1. Introduction

The use of a fuel cell (FC) to replace conventional batteries in portable systems is of great interest [1–3]. FCs open up new opportunities, mainly in the field of consumer and industrial portable devices. There is a particular interest in the field of diagnostic tools based on biofuel cells, notably in the frame of point-of-care (POC) devices and biosensors for environmental monitoring [4]. In such systems, a big challenge is to implement self-powered sensing devices [5].

The general architecture of such devices is defined mainly by three modules. On the one hand the sensor and the power source, which can be a conventional battery, sensor or a FC, and on the other hand, the electronic reader (e-reader), which is the center of interest in the present work.

Particularly, portable and wearable devices are of interest due to their applications in health monitoring, diagnostics, prevention, among others [6,7]. In most cases, these systems use batteries as power sources. Generally, developed countries have a good electricity grid and batteries are inexpensive. The problem arises if we focus on the developing world, where they are in most need of these kind of portable diagnostic devices [8]. Furthermore, batteries are limited by their reduced lifetime, negative environmental impact, large size, and weight. Different approaches are looking for the best way to power a POC solution [9]. An example is paper-based assays (PBAs), wherein sample manipulation, pre-treatment, and electronics are not required [5] since they usually use colorimetric systems to read the results [10]. Promising alternative solutions are emerging whereby the energy



from the environment is used by energy harvesters to produce power, which can be used to supply portable and wearable devices. There are many approaches to harvest energy based on biofuel cells (BFCs) [11,12], thermo-electric generators (TEG) [13], piezoelectric generators (PZT) [14], among others.

FCs are electrochemical devices that harvest electrical energy from chemical reactions. They can work as a power source and as a sensor because they produce electricity for as long as there is available fuel. Their output current is directly correlated with the concentration of fuel. Two sub-categories of FCs are enzymatic fuel cells (EFCs) and microbial fuel cells (MFCs) [15,16]. Both have similar operational principles for energy production. EFCs produce electrical power using enzymes as a catalyst to oxidize their fuel, while MFCs use bacteria as the catalysts to oxidize organic and inorganic matter.

So far, it is only possible to power low-consumption microelectronic systems with these kinds of FCs since their power density output ranges from  $\mu\text{W}$  up to  $\text{mW}$ . Due to the fact that EFCs have higher power density and a more compact size, they are suitable to power portable and wearable electronic solutions [11,16]. Nevertheless, MFCs are an eco-friendly way of producing electrical energy from waste, since the electricity can come from waste material. This waste material becomes cleaner after the break-down process and can be directly discharged to the environment [17]. Moreover, MFCs may be employed as long-term power generating systems for online environment quality monitoring [18].

An ideal scenario is based on an FC which uses the same sample to power electronics and sense the concentration. However, the FC can be replaced by other power sources like standard batteries, printed batteries, energy-harvesting resources or a combination of such solutions. For instance, a possible scenario is a FC that supplies the electronics and a sensor that measures the analyte concentration. The sensor can be an amperometric biosensor to monitor oxygen and catechol [19] or glucose [20]. Furthermore, there are examples of amperometric systems based on the detection of the inhibition of glucose oxidase enzyme [21] or horseradish peroxidase activity [22]. Another interesting case is the air/water quality monitoring using FCs as a power source along with amperometric or potentiometric sensors [23,24]. In [25], a degradable battery was proposed fabricated using organic materials. It was able to operate up to 100 min with an adaptable output voltage from 1.5 to 3.0 V. The battery could be combined with amperometric biosensors to power a commercial water quality POC and detect heavy metals. Moreover, the device can be powered from polluted air generated during the treatment of wastewater [26], or in space missions [27,28] where FCs generate electrical power from hydrogen and oxygen.

Systems based on commercial off-the-shelf (COTS) integrated circuits (IC) are an affordable way to develop biomedical biosensing systems. Some examples of COTS-based systems have been reported in the literature. In this context, Baingane et al. developed a self-powered biosensor system for real-time sensing of lactic acid [29]. The system was comprised of an enzymatic biofuel cell and a simple capacitor circuit operating as a transducer. The fuel cell-based sensor generated an electrical power proportional to the lactic acid concentration, which was deduced by measuring the charging/discharging frequency of the capacitor circuit. The system did not rely on external power sources, although it required external equipment, like an oscilloscope, to monitor the capacitor frequency. Some works proposed the use of FC to monitor lactate in sweat. An example is a non-invasive system designed by Garcia et al. [30]. The device was composed of an enzymatic sensor, a biological FC as a power source and an electronic system. The electronic circuit consisted of an energy harvester, which boosted the FC voltage, and a potentiostat that performed a chronoamperometric detection. However, the system needed an external multimeter to perform the readout. In this context, an electronic-skin-based biofuel cell was developed by Bandothkar et al. [31]. The device harvested lactate present in human sweat to power a light-emitting diode and a bluetooth low energy radio. Other authors also proposed wireless systems [32], in which an operation using an organic biofuel cell was demonstrated. The full-custom circuit was able to operate with a voltage supply of 0.23 V. Besides, the authors designed and validated a receiver and off-chip inductor to transmit the data.

In the particular case of glucometers, recent innovative concepts have been proposed, which are capable of generating electrical power from the biochemical energy stored in glucose [33,34]. An example

is the self-powered fuel cell-based system for glucose monitoring developed by Fischer et al. [35]. The low-cost device operated with a single drop of 20  $\mu\text{L}$  and lacked external power sources with the capacity to generate rapid results, although it required a digital multi-meter for signal readout. These monitoring approaches have a simple electronic system capable of extracting the glucose level from the sample. However, most of them are subjective because they cannot store and process the information [12,36].

The motivation of the batteryless e-reader derives from the needs of POC devices in different scenarios [8,37,38]. The e-reader is an equipment with a quantitative output reading that seeks to achieve the requirements defined by the World Health Organization with the ASSURED criteria (Affordable, Sensitive, Specific, User-friendly, Rapid and Robust, Equipment-free, and Deliverable to users [39]).

In this work, we present in detail, the electronic modules that build up an e-reader based on the use of FC, following two approaches: Using the FC as a power element or as a dual power/sensor element. This power/sensor element is an external item that is inserted into the e-reader in which the same sample is used for powering and detecting. The e-reader was previously validated with a custom disposable test strip composed of a glucose battery, which supplied the device, and a glucose FC, which monitored the glucose concentration [20]. However, the e-reader can be adapted to operate in other scenarios, with another kind of FC, as power sources or biosensors. The e-reader was validated with a FC of simulated body fluid with an ionic composition similar to human blood plasma enriched with ethanol [40]. This FC has an open circuit voltage (OCV) of 930 mV with a maximum power density close of  $1.237 \text{ mW}\cdot\text{cm}^{-2}$ . Another example of application is the urine/Cr(VI) FC with an OCV of 1.3 V and a power of  $340 \text{ }\mu\text{W}\cdot\text{cm}^{-2}$  [41]. In both cases, the e-reader could be supplied from the energy extracted by the fuel. At the same time, the concentration could be obtained from the current provided by the FC. Also, it is possible to perform a combination with another power source, like a direct methanol fuel cell (DMFC) for portable applications [42,43], with a specific amperometric sensor [44,45]. We describe in detail the conception, design, implementation, and characterization of the electronic modules that build-up the electronic reader based on a FC as a power source and a direct reading interface for a FC or an amperometric biosensor. Moreover, the operation of the reader is validated for different scenarios by emulating different FCs and sensors.

## 2. Materials and Methods

### 2.1. Architecture of the Self-Powered Measurement

As it has been pointed out before, the e-reader is conceived to operate with a FC as a power source and as a sensor, taking a direct amperometric reading of the FC current. Also, it is possible to use any amperometric biosensor based on a two-electrode configuration, although configuration can be easily extended to a three-electrode configuration. Using this technique, when a potential is applied to the counter electrode (CE), a current is produced as a consequence of the reaction at the working electrode (WE) surface.

The general architecture of the system is defined mainly by two modules: The power and sensor unit and the e-reader unit. The power source can be based on paper, as was presented in [20], where the device was validated with different glucose concentrations.

The architecture of the e-reader is divided into four modules (Figure 1): A power management unit (PMU), a front-end unit (FEU), a control and signal processing unit (CSPU) and a display unit (DU). The PMU extracts the power from the power source and manages it to generate the control signals and voltage supplies. All the while, the FEU picks up the measurement signal, which is proportional to the concentration of the agent to be detected. Lastly, the output signal is converted and processed by the CSPU and it is sent to the DU, where the measurement result is shown.

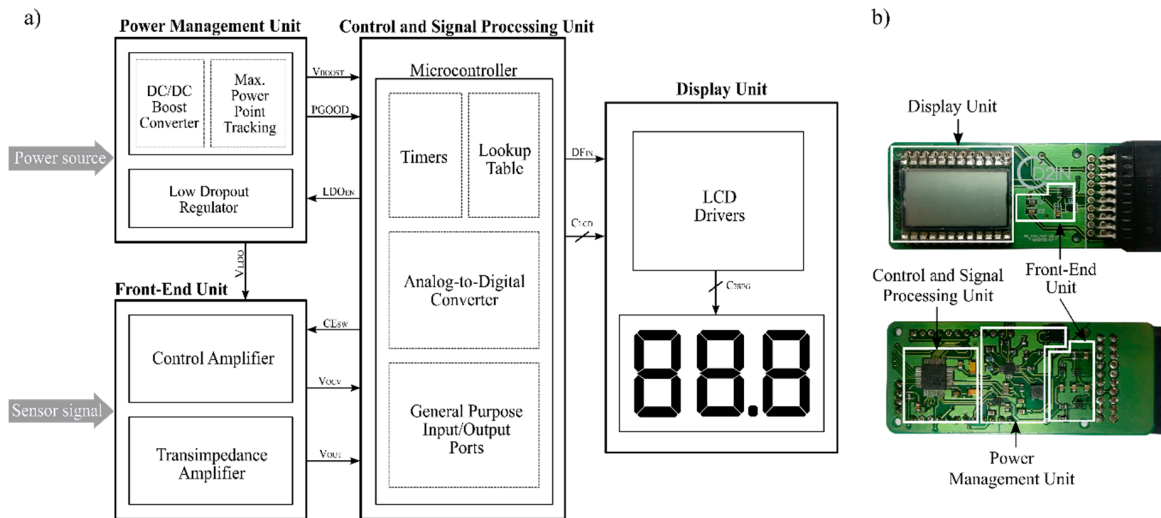


Figure 1. (a) Block diagram of the e-reader, and (b) picture of the e-reader, the four principal modules are labeled, derived from [20].

2.1.1. Power Management Unit

The PMU extracts the energy from the power source and generates a regulated output voltage to supply the electronic modules that compose the e-reader. It is comprised of a DC/DC boost converter in cascade with a low drop out (LDO) linear regulator (Figure 2a). The DC/DC boost converter steps up the voltage provided by the power source to 3.0 V ( $V_{BOOST}$ ) to supply both the CSPU and the DU.

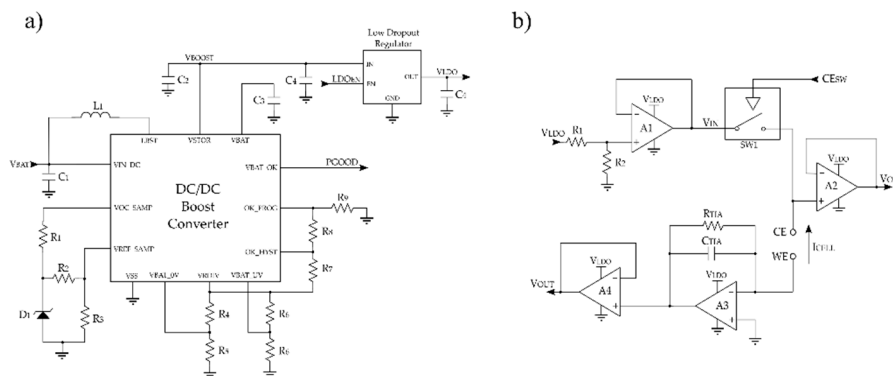


Figure 2. Circuits that compose the (a) power management unit, and (b) front-end unit circuit.

The LDO provides a 1.8 V ( $V_{LDO}$ ) regulated voltage with high noise rejection, which is used to supply the analog components that compose the FEU. This electronic module provides a stable and regulated voltage avoiding the switching noise of the boost converter and the voltage variations of the power supply.

Moreover, a maximum power point tracking (MPPT) module is implemented in the PMU. It guarantees an efficient energy extraction from the power source. This module can cope with a punctual high-power demand, such as the system’s start-up. For that purpose, the MPPT module adapts the input impedance of the DC/DC boost converter and changes the operating point of the power source to the voltage at which the power source provides the maximum power. This module allows managing the energy intelligently through the microcontroller. The DC/DC boost converter incorporates the PGOOD (power good) signal (Figure 2a). This signal is at a low level by default but, when the converter ( $V_{BOOST}$ ) reaches 2.9 V, this signal goes high state. However, if the voltage falls below 2.4 V, it returns to a low level. In this way, the microcontroller, which operates at 1.8 V, can enable/disable the LDO through the  $LDO_{EN}$  signal. Moreover, as it will be explained in the next

sections, the microcontroller has different ultra-low-power modes (LPMs) in order to adapt the system operation to the available energy.

The PMU module is based on the BQ25504 and the LP5910 LDO (Texas Instruments; Dallas, TX, USA). Both devices have a very marked low power character with a typical quiescent current of 330 nA for the first one and 12  $\mu$ A for the second one in shutdown mode. The total consumption of this PMU module is 21  $\mu$ A.

### 2.1.2. Front-End Unit

The current measurement was performed by a potentiostat amplifier (Figure 2b). The main tasks of this module are: (a) To apply a stable voltage difference between the electrodes of the electrochemical cell, and (b) to readout and process the output signal.

In order to control the potential applied to the cell, an operational amplifier (Op-Amp) is used as a control amplifier (A1). A1 provides the optimal bias voltage to the sensor ( $V_{IN}$ ), which is the voltage that enables the best sensor's performance. The e-reader is designed to adjust the voltage  $V_{IN}$ , adapting the system to a wide range of applications. The voltage  $V_{IN}$  is generated through the low-dropout regulator ( $V_{LDO}$ ), and a voltage divider resistor network ( $R_1$  and  $R_2$ ). Because the resistor network modifies the measure, a unity gain buffer amplifier (A1) is introduced between the network and the sensor to isolate both parts.

As stated above, it is possible that the power source needs some time to reach the voltage to supply the electronic components (1.8 V). Therefore, when the PGOOD signal is at a high-level voltage, the microcontroller sends a high-level signal ( $LDO_{EN}$ ) to turn on the LDO ensuring the e-reader measures when enough energy is harvested to start the application operation.

For the best performance, the open circuit voltage ( $V_{OCV}$ ) applied to the counter electrode (CE) is monitored by an analog to digital converter (ADC) pin of the microcontroller. The ADC controls the  $V_{OCV}$  applied to the sensor and when the sample is available, it starts the measurement turning on the analog switch (SW1) through the  $CE_{SW}$  signal, depicted in Figure 2b. Since the microcontroller's port impedance can affect the measurement, a unity gain buffer amplifier (A2) is connected between the CE and the microcontroller.

The Transimpedance Amplifier circuit (TIA) (A3), connected to the working electrode (WE), provides the output voltage ( $V_{OUT}$ ) that is proportional to the cell current ( $I_{CELL}$ ). It translates the current signal into a voltage signal by means of transimpedance gain resistor ( $R_{TIA}$ ). The expression that relates both magnitudes is shown in Equation (1). In this configuration, the working electrode is kept to the virtual ground by the TIA. As before, a unity gain buffer amplifier (A4) is connected between the TIA and the microcontroller so as not to affect the measurement value.

$$V_{OUT} = R_{TIA} \cdot I_{CELL} \quad (1)$$

The current generated by the sensor is amplified by the TIA and translated to an output voltage through the  $R_{TIA}$ . Ideally, this current flows through  $R_{TIA}$ , but in fact, the op-amp takes some of this current (called input bias current). A similar error is derived from the input offset voltage, which is caused by a mismatch in the input terminals of the op-amp. It specifies the voltage across the terminals that must be applied in order to get an output voltage of zero. This input bias current and input offset voltage results in an error voltage at the output and limits the dynamic range of the FEU circuit. Therefore, it is important to select an op-amp with low input bias current and low input offset voltage, to achieve the required dynamic range and overall accuracy. The selected op-amp in the FEU is the LPV521 (Texas Instruments; Dallas, TX, USA). It is a nano-power amplifier which is able to operate from 1.6 V up to 5.5 V with typically 345 nA of supply current. It also presents a very low offset voltage (0.1 mV, typically at 1.8 V) and an ultra-low bias current (0.01 pA, typically at 1.8 V). The maximum output current is 3 mA, which is the maximum current that the e-reader can read.

The analog switch used is the SN74AUC1G66 (Texas Instruments; Dallas, TX, USA). It presents a low power character since it is able to operate at 0.8 V to 2.7 V with only 10  $\mu\text{A}$  of typical quiescent current. In addition, the design is made up of accurate resistors with 1% tolerance. The total consumption of the front-end unit circuit is 7.5  $\mu\text{A}$ .

### 2.1.3. Control and Signal Processing Unit

This unit is based on a low power microcontroller, which has three main tasks: a) Generate the signals that control the modules of the system; b) process the data and; c) show it on the display.

Figure 3 shows the flow diagram of the application. Initially, the device is switched off, waiting for the introduction of the power and sensor module (“Disconnected phase”) into the reader. As soon as it is inserted and the sample deposited, the “start-up phase” begins.

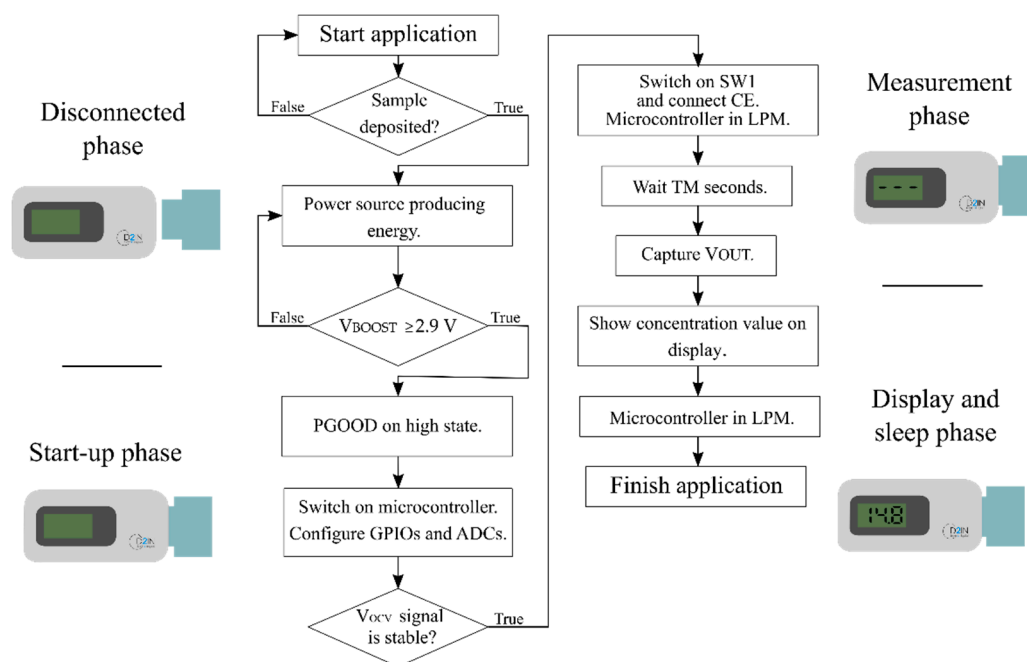


Figure 3. Diagram of the application’s flow.

Thereafter, the FC-based power source starts to deliver energy to the system, and when the output voltage of the boost converter ( $V_{\text{BOOST}}$ ) reaches 1.8 V (the minimum voltage to turn on the microcontroller) the microcontroller is switched on. It configures and initializes general-purpose input/output (GPIO) pins as well as the ADCs to monitor the sample and control the power delivered by the FC.

The PGOOD signal (Figure 2b) monitors the state of the regulated voltage supply ( $V_{\text{BOOST}}$ ). It ensures that the e-reader performs the measurement when enough energy is harvested to start the application operation. In order to minimize power consumption, meanwhile there is not enough energy to start the measurement (PGOOD signal in a low state), the LDO remains disabled and the microcontroller stays in the low power mode (LPM). When the boost converter ( $V_{\text{BOOST}}$ ) reaches 2.9 V, the PGOOD changes to the high state. Afterwards, an interruption event wakes up the microcontroller from LPM, and it enables the LDO, which supplies the FEU’s components.

Then, the ADC pin ( $V_{\text{OCV}}$ ) begins to monitor the state of the sensor’s voltage. The “measurement phase” starts as soon as the signal provided by the sensor is stable.

Afterwards, the microcontroller turns on the analog switch (SW1), which connects the CE, and applies a DC bias voltage ( $V_{\text{IN}}$ ) to the sensor as is depicted in Figure 2b. Then, a timer starts to count until the moment in which the measurement takes place, TM. TM is the time that elapses between the CE’s connection and the measurement takes place, fixed for each particular biosensor.

During this time, the microcontroller remains in LPM. The criteria for determining the TM time is described in Section 3.2.

After the TM, the microcontroller exits the LPM state and the ADC captures the measurement signal ( $V_{OUT}$ ), which is proportional to the current provided by the sensor ( $I_{CELL}$ ).  $I_{CELL}$  can be obtained by Equation (1), as the input bias voltage ( $V_{IN}$ ), the TIA resistor ( $R_{TIA}$ ) and the output voltage ( $V_{OUT}$ ) are known.

In most situations, the relationship between the magnitude to measure and the voltage obtained is not linear. For this reason, we implemented a lookup table (LUT) [46–48] in the microcontroller to translate the data obtained to a current or concentration. A LUT is an array of data that allows linking input values to output values, replacing the runtime computation with a simple array indexing operation. It maps inputs to an output value by looking up or interpolating in a defined table of values.

Later, following Figure 3, the “display and sleep phase” takes place. In this phase, the microcontroller manages the drivers that control the display and shows the concentration value on the display. Finally, the microcontroller returns back to the LPM and remains in this state permanently.

The CSPU module is based on the MSP430FR5969 microcontroller (Texas Instruments; Dallas, Texas, USA). This microcontroller has been selected because of its good characteristics in terms of voltage, quiescent current and operating power consumption. It has a supply voltage that ranges from 1.8 V up to 3.6 V with one operating active mode and seven software-selectable low power modes. Furthermore, it consumes only 0.4  $\mu\text{A}/\text{MHz}$  in standby mode and 100  $\mu\text{A}/\text{MHz}$  in active mode. The microcontroller has an ultra-low-power 16-bit architecture that allows controlling the intelligent peripherals to extend the autonomy of the system.

#### 2.1.4. Display Unit

Different low power solutions could be used to show the detection result, like printed and flexible electrochromic displays [49,50]. In this study, a 3-digit 7-segments numerical liquid crystal display (LCD) has been used to show the result, due to its simple operation and low power consumption, it also operates at 3 V with a typical quiescent current of 0.33  $\mu\text{A}$ .

This kind of LCD uses many interconnects, to facilitate connection and control of the LCD, the CD4055B integrated circuit (IC) (Texas Instruments; Dallas, Texas, USA) has been used. It reduces the number of control signals needed to control the display and typically consumes 5  $\mu\text{A}$ . This IC is a single-digit BCD-to-7-segment decoder that allows controlling the 7-segments of each digit with only four pins. The display is controlled by the display-frequency input signal, which is a square-wave signal. The IC provides a square-wave signal to the selected segments that is 180 degrees out-of-phase with the common-signal, making these segments visible. The segments which are not selected have the square-wave signal and are in phase with the common-signal, so they are not visible. The consumption of the DU module is 16  $\mu\text{A}$ .

#### 2.2. Fuel Cells and Sensors

In order to validate the operation of the e-reader, we emulated different FCs and sensors reported in the literature (Figure 4). We emulated FCs and sensors based on urine/Cr(VI) [41] and methanol [51,52] by using a source measurement unit (SMU). Moreover, we carried out experimental tests with an emulated ethanol FC as a sensor [40] and a commercial ethanol FC as a power source.

These approaches fully validated the e-reader implementation. For each case, key design parameters are indicated, like the open-circuit voltage (OCV), and the related concentrations of the involved sample.

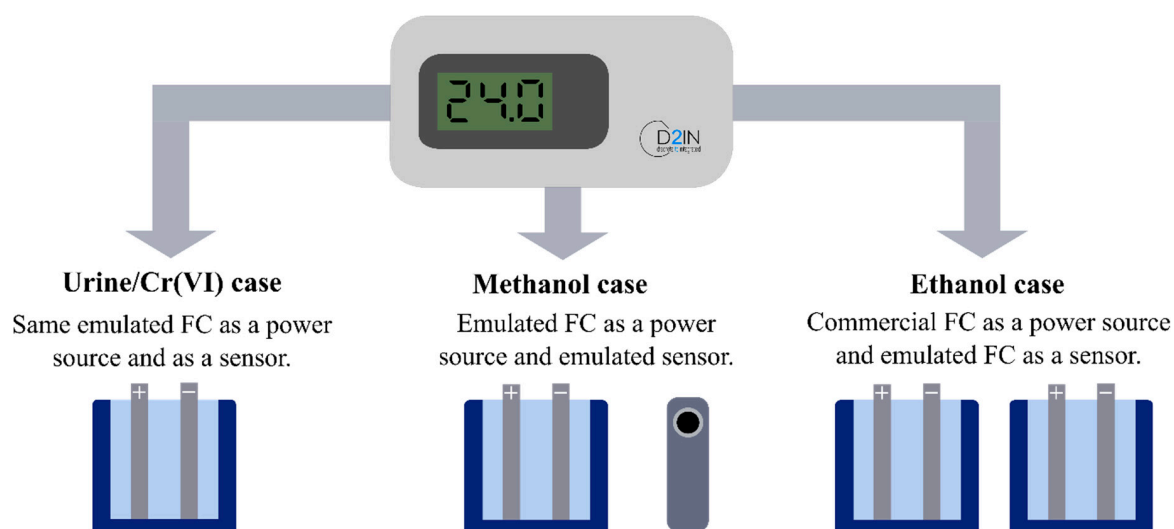


Figure 4. Summary diagram of the validation tests performed.

### 2.2.1. Urine/Cr(VI) Fuel Cell Case

The urine/Cr(VI)'s FC presented by [41] is able to generate electrical power from processing human urine and heavy metal, in this case, Cr(VI). This FC reduces Cr(VI) in human urine, using urine as fuel and Cr(VI) as oxidant. The open-circuit voltage (OCV) ranges from 1.11 V at  $13 \text{ mg}\cdot\text{L}^{-1}$  to 1.26 V at  $50 \text{ mg}\cdot\text{L}^{-1}$ . In addition, this FC provides a maximum power density going from  $3.4 \text{ W}\cdot\text{m}^{-2}$  at  $50 \text{ mg}\cdot\text{L}^{-1}$  of Cr(VI) to  $2.2 \text{ W}\cdot\text{m}^{-2}$  at  $13 \text{ mg}\cdot\text{L}^{-1}$  of Cr(VI). To validate the operation of the proposed system, we used the same urine/Cr (VI) FC as a sensor and as a power source.

### 2.2.2. Methanol Fuel Cell and Sensor Case

In this case, we used a methanol FC as a power source and as a sensor to detect methanol. We emulated and employed a passive direct methanol fuel cell (DMFC) as a power source for portable electronic devices [51]. In the study, the authors used six dual DMFC connected in series to produce energy. In order to validate the e-reader operation, we considered a single FC of  $1 \text{ cm}^2$  with a 1 M of methanol concentration. It was only necessary to use a single FC because the developed e-reader was a low power device and operated with a minimum voltage of 330 mV. A single DMFC with a 1 M of methanol concentration provides a maximum power density of  $5 \text{ mW}\cdot\text{cm}^{-2}$ , a maximum current density of  $22 \text{ mA}\cdot\text{cm}^{-2}$  and an OCV of 0.6 V.

The emulated sensor is reported in [52]. It is a wearable vapor/liquid amphibious electrochemical sensor for monitoring methanol. The sensor exhibits high selectivity, good repeatability, and reliable stability for both vapor and liquid methanol. It was tested with methanol concentrations that go from 0% to 6%, providing current densities that go from 90 to  $3.5 \mu\text{A}\cdot\text{mm}^{-2}$ . We validated the e-reader considering a methanol sensor of  $1 \text{ mm}^2$ .

### 2.2.3. Ethanol Fuel Cell Case

After emulating different approaches based on fuel cells and sensors, we carried on experimental verification working with a commercial FC. To perform the experimental test with the e-reader, we used as a power source the commercial FCJ-42 ethanol fuel cell science kit (Horizon Fuel Cell Technologies; Singapore). Due to the fact that the characteristics of this FC are not described, we characterized it, obtaining the I-V curves for different ethanol concentrations that go from 3% to 9%. This ethanol FC provides a maximum power going from 0.23 W at 9% to 0.186 W at 3%. The maximum current given is 700 mA at 9% and 540 mA at 3%. All concentrations tested presented an OCV close to 1 V. To validate the system, we used the commercial ethanol FC with 3% of concentration as a power source.

The chosen FC used to sense ethanol was presented in [40]. It is a single-cell membraneless microfluidic FC that operates in the presence of simulated body fluids, human serum, and blood enriched with ethanol as the fuel. It provides current densities up to  $6.5 \text{ mA}\cdot\text{cm}^{-2}$ .

### 2.3. Experimental Set-Up

The electronics validation and characterization were carried out with a source measurement unit (SMU) B2962A by Keysight Technology (Santa Rosa, CA, USA) and an Agilent Technologies oscilloscope MSO-X 3034A (Santa Clara, CA, USA).

In order to emulate the FCs and sensors previously presented, we introduced their I–V polarization curves into the SMU and performed a piecewise linear (PWL) interpolation. The PWL interpolation is a technique used in engineering to approximate a complex function by a simple linear function, which allows expressing the non-linear I–V characteristics that present FCs. Next, we analyzed the start-up of the power management unit (PMU) and emulated the current ( $I_{\text{CELL}}$ ) provided by the sensors and FCs.

Furthermore, we obtained the I–V curves in potentiodynamic mode at a scan rate of  $2 \text{ mV}\cdot\text{s}^{-1}$  to characterize the ethanol FC. We performed the ethanol concentrations with deionized water obtained from a Milli-Q<sup>®</sup> Advantage A10 water purification system and absolute ethanol for analysis (ACS grade) at a concentration of 99.8% (Panreac, Barcelona, Spain).

## 3. Results and Discussion

### 3.1. Electronic Reader Manufacturing

We developed a printed circuit board (PCB) and an outer case, both items build up the e-reader (Figure 5). The PCB is a double-sided printed circuit made in glass-reinforced epoxy laminate material (FR4) with silver-finish. The total size of the board was  $77.5 \text{ mm} \times 32.5 \text{ mm} \times 2 \text{ mm}$ . The case of the device had a size of  $85 \text{ mm} \times 42 \text{ mm} \times 21 \text{ mm}$  and was developed using three-dimensional (3D) printing. The case was made of a photosensitive epoxy resin called Accura<sup>®</sup> 25 and it was created with the solid-state stereolithography (SLA<sup>®</sup>) printing technology.

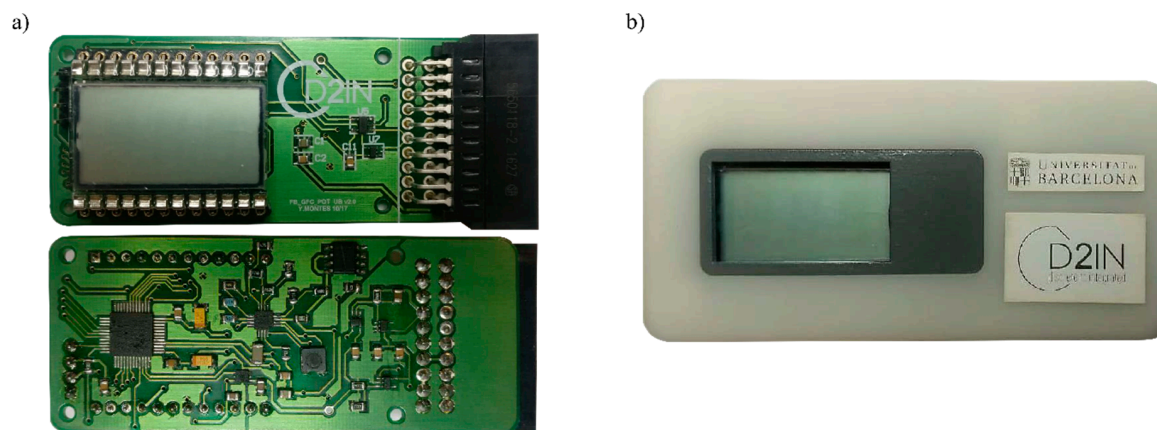


**Figure 5.** (a) Picture of the e-reader's printed circuit board (PCB). (b) Picture of the whole self-powered electronic reader: PCB and outer case.

### 3.2. Characterization and Calibration of the Self-Powered Electronic Reader

We characterized the e-reader in order to analyze its performance and uncertainty translating the cell current ( $I_{\text{CELL}}$ ) into a voltage ( $V_{\text{OUT}}$ ). The procedure followed was previously explained, in which the SMU and the oscilloscope were used.

First, we connected the SMU to the e-reader and we applied a current ramp ( $I_{\text{C}}$ ) from  $13 \mu\text{A}$  to  $0 \mu\text{A}$  with a change rate of  $1.85 \mu\text{A/s}$ . Then, we captured the potentiostat output voltage ( $V_{\text{OUT}}$ ) by the oscilloscope. We translated  $V_{\text{OUT}}$  into the measurement current ( $I_{\text{M}}$ ) with Equation (1). As is



shown in Figure 6, we compared the current measured by the e-reader ( $I_M$ ) with those applied by the SMU ( $I_G$ ). This test allowed us to obtain the uncertainty between the current generated ( $I_G$ ) and the current measured by the e-reader ( $I_M$ ). Analyzing these data, we obtained that the maximum relative uncertainty between  $I_G$  and  $I_M$  is 1.8%, which is the uncertainty associated with the FEU module. This maximum uncertainty was obtained at a nominal current value of 12.91  $\mu\text{A}$ , and it had an absolute uncertainty value of 0.24  $\mu\text{A}$ .

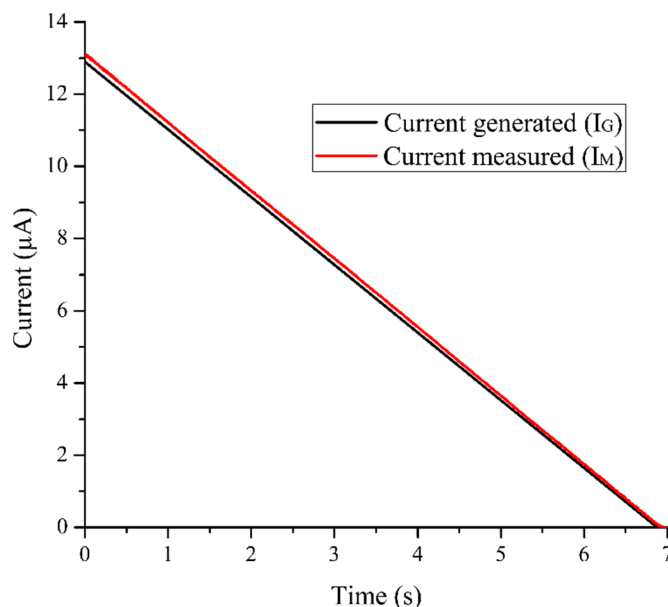


**Figure 6.** Uncertainty between the current generated by the SMU ( $I_G$ ) and the current measured by the front-end unit ( $I_M$ ).

As it is stated in Section 2.1.3., the definition of the moment in which the measurement takes place,  $T_M$ , is the key point. It depends mainly on two aspects: (a) The device resolution, which is constrained by the electronics' resolution, and (b) the measurement uncertainty. This depends on the change rate of the current because a slight deviation in the measurement time can affect the current value, since initially the current decreased quickly. In order to obtain the ideal moment to perform the measurement, the e-reader was calibrated for each sensor.

First, we established the polarization voltage ( $V_{IN}$ ) from the sensor's characterization, and we programmed the e-reader to drive the sensor to  $V_{IN}$ . Then, we connected the sensor to the e-reader and polarized it. After that, we captured the chronoamperometry curves with the SMU and analyzed the device resolution and the measurement.

The e-reader resolution is defined by the ADC resolution, which is time-invariant and has a value of 13 nA.

In a chronoamperometry, a redox reaction occurs when a potential step is applied to the electrode. The current decays  $t^{1/2}$ , obeying the Cottrell equation for reactions that are under diffusion control [53]. Consequently, the initial and the final region cannot afford to extract a measurement. During the initial time, a small deviation in the moment to extract the measurement is translated into a large current uncertainty. While in the final region, it is difficult to distinguish between concentrations because they are too close.

Considering these facts, we found the measurement uncertainty for different concentrations. As a result, we were able to establish the best moment to extract the measurement ( $T_M$ ). The time chosen in each case was the one which presented the lower uncertainty value for the worst case of detection, which was the detection of the lowest level of concentration.

### 3.3. Start-Up and Power Consumption of the E-Reader

Figure 7a shows the startup curve graph of the e-reader when it is powered by a commercial ethanol FC as an example case. The upper graph shows the voltage provided by the ethanol FC ( $V_{FC}$ ). While, the middle graph shows the boost converter voltage ( $V_{BOOST}$ ), which is used to supply both CSPU and the DU. In the end, the bottom graph displays the voltage provided by the low-dropout voltage regulator ( $V_{LDO}$ ), which supplies the analog components that comprise the FEU.

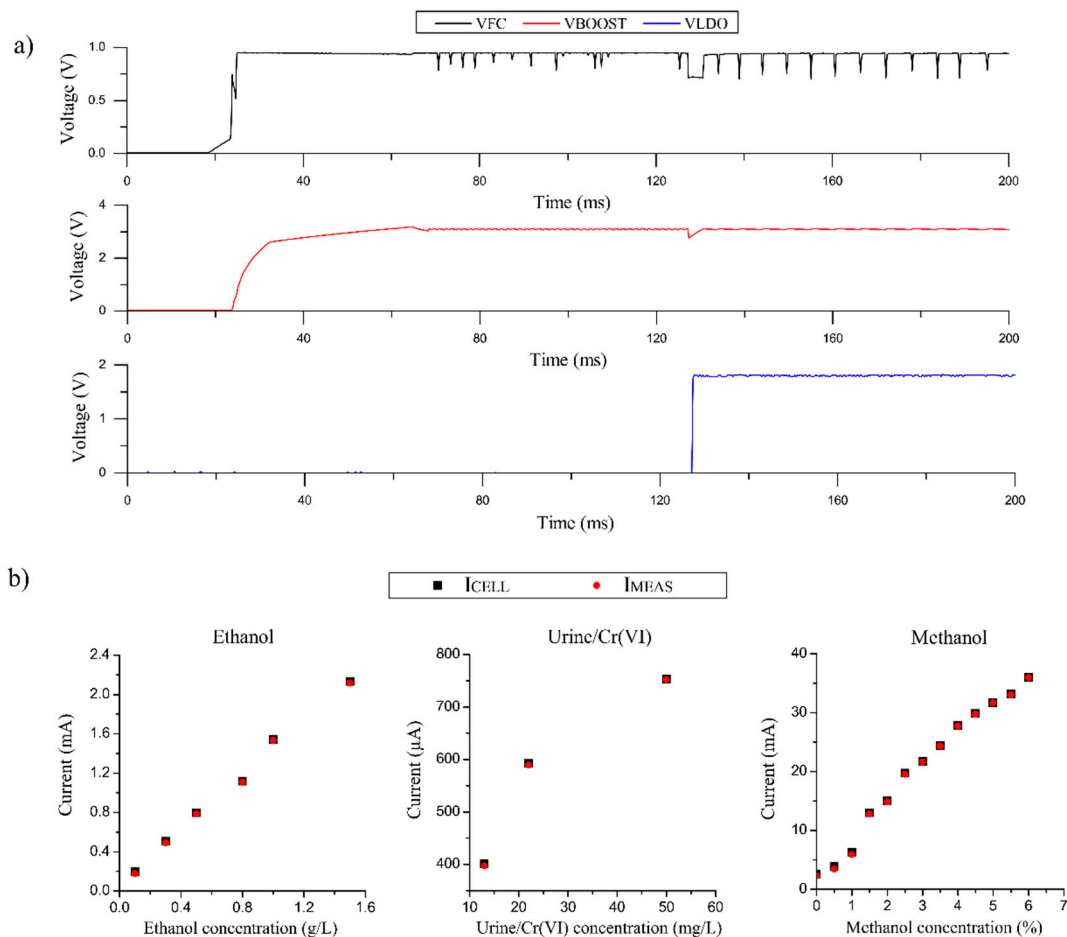


**Figure 7.** (a) Start-up curves of the e-reader powered by an ethanol FC. (b) Transfer function that relates the measured current by the e-reader with different emulated sensors and fuel cell concentrations (ethanol, urine and methanol), and the comparison against the current produced by the sensor ( $I_{CELL}$ ).

When the FC is connected to the e-reader, the PMU is enabled. It starts collecting energy and the  $V_{BOOST}$  signal increases. During 100 ms the  $V_{LDO}$  signal remains in a low state since there is not enough energy to start the whole system. When the PMU has harvested enough energy, the  $V_{LDO}$  signal changes to a high state and the system begins to operate. The peaks that appear in the  $V_{FC}$  signal correspond to the MPPT sampling system that optimizes the energy extraction from the power source. As it is shown in Figure 7a,  $V_{FC}$  is a noisy signal. For this reason,  $V_{FC}$  did not power any electronic components directly. The periodical peaks of  $V_{FC}$  were reduced by DC/DC boost converter ( $V_{BOOST}$ ), which supplies both CSPU and the DU. The FEU was the most sensitive circuit because it is the circuit that carried out the measurement. Thus, the voltage which supplied the FEU circuit ( $V_{LDO}$ ) was stabilized and regulated by a low-dropout voltage regulator (LDO).

We also obtained the e-reader's power consumption. When the power source was connected to the e-reader, it had a typical inrush current peak of 5 mW. At this moment, the e-reader enters into a low power operation mode, and consumes only 900  $\mu$ W. The system waits in this low power mode

until the voltage provided by the power source is stable. Then, the FEU module is switched on and the measurement is performed. Lastly, the numerical data is processed and displayed, and the e-reader returns to the low power mode. During the device's operation, the power consumption presents two peaks that increase the consumption instantly to 1 mW. These peaks occur when the FEU module is activated and when the data is processed and displayed.

### 3.4. Validation of the E-Reader

The system has been validated in different conditions and cases, with FCs of urine/Cr(VI), methanol and ethanol, and the methanol sensor.

We verified the efficient extraction of energy from the sample in different cases, enabling the operation of both the DC/DC boost converter and the LDO, components that supply the FEU and the CPSU. The transitory performance of the commercial FC was obtained, extracting the curves shown in Figure 7a. This figure shows the behavior of the power signals in the "disconnected phase" and the "start-up phase", explained in Figure 3. Moreover, we validated the stationary behavior of the device with the emulated FCs of methanol and urine. These tests confirmed the self-powered performance of the system, which can power the e-reader circuits with the same monitored sample.

Furthermore, we validated the FEU's module operation, measuring different current ranges produced by the FCs of urine/Cr(VI) and ethanol, and the methanol sensor. For all these experiments, we followed the same procedure. Firstly, we connected the sensor to the e-reader, and we polarized it to the proper bias voltage ( $V_{IN}$ ). When the sensor is polarized, it produces a current proportional to the concentration of the analyte ( $I_{CELL}$ ).  $I_{CELL}$  flows through the potentiostat circuit, which translates it into the voltage ( $V_{OUT}$ ). The microcontroller's ADC reads  $V_{OUT}$  and translates it to current ( $I_{MEAS}$ ) by a LUT, as stated in Section 2.1.3.

Figure 7b shows the comparison between the current produced by the emulated FC/sensor ( $I_{CELL}$ ) and the current measured by the e-reader ( $I_{MEAS}$ ). The figure depicts that the current measured by the e-reader is practically the same as the nominal current injected by the emulated FC. The results show that the maximum difference between  $I_{CELL}$  and  $I_{MEAS}$  is 1.8%, validating the operation of the FEU module of the e-reader with different ranges of current and demonstrating the accuracy of the e-reader.

These tests validated the operation of the system, demonstrating the ability of the device to power the whole system while measuring the concentration of the sample and displaying the numerical result on the e-reader's display. The validation has been carried out with three different FCs, although it can be adapted to operate with other FCs, measuring a wide range of analytes.

## 4. Conclusions

In this work, we presented and described, in detail, the full implementation of an electronic reader for self-powered POC solutions based on the use of FCs as a power source or as a power source and as a sensor. The operation of the e-reader was validated in different cases, using a commercial ethanol FC, three emulated FCs (urine, ethanol, and methanol) and a sensor (methanol), showing its capability of adaptation to different scenarios.

Due to its low power design, the platform can operate with a minimum voltage of 330 mV, consuming only 900  $\mu$ W in the low power mode. The device has been proven to exhibit reliable, robust, and effective results. It has a measurement uncertainty below 1.8%, a minimum resolution of 13 nA and a maximum measurement current of 3 mA. Furthermore, the plug-and-play device performs amperometric measurements automatically, in only a few seconds. The device presented in this work could be the first step towards the future of point-of-care since the system provides quantitative data, showing the numerical result on the display. Some advantages of the proposed device include: (i) No need for external power sources, since the same sample is used to power and sense; (ii) the ease of use; (ii) compactness and portability; (iii) the possibility of showing the data on a display, without the need for external laboratory equipment; (iv) adaptability to wide range of cases; and (v) the rapidity and accuracy of results. The portable device can operate with conventional lithium

batteries or biodegradable batteries [25] or with the sensing sample. It is a valuable characteristic in disadvantaged regions without a good electricity grid and batteries.

As future work, we propose to introduce a wireless communication system to show the resulting data on a smartphone or a laptop, a module to set the polarization voltage (VIN) externally, or an adjustable signal generator to perform cyclic voltammetry. A big challenge would be to integrate the device in a single chip, developing the system in a flexible substrate.

**Author Contributions:** Y.M.-C. developed, implemented and tested the point-of-care (POC) electronic device and acquisition software, performed the experimental study and analyzed and interpreted the acquired data. She wrote the manuscript and approved the final version of the manuscript. A.Á.-C. designed the power management unit and the outer case of the device as well as developed acquisition software. Besides, P.L.M.-C., M.P.-V. and J.C.-F. supervised the development of the POC device. P.L.M.-C., J.C.-F., M.P.-V. and A.Á.-C. have discussed the resultant data, contributed in the manuscript and approved the final version for its publication.

**Funding:** This research was funded by the Spanish Ministry of Economy, Agencia Estatal de Investigación, and Fondo Europeo de Desarrollo Regional (AEI/FEDER, UE), through the project Circuits for Energy Harvesting Management for Low-Voltage Low-Power Applications (MINAUTO) – grant number TEC2016-78284-C3-3-R).

**Conflicts of Interest:** The authors declare no conflict of interest.

## References

1. Dyer, C.K. Fuel cells and portable electronics. In Proceedings of the 2004 Symposium on VLSI Circuits. Digest of Technical Papers (IEEE Cat. No.04CH37525), Honolulu, HI, USA, 17–19 June 2004; pp. 124–127.
2. Stone, C. Fuel cell technologies powering portable electronic devices. *Fuel Cells Bull.* **2007**, *2007*, 12–15. [[CrossRef](#)]
3. Safdar, M.; Jänis, J.; Sánchez, S. Microfluidic fuel cells for energy generation. *Lab Chip* **2016**, *16*, 2754–2758. [[CrossRef](#)] [[PubMed](#)]
4. Justino, C.I.L.; Duarte, A.C.; Rocha-Santos, T.A.P. Recent progress in biosensors for environmental monitoring: A review. *Sensors* **2017**, *19*, 2918. [[CrossRef](#)] [[PubMed](#)]
5. Grattieri, M.; Minter, S.D. Self-Powered Biosensors. *ACS Sens.* **2018**, *3*, 44–53. [[CrossRef](#)] [[PubMed](#)]
6. Kim, J.; Campbell, A.S.; de Ávila, B.E.-F.; Wang, J. Wearable biosensors for healthcare monitoring. *Nat. Biotechnol.* **2019**, *37*, 389–406. [[CrossRef](#)] [[PubMed](#)]
7. Hong, Y.J.; Jeong, H.; Cho, K.W.; Lu, N.; Kim, D. Wearable and Implantable Devices for Cardiovascular Healthcare: From Monitoring to Therapy Based on Flexible and Stretchable Electronics. *Adv. Funct. Mater.* **2019**, *29*, 1808247. [[CrossRef](#)]
8. Zarei, M. Portable biosensing devices for point-of-care diagnostics: Recent developments and applications. *TrAC-Trends Anal. Chem.* **2017**, *91*, 26–41. [[CrossRef](#)]
9. Choi, S. Powering point-of-care diagnostic devices. *Biotechnol. Adv.* **2016**, *34*, 321–330. [[CrossRef](#)]
10. Yetisen, A.K.; Akram, M.S.; Lowe, C.R. Paper-based microfluidic point-of-care diagnostic devices. *Lab Chip* **2013**, *13*, 2210–2251. [[CrossRef](#)]
11. Jia, W.; Wang, X.; Imani, S.; Bandodkar, A.J.; Ramírez, J.; Mercier, P.P.; Wang, J. Wearable textile biofuel cells for powering electronics. *J. Mater. Chem. A* **2014**, *2*, 18184–18189. [[CrossRef](#)]
12. Slaughter, G.; Kulkarni, T. A self-powered glucose biosensing system. *Biosens. Bioelectron.* **2016**, *78*, 45–50. [[CrossRef](#)]
13. Bahk, J.-H.; Fang, H.; Yazawa, K.; Shakouri, A. Flexible thermoelectric materials and device optimization for wearable energy harvesting. *J. Mater. Chem. C* **2015**, *3*, 10362–10374. [[CrossRef](#)]
14. Dagdeviren, C.; Joe, P.; Tuzman, O.L.; Park, K.-I.; Lee, K.J.; Shi, Y.; Huang, Y.; Rogers, J.A. Recent progress in flexible and stretchable piezoelectric devices for mechanical energy harvesting, sensing and actuation. *Extrem. Mech. Lett.* **2016**, *9*, 269–281. [[CrossRef](#)]
15. Slate, A.J.; Whitehead, K.A.; Brownson, D.A.C.; Banks, C.E. Microbial fuel cells: An overview of current technology. *Renew. Sustain. Energy Rev.* **2019**, *101*, 60–81. [[CrossRef](#)]
16. Gonzalez-Solino, C.; Lorenzo, M. Enzymatic Fuel Cells: Towards Self-Powered Implantable and Wearable Diagnostics. *Biosensors* **2018**, *8*, 11. [[CrossRef](#)] [[PubMed](#)]
17. Winfield, J.; Ieropoulos, I.; Greenman, J. Investigating a cascade of seven hydraulically connected microbial fuel cells. *Bioresour. Technol.* **2012**, *110*, 245–250. [[CrossRef](#)]

18. Pasternak, G.; Greenman, J.; Ieropoulos, I. Self-powered, autonomous Biological Oxygen Demand biosensor for online water quality monitoring. *Sens. Actuators B Chem.* **2017**, *244*, 815–822. [[CrossRef](#)]
19. Majdecka, D.; Draminska, S.; Janusek, D.; Kryszynski, P.; Bilewicz, R. A self-powered biosensing device with an integrated hybrid biofuel cell for intermittent monitoring of analytes. *Biosens. Bioelectron.* **2018**, *102*, 383–388. [[CrossRef](#)]
20. Montes-Cebrián, Y.; del Torno-de Román, L.; Álvarez-Carulla, A.; Colomer-Farrarons, J.; Minter, S.D.; Sabaté, N.; Miribel-Català, P.L.; Esquivel, J.P. 'Plug-and-Power' Point-of-Care diagnostics: A novel approach for self-powered electronic reader-based portable analytical devices. *Biosens. Bioelectron.* **2018**, *118*, 88–96. [[CrossRef](#)]
21. Mugheri, A.Q.; Tahira, A.; Sherazi, S.T.H.; Abro, M.I.; Willander, M.; Ibupoto, Z.H. An Amperometric Indirect Determination of Heavy Metal Ions through Inhibition of Glucose Oxidase Immobilized on Cobalt Oxide Nanostructures. *Sens. Lett.* **2016**, *14*, 1178–1186. [[CrossRef](#)]
22. Nomngongo, P.N.; Ngila, J.C.; Nyamori, V.O.; Songa, E.A.; Iwuoha, E.I. Determination of Selected Heavy Metals Using Amperometric Horseradish Peroxidase (HRP) Inhibition Biosensor. *Anal. Lett.* **2011**, *44*, 2031–2046. [[CrossRef](#)]
23. Szulczyński, B.; Gębicki, J. Currently Commercially Available Chemical Sensors Employed for Detection of Volatile Organic Compounds in Outdoor and Indoor Air. *Environments* **2017**, *4*, 21. [[CrossRef](#)]
24. Spinelle, L.; Gerboles, M.; Kok, G.; Persijn, S.; Sauerwald, T. Review of portable and low-cost sensors for the ambient air monitoring of benzene and other volatile organic compounds. *Sensors* **2017**, *17*, 1520. [[CrossRef](#)] [[PubMed](#)]
25. Esquivel, J.P.; Alday, P.; Ibrahim, O.A.; Fernández, B.; Kjeang, E.; Sabaté, N. A Metal-Free and Biotically Degradable Battery for Portable Single-Use Applications. *Adv. Energy Mater.* **2017**, *7*, 1700275. [[CrossRef](#)]
26. Hamoda, M.F. Air pollutants emissions from waste treatment and disposal facilities. *J. Environ. Sci. Heal.—Part A Toxic/Hazard. Subst. Environ. Eng.* **2006**, *41*, 77–85. [[CrossRef](#)] [[PubMed](#)]
27. Brey, J.; Muñoz, D.; Mesa, V.; Guerrero, T. Use of Fuel Cells and Electrolyzers in Space Applications: From Energy Storage to Propulsion/Deorbitation. In Proceedings of the E3S Web of Conferences, Seville, Spain, 3–7 October 2016.
28. Burke, K.A. Fuel Cells for Space Science Applications. In Proceedings of the 1st International Energy Conversion Engineering Conference IECEC, Cleveland, OH, USA, 17–21 August 2003.
29. Baingane, A.; Slaughter, G. Self-Powered Electrochemical Lactate Biosensing. *Energies* **2017**, *10*, 1582. [[CrossRef](#)]
30. Garcia, S.O.; Ulyanova, Y.V.; Figueroa-Teran, R.; Bhatt, K.H.; Singhal, S.; Atanassov, P. Wearable Sensor System Powered by a Biofuel Cell for Detection of Lactate Levels in Sweat. *ECS J. Solid State Sci. Technol.* **2016**, *5*, M3075–M3081. [[CrossRef](#)] [[PubMed](#)]
31. Bhandodkar, A.J.; You, J.-M.; Kim, N.-H.; Gu, Y.; Kumar, R.; Mohan, A.M.V.; Kurniawan, J.; Imani, S.; Nakagawa, T.; Parish, B.; et al. Soft, stretchable, high power density electronic skin-based biofuel cells for scavenging energy from human sweat. *Energy Environ. Sci.* **2017**, *10*, 1581–1589. [[CrossRef](#)]
32. Niitsu, K.; Kobayashi, A.; Nishio, Y.; Hayashi, K.; Ikeda, K.; Ando, T.; Ogawa, Y.; Kai, H.; Nishizawa, M.; Nakazato, K. A Self-Powered Supply-Sensing Biosensor Platform Using Bio Fuel Cell and Low-Voltage, Low-Cost CMOS Supply-Controlled Ring Oscillator With Inductive-Coupling Transmitter for Healthcare IoT. *IEEE Trans. Circuits Syst. I Regul. Pap.* **2018**, *65*, 2784–2796. [[CrossRef](#)]
33. Narvaez Villarrubia, C.W.; Soavi, F.; Santoro, C.; Arbizzani, C.; Serov, A.; Rojas-Carbonell, S.; Gupta, G.; Atanassov, P. Self-feeding paper based biofuel cell/self-powered hybrid  $\mu$ -supercapacitor integrated system. *Biosens. Bioelectron.* **2016**, *86*, 459–465. [[CrossRef](#)] [[PubMed](#)]
34. Slaughter, G.; Kulkarni, T. Highly Selective and Sensitive Self-Powered Glucose Sensor Based on Capacitor Circuit. *Sci. Rep.* **2017**, *7*, 1417. [[CrossRef](#)] [[PubMed](#)]
35. Fischer, C.; Fraiwan, A.; Choi, S. A 3D paper-based enzymatic fuel cell for self-powered, low-cost glucose monitoring. *Biosens. Bioelectron.* **2016**, *79*, 193–197. [[CrossRef](#)] [[PubMed](#)]
36. Lee, I.; Sode, T.; Loew, N.; Tsugawa, W.; Lowe, C.R.; Sode, K. Continuous operation of an ultra-low-power microcontroller using glucose as the sole energy source. *Biosens. Bioelectron.* **2017**, *93*, 335–339. [[CrossRef](#)] [[PubMed](#)]
37. Bissonnette, L.; Bergeron, M.G. Portable devices and mobile instruments for infectious diseases point-of-care testing. *Expert Rev. Mol. Diagn.* **2017**, *17*, 471–494. [[CrossRef](#)] [[PubMed](#)]

38. Stoot, L.J.; Cairns, N.A.; Cull, F.; Taylor, J.J.; Jeffrey, J.D.; Morin, F.; Mandelman, J.W.; Clark, T.D.; Cooke, S.J. Use of portable blood physiology point-of-care devices for basic and applied research on vertebrates: A review. *Conserv. Physiol.* **2014**, *2*, 1. [[CrossRef](#)] [[PubMed](#)]
39. Vashist, S.K.; Luppia, P.B.; Yeo, L.Y.; Ozcan, A.; Luong, J.H.T. Emerging Technologies for Next-Generation Point-of-Care Testing. *Trends Biotechnol.* **2015**, *33*, 692–705. [[CrossRef](#)]
40. Galindo-de-la-Rosa, J.; Arjona, N.; Moreno-Zuria, A.; Ortiz-Ortega, E.; Guerra-Balcázar, M.; Ledesma-García, J.; Arriaga, L.G. Evaluation of single and stack membraneless enzymatic fuel cells based on ethanol in simulated body fluids. *Biosens. Bioelectron.* **2017**, *92*, 117–124. [[CrossRef](#)]
41. Xu, W.; Zhang, H.; Li, G.; Wu, Z. A urine/Cr(VI) fuel cell—Electrical power from processing heavy metal and human urine. *J. Electroanal. Chem.* **2016**, *764*, 38–44. [[CrossRef](#)]
42. Wang, L.; He, M.; Hu, Y.; Zhang, Y.; Liu, X.; Wang, G. A “4-cell” modular passive DMFC (direct methanol fuel cell) stack for portable applications. *Energy* **2015**, *82*, 229–235. [[CrossRef](#)]
43. Kamarudin, S.K.; Achmad, F.; Daud, W.R.W. Overview on the application of direct methanol fuel cell (DMFC) for portable electronic devices. *Int. J. Hydrog. Energy* **2009**, *34*, 6902–6916. [[CrossRef](#)]
44. Rashid, M.; Jun, T.-S.; Jung, Y.; Kim, Y.S. Bimetallic core-shell Ag@Pt nanoparticle-decorated MWNT electrodes for amperometric H<sub>2</sub> sensors and direct methanol fuel cells. *Sens. Actuators B Chem.* **2015**, *208*, 7–13. [[CrossRef](#)]
45. Sales, M.G.F.; Brandão, L. Autonomous electrochemical biosensors: A new vision to direct methanol fuel cells. *Biosens. Bioelectron.* **2017**, *98*, 428–436. [[CrossRef](#)] [[PubMed](#)]
46. Liang, K.-F.; Chen, J.-H.; Chen, Y.-J.E. A Quadratic-Interpolated LUT-Based Digital Predistortion Technique for Cellular Power Amplifiers. *IEEE Trans. Circuits Syst. II Express Briefs* **2014**, *61*, 133–137. [[CrossRef](#)]
47. Bandyopadhyay, S.; Das, A.; Mukherjee, A.; Dey, D.; Bhattacharyya, B.; Munshi, S. A Linearization Scheme for Thermistor-Based Sensing in Biomedical Studies. *IEEE Sens. J.* **2016**, *16*, 603–609. [[CrossRef](#)]
48. Shyu, L.-H.; Wang, Y.-C.; Chang, C.-P.; Shih, H.-T.; Manske, E. A signal interpolation method for Fabry–Perot interferometer utilized in mechanical vibration measurement. *Measurement* **2016**, *92*, 83–88. [[CrossRef](#)]
49. Andersson Ersman, P.; Kawahara, J.; Berggren, M. Printed passive matrix addressed electrochromic displays. *Org. Electron.* **2013**, *14*, 3371–3378. [[CrossRef](#)]
50. Cao, X.; Lau, C.; Liu, Y.; Wu, F.; Gui, H.; Liu, Q.; Ma, Y.; Wan, H.; Amer, M.R.; Zhou, C. Fully Screen-Printed, Large-Area, and Flexible Active-Matrix Electrochromic Displays Using Carbon Nanotube Thin-Film Transistors. *ACS Nano* **2016**, *10*, 9816–9822. [[CrossRef](#)] [[PubMed](#)]
51. Achmad, F.; Kamarudin, S.K.; Daud, W.R.W.; Majlan, E.H. Passive direct methanol fuel cells for portable electronic devices. *Appl. Energy* **2011**, *88*, 1681–1689. [[CrossRef](#)]
52. Jiang, Y.; Ma, J.; Lv, J.; Ma, H.; Xia, H.; Wang, J.; Yang, C.; Xue, M.; Li, G.; Zhu, N. Facile Wearable Vapor/Liquid Amphibious Methanol Sensor. *ACS Sens.* **2019**, *7*, 56. [[CrossRef](#)]
53. Bard, A.J.; Faulkner, L.R. *Electrochemical Methods: Fundamentals and Applications*; Wiley: New York, NY, USA, 2001; ISBN 0471043729.





## 2.3 Publication 3

### Competitive USB-Powered Hand-Held Potentiostat for POC Applications: An HRP Detection Case

*By*

**‘Yaiza Montes-Cebrián<sup>1\*</sup>**, Albert Álvarez-Carulla<sup>1</sup>, Gisela Ruiz-Vega<sup>1</sup>, Jordi Colomer-Farrarons<sup>1</sup>, Manel Puig-Vidal<sup>1</sup>, Eva Baldrich<sup>2,3</sup> and, Pere Ll. Miribel-Catalá<sup>1</sup>.

<sup>1</sup> *Discrete-to-Integrated (D2In) Research Group, Department of Electronic and Biomedical Engineering, Faculty of Physics, University of Barcelona (UB), 1st Martí i Franqués St., 08028 Barcelona, Spain*

<sup>2</sup> *Diagnostic Nanotools Group, Cibbim-Nanomedicine, Vall Hebron Research Institute (VHIR), Universitat Autònoma de Barcelona, 08035 Barcelona, Spain*

<sup>3</sup> *CIBER de Bioingeniería, Biomateriales y Nanobiomedicina (CIBER-BNN), 28029 Madrid, Spain*

*Published in*

**Sensors** 2019, 19, 5388; doi:10.3390/s19245388





Article

# Competitive USB-Powered Hand-Held Potentiostat for POC Applications: An HRP Detection Case

Yaiza Montes-Cebrián <sup>1,\*</sup>, Albert Álvarez-Carulla <sup>1</sup>, Gisela Ruiz-Vega <sup>2</sup>,  
Jordi Colomer-Farrarons <sup>1</sup>, Manel Puig-Vidal <sup>1</sup>, Eva Baldrich <sup>2,3</sup> and Pere Ll. Miribel-Català <sup>1</sup>

<sup>1</sup> Department of Electronics and Biomedical Engineering, Faculty of Physics, Universitat de Barcelona, 08028 Barcelona, Spain; albertalvarez@ub.edu (A.Á.-C.); jcolomerf@ub.edu (J.C.-F.); manel.puig@ub.edu (M.P.-V.); peremiribelcatala@ub.edu (P.L.M.-C.)

<sup>2</sup> Diagnostic Nanotools Group, Cibbim-Nanomedicine, Vall Hebron Research Institute (VHIR), Universitat Autònoma de Barcelona, 08035 Barcelona, Spain; gisela.ruiz@vhir.org (G.R.-V.); eva.baldrich@vhir.org (E.B.)

<sup>3</sup> CIBER de Bioingeniería, Biomateriales y Nanomedicina (CIBER-BBN), 28029 Madrid, Spain

\* Correspondence: ymontes@ub.edu; Tel.: +34-93-4020876

Received: 10 November 2019; Accepted: 3 December 2019; Published: 6 December 2019



**Abstract:** Considerable efforts are made to develop Point-of-Care (POC) diagnostic tests. POC devices have the potential to match or surpass conventional systems regarding time, accuracy, and cost, and they are significantly easier to operate by or close to the patient. This strongly depends on the availability of miniaturized measurement equipment able to provide a fast and sensitive response. This paper presents a low-cost, portable, miniaturized USB-powered potentiostat for electrochemical analysis, which has been designed, fabricated, characterized, and tested against three forms of high-cost commercial equipment. The portable platform has a final size of 10.5 × 5.8 × 2.5 cm, a weight of 41 g, and an approximate manufacturing cost of \$85 USD. It includes three main components: the power module which generates a stable voltage and a negative supply, the front-end module that comprises a dual-supply potentiostat, and the back-end module, composed of a microcontroller unit and a LabVIEW-based graphic user interface, granting plug-and-play and easy-to-use operation on any computer. The performance of this prototype was evaluated by detecting chronoamperometrically horseradish peroxidase (HRP), the enzymatic label most widely used in electrochemical biosensors. As will be shown, the miniaturized platform detected HRP at concentrations ranging from 0.01 ng·mL<sup>-1</sup> to 1 µg·mL<sup>-1</sup>, with results comparable to those obtained with the three commercial electrochemical systems.

**Keywords:** horseradish peroxidase (HRP) chronoamperometry; electrochemical biosensor; reconfigurable potentiostat; portable; low-cost electronics; USB-powered

## 1. Introduction

Traditionally, diagnostic tests are performed at central laboratories equipped with automated bench-top analyzers that provide highly reproducible and quantitative diagnostic results. Consequently, patients must often wait for long periods before receiving their test results. This circumstance is most common in developing countries and rural areas, where the lack of access to basic diagnostic equipment and trained personnel is an additional challenge [1]. This issue has resulted in an interest to develop Point-of-Care (POC) testing devices in recent years [2]. POC systems are diagnostic instruments that provide rapid results geographically near the patient, even when handled by untrained personnel. Rigorous requirements are set for POC diagnostic systems following the World Health Organization (WHO) ASSURED criteria (Affordable, Sensitive, Specific, User-friendly, Rapid and Robust, Equipment-free and Delivered to end-users) [3]. According to this standard, POC

platforms must deliver quick results for early-stage disease detection to enable rapid intervention and improve patient quality of life. The provided results must be accurate, reproducible, and optimally quantitative, and they must be comparable to those obtained by bench-top analyzers at central laboratories. Furthermore, these POC devices must be inexpensive, handheld, or at least portable and easy-to-use, making them usable by non-professional personnel.

Many portable POCs are based on electrochemical detection [4–6]. Nowadays, glucose monitoring POC devices (glucometers) are the most widespread miniaturized test systems. Of the main reasons, glucose sensors are inexpensive, easy to produce, small, and easy-to-use [7]. Most glucometers are based on potentiostats, measurement equipment that allow for the studying of oxidation-reduction (redox) reactions taking place in a test solution or at the electrode surface. In this context, the redox activity generates a current proportional to the concentration of the electrochemically active molecules that are being monitored. These systems are suitable in a wide range of applications, such as medical and health care monitoring [8], environmental measurements [9], or construction and characterization of portable biosensors [10], among others. There are different approaches to implement such solutions depending on the requirements of each situation [2], where the budget constraints are one of the main considerations. For instance, conventional bench-top potentiostats designed for research can perform a wide variety of electrochemical analysis. However, they are typically complex, expensive, and tend to be bulky, making them unsuitable for POC applications. In contrast, some research groups have developed miniaturized potentiostat-based single-chip platforms [11,12]. These devices are very small, low-powered, and customizable for specific applications, although the fabrication costs are too elevated for POC implementation.

The use of commercial off-the-shelf (COTS) integrated circuits (IC) is an affordable way to miniaturize instrumentation at minimum cost. Some examples based on potentiostats constructed with COTS components can be found in the state-of-the-art for a wide range of applications [13–16]. For instance, a portable system was developed based on a LMP91000EVM potentiostat (Texas Instruments; Dallas, TX, USA) and a Raspberry Pi 2 Model B microcontroller, which accomplished amperometric detection of progesterone in undiluted saliva making use of disposable immunosensors [17]. A similar COTS-based potentiostat was proposed in [18], which included a wireless module to transmit the measurements to a remote database. The effectiveness of the proposal was assessed by measuring ascorbic acid and comparing the results with those provided by a commercial potentiostat. Another example able to transmit data to a PC or via Bluetooth communication is the portable electrochemical amperometric analyzer proposed in [19]. In this study, the performance and reliability of the platform were validated using an indium tin oxide glass electrode. The low-cost miniaturized potentiostat reported in [20] was also based on an LMP91000 evaluation board, this time assembled to a BeagleBone development board. The system performed cyclic voltammetry (CV) measurements to achieve electrochemical cortisol immunosensing, obtaining a limit of detection of 1 pM of cortisol with a sensitivity of 1.24  $\mu$ M. In a different approach, Muñoz-Martinez et al. [21] described a system capable of performing electrochemical sensing over system-on-a-chip platforms. To validate the system, they performed diverse electrochemical experiments and a comparison between the COTS system and a commercial potentiostat. Alternatively, smartphones have been exploited as a resource for powering the system, data processing, and Big-Data management [22,23]. One of the most recent advances in the field is the employment of self-powered platforms based on the use of a fuel cell (FC) acting as a power source. In this scenario, the same FC may even act simultaneously as a power source and as a sensor [24]. These solutions use smartphone resources like an audio earphone port [25] or NFC functionality [26].

The main features required for portable electrochemical instrumentation systems are the following: to have a small size, low power consumption, high precision measurements and low fabrication, and maintenance costs. Taking into account these considerations, we have designed a miniaturized, robust, and customizable USB-based system for amperometric detection. The presented system, dubbed AmpStat, is composed of three parts: (a) a connector that houses the disposable amperometric sensor,

(b) an embedded electronic system for measurement acquisition, and (c) AmpView, custom software which displays and stores the results. The size of the miniaturized platform is  $10.5 \times 5.8 \times 2.5$  cm and it weighs 41 g. The full-custom circuit, which contains the power module and the front-end module, operates a low-voltage condition of 3.6 V and only consumes up to 235  $\mu\text{A}$ . Moreover, a single prototype has an approximate manufacturing cost of \$85 USD.

Operation of the proposed system was initially evaluated by detecting amperometrically horseradish peroxidase (HRP). HRP has a particular commercial and medical interest in the molecular biology, medicine, biotechnology, and diagnostic industry fields, as well as broad applicability in life sciences [27]. For instance, HRP is very common in biomedical applications, in which it is used to catalyze hydrogels [28]. On the other hand, HRP and a wide variety of peroxidase enzyme mimetics are extensively employed as electrode modifiers, bioreceptors, and labels to produce enzymatic and sandwich electrochemical biosensors [29–31].

As will be shown, the USB-powered prototype developed here provided current measurement from 5 nA to 11  $\mu\text{A}$  in real-time and could be adjusted to register currents up to 3 mA. This allowed detecting HRP at concentrations ranging from  $0.01 \text{ ng}\cdot\text{mL}^{-1}$  to  $1 \text{ }\mu\text{g}\cdot\text{mL}^{-1}$  using screen-printed carbon electrodes (SPCE) and a ready-to-use commercial substrate solution, with results comparable to those obtained with three-commercial potentiostats.

## 2. Materials and Methods

### 2.1. Portable Potentiostat

The architecture of the POC system is divided into three parts (Figure 1): (a) a Front-End Module (FEM), which drives the sensor, measures the current provided by the sensor ( $I_{\text{SENSE}}$ ) and translates the current into voltage ( $V_{\text{OUT}}$ ), (b) a Power Module (PM) that generates a stable voltage and virtual ground, creating a negative supply that allows measuring negative signals, and (c) a Back-End Module (BEM), comprised of a microcontroller unit (MCU), which processes the  $V_{\text{OUT}}$ , translates it into a current and sends the result via USB to the computer, and a graphic user interface (GUI), which displays the data on the computer. The block diagram of the system is depicted in Figure 1.

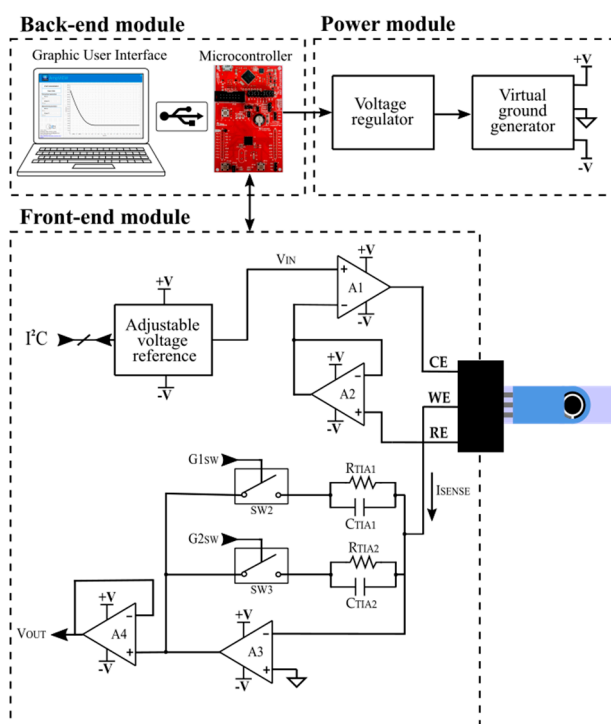


Figure 1. Block diagram of the miniaturized portable potentiostat.

### 2.1.1. Front-End Module (FEM): Signal Acquisition Module Description

This module performs two tasks: (a) drives the sensor electrodes to the desired voltage ( $V_{IN}$ ) and (b) measures the current provided by the sensor ( $I_{SENSE}$ ), translating it into voltage ( $V_{OUT}$ ) through a Transimpedance Amplifier (TIA) to be read by the MCU.

For  $V_{IN}$  generation, we use an adjustable voltage reference based on the AD5321 IC (Analog Devices; Norwood, Massachusetts, USA). This is a 12-bit voltage output Digital-to-Analog Converter (DAC), which has a typical consumption of 120  $\mu$ A at 3 V and 0.05  $\mu$ A in power-down mode. The DAC is controlled by the MCU through a 2-wire serial interface, compatible with the I2C protocol.

The designed potentiostat is based on a three-electrode topology. Two operational amplifiers (A1 and A2) polarize the sensor and track  $V_{IN}$  to the reference electrode (RE), whose low-input-bias current avoids voltage distortion. An operational amplifier in transimpedance configuration (A3) performs the current readout and translates the current registered between the counter (CE) and the working electrodes (WE) into a voltage signal ( $V_{OUT}$ ) by means of a sensing resistor ( $R_{TIA}$ ). The system includes two gain resistors ( $R_{TIA1}$  and  $R_{TIA2}$ ) to measure a wide current range. Two switches ( $SW_1$  and  $SW_2$ ) connect the suitable resistor, depending on the current range to measure. In this way, if the system detects that the measurement is out of range, it automatically changes the  $R_{TIA}$  to adjust the measurement circuit to the current range. Two capacitors,  $C_{TIA1}$  and  $C_{TIA2}$ , are connected in parallel with the gain resistors. Both passive components act as a filter, avoiding noise in the corresponding measurement range. Finally, a unity gain buffer amplifier (A4), located between the TIA and the MCU, isolates both parts in order to avoid errors in measurement.

As stated before, the potentiostat circuit translates  $I_{SENSE}$  into  $V_{OUT}$  through  $R_{TIA}$ . Both parameters are related according to Equation (1),

$$V_{OUT} = -R_{TIA} \cdot I_{SENSE} \quad (1)$$

in which  $V_{OUT}$  has a negative value. Accordingly, a dual-supply operational amplifier (positive and negative operation voltage) is required to perform the electrochemical measurement. The operational amplifier used here is a LPV521 (Texas Instruments, Dallas, TX, USA). This nano-power amplifier operates from 1.6 V up to 5.5 V with a typical current consumption of 345 nA. It has a typical offset voltage of 0.1 mV at 1.8 V and a typical bias current of 0.01 pA at 1.8 V. A low-resistance and low-power consumption switch (ADG702; Analog Devices; Norwood, MA, USA) is used to change the current range, which has a typical current consumption of 1 nA and a typical on-resistance of 40  $\Omega$ . Moreover, all the resistors used in the system have a 1% tolerance to assure a minimum uncertainty in the measurement.

### 2.1.2. Back-End Module (BEM): Processing and Display Module Description

The Back-end module is composed of a MCU and a GUI. The MCU used is the MSP430FR5969 LaunchPad development kit. It is a low-cost evaluation module for rapid prototyping, which is based on the MSP430FR5969 microcontroller and includes on-board emulation for programming and debugging. In addition, it is simplified by a 20-pin header, which allows for quick access to General Purpose Input/Output ports (GPIOs), peripherals for communication, Analog-to-Digital Converters (ADC), timers, etc. The MCU controls the DAC, which generates  $V_{IN}$  signal through an I<sup>2</sup>C protocol and acquires the  $V_{OUT}$  from the FEM by means of the ADC. It also activates the suitable switch, which sets the best  $R_{TIA}$  value assuring the maximum measurement range. Furthermore, it processes the obtained data, translating it into current and sending it to the computer via USB port.

The full-custom GUI, AmpVIEW, is developed using LabVIEW (National Instruments; Austin, TX, USA), a development software for visual language programming. AmpVIEW controls the system, including the measurement time and applied voltage and, at the same time, it registers and displays the chronoamperometry measurement in real-time. Figure 2 summarizes the procedure followed to perform measurements and a picture of the GUI. Once the program has been turned on, the user must

set the pretreatment and measurement parameters (time and sensor's polarization voltage) and must press the "Start Measurement" button. An error message appears on the display when the device has not been connected to the computer and the process ends. In the case of having the device connected, the MCU configures the GPIOs and the ADCs ports, it controls the DAC through the I<sup>2</sup>C protocol and it starts the chronoamperometry. While the FEM drives the sensor, the MCU acquires the  $V_{OUT}$  signal and it sends the result via USB to the GUI, which displays the data in real-time. When the measurement is finished, the user can save the data in a file pressing the "Export Data" button, which generates a csv or xlsx file with the chronoamperometry data. In addition, the measurement can be aborted at any moment by pressing the "Stop Measurement" button.

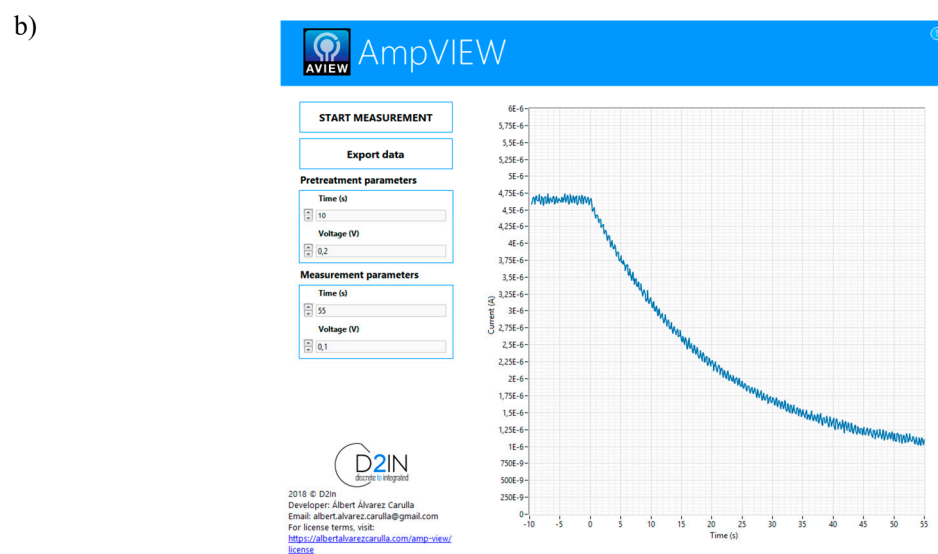
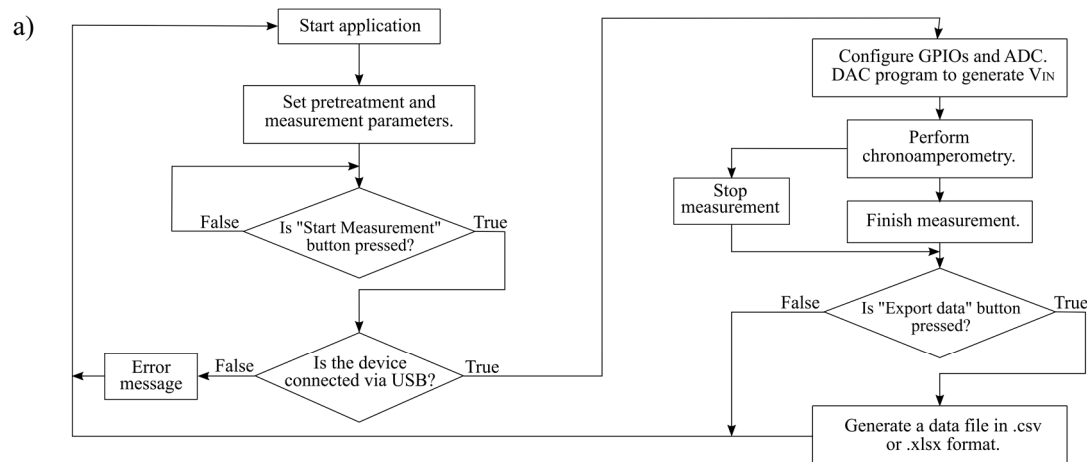


**Figure 2.** (a) Diagram flow of the designed program. (b) Chronoamperometry curve measured with AmpVIEW.

### 2.1.3. Power Module (PM): Power Supply Module Description

The full-custom circuit board is connected to the MCU board, which operates with the power provided by the computer USB port. The MCU board provides 3.6 V ( $V_{MCU}$ ) to the full-custom circuit that contains the FEM and the PM. In order to avoid variations in the power supply, the  $V_{MCU}$  is sent to the AP3330 Low Dropout linear Regulator (LDO), which provides an output with a stable and regulated voltage of 3.6 V ( $V_{PM}$ ). As stated in the previous section, it is necessary to have dual supply operational amplifiers to measure the negative voltage obtained at the potentiostat's output ( $V_{OUT}$ ).

To generate the negative voltage supply, we created a virtual ground with a low quiescent current LDO (ADP125 IC; Analog Devices; Norwood, Massachusetts, USA). This provides an output voltage of 3 V that is set as a virtual ground, by creating a non-symmetrical power supply of 0.6 V (+V) and −3 V (−V), allowing a wide negative measurement range. The ADP125 has a quiescent current of 45  $\mu\text{A}$  with no-load and a maximum quiescent current of 210  $\mu\text{A}$  in case of maximum load (500 mA).

## 2.2. Electrochemical Measurements

### 2.2.1. Electrochemical HRP Detection Procedure

The chronoamperometric detection of HRP (Ref. P6782, Sigma Aldrich, San Luis, MO, USA) was performed in parallel using the full-custom AmpStat potentiostat and three commercial potentiostats. Disposable screen-printed carbon electrodes (SPCE; Ref. DRP-110; Dropsens; Llanera, Spain) were employed for this purpose, each one featuring a 4-mm carbon working electrode, a carbon counter electrode, and a silver pseudo-reference electrode. Before they were used, SPCE were rinsed with ethanol 70% and water, dried under airflow and characterized by CV in 0.1 M KCl, 1 mM  $\text{K}_4\text{Fe}(\text{CN})_6$ .

For detection, HRP was diluted serially in miliQ water, obtaining eight final HRP concentrations (0.01, 1, 10, 25, 50, 100, 500, and 1000  $\text{ng}\cdot\text{mL}^{-1}$ ) and a negative control without HRP. The measurement equipment was turned on to register current at 0.00 V vs. the Ag pseudo-reference. Then, the SPCE was plugged and 45  $\mu\text{L}$  of ready-to-use 3,3',5,5'-Tetramethylbenzidine (TMB) Liquid Substrate System (Sigma Aldrich, Ref. T0440, which contains a mixture of TMB and  $\text{H}_2\text{O}_2$  in a buffer of undisclosed composition) were pipetted onto the electrodes. Next, 5  $\mu\text{L}$  of HRP were added and the enzymatic reaction proceeded while the current was registered for 300 s more.

### 2.2.2. Data Analysis

Data shown in the graphs correspond to the averages of no less than three independent replicates, each one obtained using a new SPCE, and the error bars show their standard deviation (SD). The assay limits of detection (LOQ) and quantification (LOQ) were calculated using the average of the blanks plus 3 and 10 times their SD, respectively. The variability was estimated in terms of the variation coefficient ( $\%CV = (\text{SD}/\text{mean}) \times 100$ ). The sensitivity corresponded to the slope of the linear range of the assay and the signal-to-noise ratio (SNR) was the signal registered for each HRP concentration divided by the averaged signal of the blanks.

## 3. Results and Discussion

In this work, we report the design, production, and analytical evaluation of a USB-powered portable potentiostat. The AmpStat prototype was designed to detect amperometrically the activity of HRP, an enzyme widely used for the detection of electrochemical biosensors, although it could be easily adapted for other applications.

### 3.1. Test and Calibration of the Electronic Platform

Figure 3 shows the final device composed by the full-custom Printed Circuit Board (PCB) connected to the MCU board (Figure 3a) and the control AmpVIEW software (Figure 3b). The whole system measures  $10.5 \times 5.8 \times 2.5$  cm and it weighs 41 g. The PCB, which contains the FEM and the PM, is connected to the MCU board through a 20-pin header. Since the FEM circuit measures low currents, we implemented a guard ring used to protect high-impedance circuit nodes from surface leakage currents. It is a copper ring driven by a low-impedance source to the same voltage as the high impedance node.

We designed and simulated the electronic circuit with Multisim program (National Instruments; Austin, TX, USA), and we made the PCB layout using Ultiboard software (National Instruments; Austin, TX, USA). The MCU was programmed with Code Composer Studio (Texas Instruments; Dallas, TX, USA), an integrated development environment (IDE) to develop applications for Texas Instruments embedded processors.

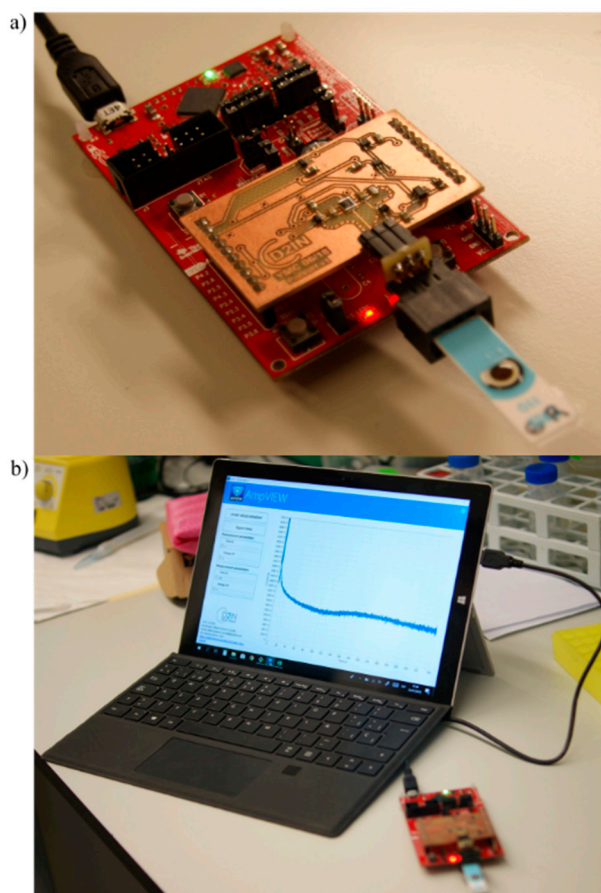


**Figure 3.** Picture of the prototype developed. (a) AmpStat potentiostat composed by the full-custom PCB (copper board) and the MCU board (red board). (b) AmpVIEW software registering an amperometry in real time.

The electronics characterization and a preliminary study towards the analytical validation of the platform were carried out with a Source Measurement Unit (SMU) B2962A (Keysight Technology; Santa Rosa, CA, USA) and an oscilloscope MSO-X 3034A (Agilent Technologies; Santa Clara, CA, USA). This allowed analyzing the AmpStat performance and deviation by measuring the  $I_{\text{SENSE}}$  current. For this purpose, the SMU was connected to the electronics platform and was programmed to apply a ramp of current from  $0 \mu\text{A}$  to  $11.2 \mu\text{A}$  (maximum current that the system can measure) while  $I_{\text{SENSE}}$  was measured. The maximum deviation between the current measured and the current applied was of 4.26%. The AmpStat potentiostat, composed by the PCB and MCU board, consumes 6.45 mA at 5 V, although the PCB, which contains the FEM and PM, only consumes  $235 \mu\text{A}$ , and can work with voltages of 3.6 V. The difference between consumptions is due to the MCU board, which contains many functionalities that increase prototype consumption. The developed system is able to measure currents up to  $11.2 \mu\text{A}$  with resolution  $0.13 \text{ nA}$ . However, it can be configured to measure currents up to 3 mA. Furthermore, the system can polarize the sensor electrodes to voltages up to 3.6 V.

Compared to other works, AmpStat had a broader current range and resolution, while still maintaining comparable operation voltage [32,33]. The measurement deviation of AmpStat was lower than the proposed by [34], which was the only work we could find in which this parameter was discussed. Although the potentiostat reported in [11] consumes less power, it is a fully-integrated chip designed in a  $0.35\text{-}\mu\text{m}$  bulk-CMOS technology and can measure a more limited current range.



### 3.2. System Verification by HRP Electrochemical Detection

The equipment was tested by detecting HRP concentrations ranging from  $0.01 \text{ ng}\cdot\text{mL}^{-1}$  to  $1000 \text{ ng}\cdot\text{mL}^{-1}$ , as well as a negative control without HRP. HRP was detected by monitoring its activity using a commercial ready-to-use substrate solution that contained TMB and  $\text{H}_2\text{O}_2$ . In this system, HRP catalyzed the reduction of  $\text{H}_2\text{O}_2$  coupled to the oxidation of TMB. The resulting oxidized TMB was then reduced at the surface of a SPCE, which registered a reduction current that was proportional to the amount of HRP present in solution (insert in Figure 4a). The AmpStat prototype was able to apply voltages up to 3.6 V between the WE and the RE. However, sensor characterization revealed that the best potential for this application was 0.00 V vs. the Ag pseudo-reference, and these were the measurement conditions used here.

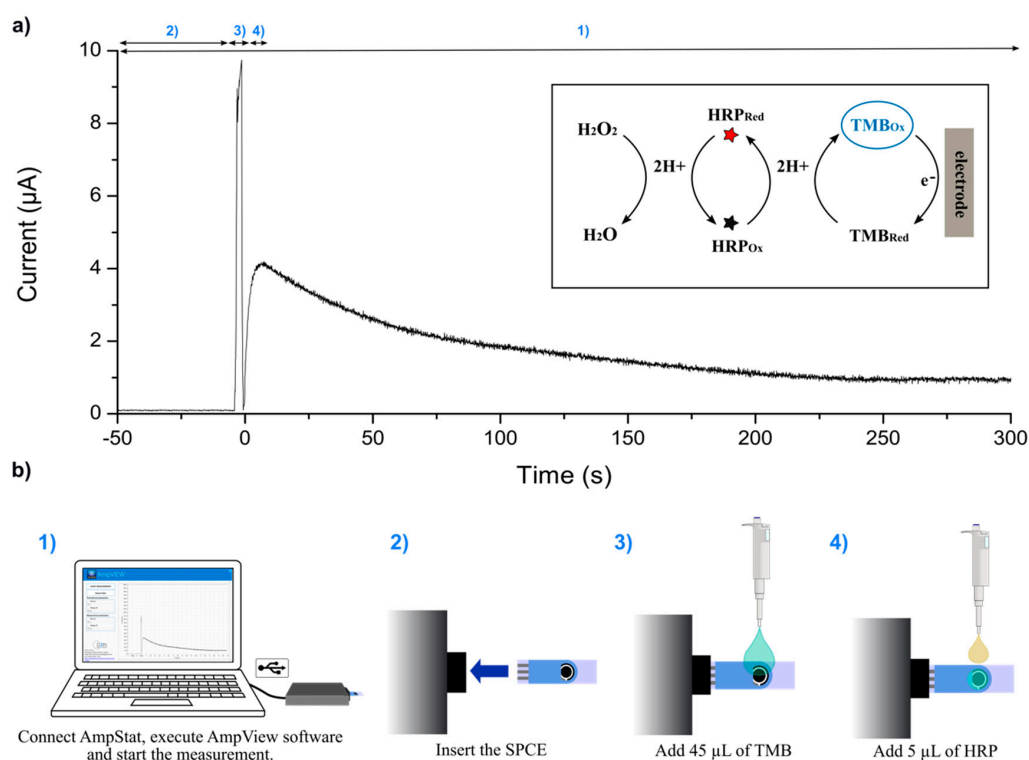


**Figure 4.** (a) Example of a chronoamperometry registered for  $500 \text{ ng}\cdot\text{mL}^{-1}$  of HRP. (b) The procedure followed for current measurement: (1) First, the AmpStat potentiostat was connected via USB to the computer, the AmpView software executed, and the “Start” button clicked on; (2) the SPCE was plugged to the connector, and (3) 45 µL of TMB were added; then, to begin the enzymatic reaction, (4) 5 µL of HRP were pipetted on the electrodes, and the current was registered during 300 s; finally, the “Stop” button was pressed and the data saved.

Figure 4 shows an example of chronoamperometric detection for  $500 \text{ ng}\cdot\text{mL}^{-1}$  of HRP, and the procedure followed to perform each detection. First, we connected the AmpStat to the computer, executed the AmpView program, and pressed the “Start” button to record the current signal (Figure 4b(1)). The software started showing the chronoamperometry in real-time on the computer display. Then, we plugged the SPCE to the potentiostat (Figure 4b(2)) and pipetted 45 µL of TMB onto the electrodes, which produced a transient current fluctuation (Figure 4b(3)). We then added 5 µL of HRP (Figure 4b(4)), and allowed the enzymatic reaction to take place while the current was registered for 300 s. Finally, when the measurement ended, or the “Stop” button was pressed, data was saved in csv or xls format.

Figure 5a shows a histogram summarizing the currents registered over time for increasing HRP concentrations and employing alternatively the customized AmpStat and the three commercial potentiostats used in parallel as the reference standards. As can be seen, the equipment generated

comparable results. In general, the enzymatic reaction was fast, and the highest currents were registered over the first 100 s for HRP concentrations above 25  $\text{ng}\cdot\text{mL}^{-1}$ . In contrast, detection of lower HRP concentrations improved for longer measurement times. Additionally, the fourth equipment displayed the highest reproducibility at 300 s, when current stabilization had been reached. In all cases, the currents registered ranged 20–50 nA for the blanks, increased proportionally to HRP concentration up to 100  $\text{ng}\cdot\text{mL}^{-1}$ , and increased to a lesser extent or plateaued for higher HRP contents when the reaction was substrate-limited (Figure 5b).

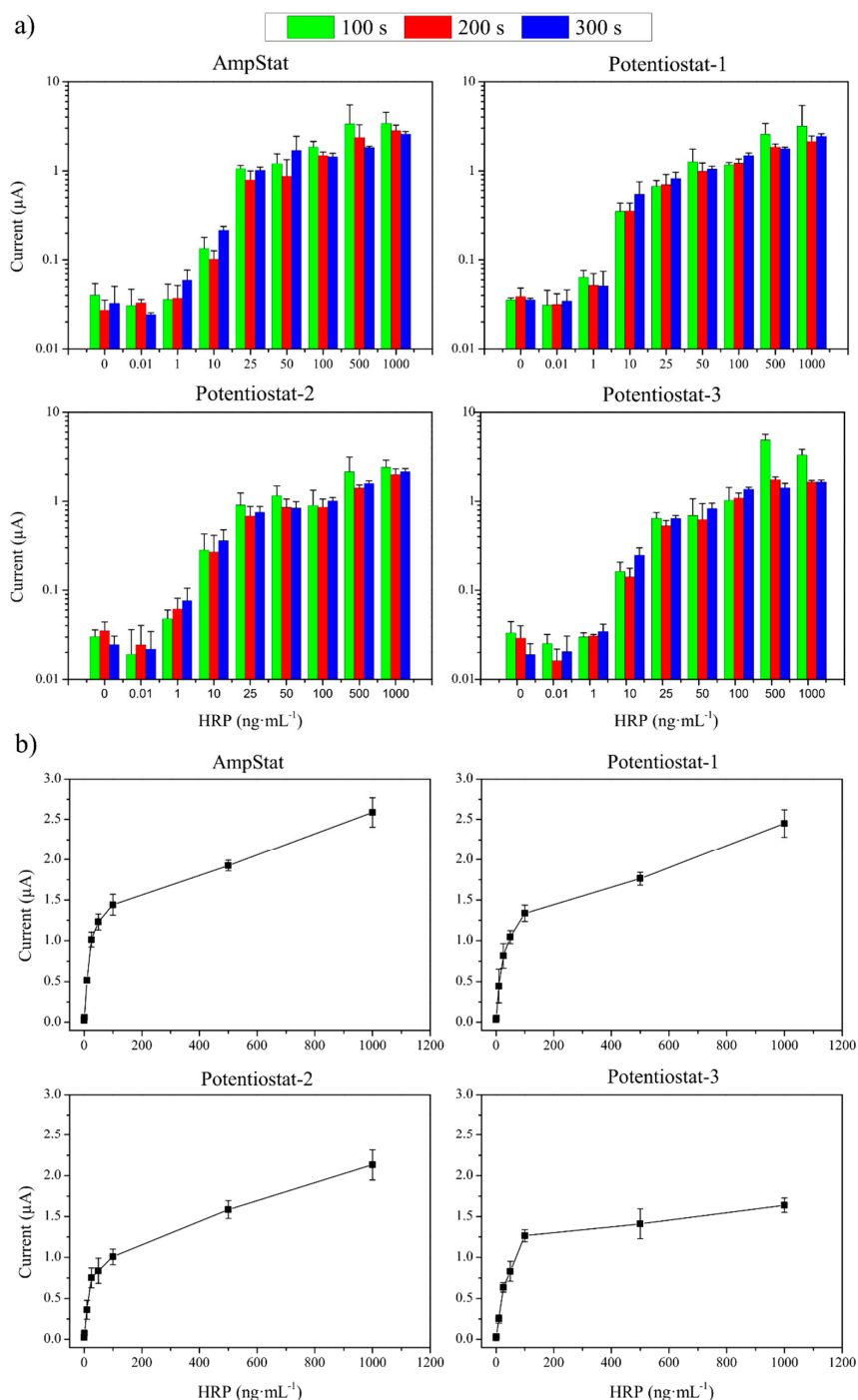


**Figure 5.** (a) Currents recorded by the four potentiostats used for HRP concentrations ranging from 0 to 1000  $\text{ng}\cdot\text{mL}^{-1}$  after 100 s, 200 s and 300 s of reaction with the substrate. (b) Currents registered after 300 s of reaction with the substrate ( $n = 3$ ).

Among the three commercial equipment that were studied, the potentiostat-3 was the one that measured the lowest currents for all HRP concentrations, but also presented the smallest data dispersion. On the other hand, the potentiostat-2 registered the highest currents and the most stable and reproducible background noise in the blanks (see the currents registered over time for the blanks in Figure 5a). Interestingly, the AmpStat portable system developed here measured similar currents and comparable result dispersion than the potentiostat-2 (%CV ranging of 4.7–21% in both cases). Nevertheless, the AmpStat displayed more variable blank measures. This negatively affected the assay SNR, which was calculated by using the blank values (Figure 6).

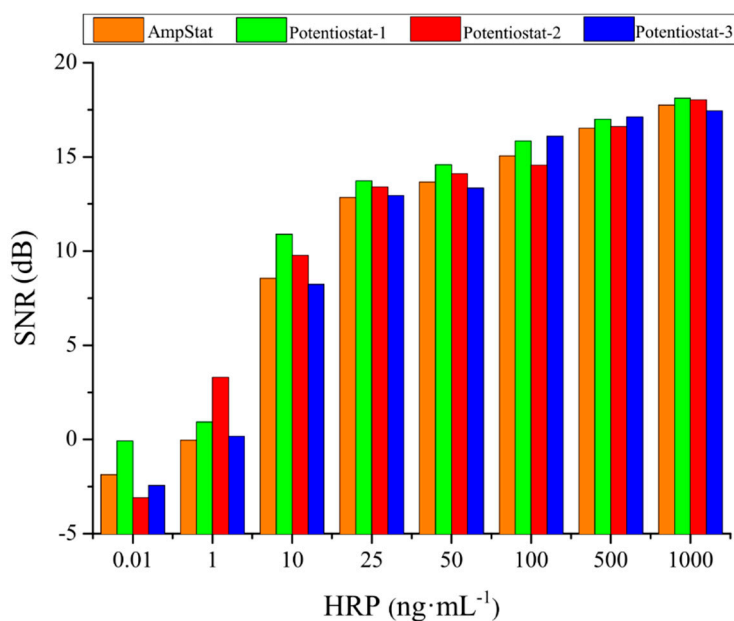


**Figure 6.** SNR of the four potentiostats for HRP concentrations ranging from 0.1 to 1000 ng mL<sup>-1</sup>.

Table 1 summarizes the figures of merit calculated for the HRP detection assay, carried out with the four electrochemical systems. The four potentiostats displayed comparable LOD and LOQ in terms of minimal current measurable and quantifiable, respectively. However, in terms of HRP concentration, both LOD and LOQ were higher (and thus worse) if HRP was measured using the potentiostat-3. The customized AmpStat potentiostat designed here exhibited an LOD of 0.83 ng·mL<sup>-1</sup> and an LOQ of 1.52 ng·mL<sup>-1</sup> of HRP, which were values only slightly higher than those provided by the potentiostat-1 and the potentiostat-2 (0.52–0.56 ng·mL<sup>-1</sup> and 1.16–1.61 ng·mL<sup>-1</sup>, respectively). Additionally, assay sensitivity, calculated as the slope of the corresponding assay linear range (spanning from 0.01 ng·mL<sup>-1</sup> to 50 ng·mL<sup>-1</sup>), was comparable for all three equipment. These parameters were reasonably accurate, taking into account that the AmpStat is a homemade prototype with an approximate manufacturing cost of \$85 USD.

**Table 1.** Comparison of the figures of merit of the HRP detection assay, carried out with the four tested potentiostats.

	AmpStat	Potentiostat-1	Potentiostat-2	Potentiostat-3
LOD				
Current (μA)	0.05	0.05	0.04	0.04
Concentration (ng·mL <sup>-1</sup> )	0.83	0.52	0.56	1.27
LOQ				
Current (μA)	0.07	0.08	0.07	0.06
Concentration (ng·mL <sup>-1</sup> )	1.52	1.16	1.61	2.89

Table 1. Cont.

	AmpStat	Potentiostat-1	Potentiostat-2	Potentiostat-3
Sensitivity (ng·mL <sup>-1</sup> ·μA <sup>-1</sup> )	0.0328	0.0326	0.0305	0.0219
Weight (g)	41	1600	480	5433
Dimensions (cm)	10.5 × 5.8 × 2.5	22.2 × 20.5 × 7.5	13.2 × 10.0 × 3.6	360.7 × 233.7 × 116.9
Cost (USD)	85	11,013	4087	16,000

#### 4. Conclusions

In this paper, we demonstrated experimentally the performance of AmpStat, a full-custom low-cost potentiostat. We described in detail the design, production, and preliminary analytical evaluation of this portable high-performance prototype, which is entirely powered and controlled by USB and includes a user-friendly interface that makes it plug-and-play and easy-to-use.

The potentiostat is composed of three blocks: the PM, which generates a stable voltage and a virtual ground, the potentiostat-based FEM, and the BEM, which includes an MCU and the GUI. Furthermore, we developed a full-custom software, called AmpVIEW, which controls the system, presents the chronoamperometry in real-time on a computer display, and allows saving the data in different file formats. The low-cost platform consumes 6.45 mA at 3.6 V. However, the full-custom designed PCB, which contains the instrumentation, only consumes 235 μA. Furthermore, the developed potentiostat can drive the sensor electrodes to voltages up to 3.6 V and measure currents up to 11.2 μA, although it can be adjusted to measure a maximum current of 3 mA.

We confirmed the efficacy of the AmpStat prototype by detecting HRP in a concentration range from 0.01 ng·mL<sup>-1</sup> to 1 μg·mL<sup>-1</sup>. As has been shown, the results obtained with the AmpStat were comparable to those obtained using three commercial electrochemical systems that were significantly more expensive. Our equipment displayed LOD of 0.83 ng·mL<sup>-1</sup>, LOQ of 1.52 ng·mL<sup>-1</sup>, and sensitivity of 0.0305 μA·mL·ng<sup>-1</sup>.

Furthermore, this platform could be additionally optimized in the future to produce a tailored compact system. For instance, size reduction could be achieved by creating a full-custom board with an integrated microcontroller unit. The software could also be upgraded to perform current averaging within defined measurement time ranges and/or interpolation in preloaded calibration plots. Also, the system could integrate additional functionalities based on mobile resources. For example, the incorporation of a Bluetooth module to connect the system to a smartphone and a rechargeable battery would facilitate the employment in POC testing, resulting in a more compact and flexible electrochemical detection solution.

**Author Contributions:** Y.M.-C. developed, implemented and tested the Point-of-Care (POC) electronic device and A.Á.-C. developed the acquisition software. Y.M.-C. and G.R.-V. did the experimental study and analyzed and interpreted the acquired data. Y.M.-C. wrote the manuscript and approved the final version of the manuscript. Besides, P.L.M.-C., E.B., M.P.-V. and J.C.-F. supervised the development of the device. P.L.M.-C., J.C.-F., M.P.-V., G.R.-V. and A.Á.-C. have discussed the resultant data, contributed in the manuscript and approved the final version for its publication.

**Funding:** This research was funded by the Spanish Ministry of Economy, Agencia Estatal de Investigación, Fondo de Investigaciones Sanitarias of Instituto de Salud Carlos III (ISCIII) and Fondo Europeo de Desarrollo Regional (AEI/FEDER, UE), through projects TEC2016-78284-C3-3-R and DTS17/00145. EB is funded by a Miguel Servet II contract from ISCIII-FEDER (CPII18/00025). GR is supported by a VHIR predoctoral fellowship funded by Amics del VHIR. Diagnostic Nanotools is a Consolidated Group supported by the Secretaria d'Universitats i Recerca of Generalitat de Catalunya (Grant 2017 SGR 240).

**Conflicts of Interest:** The authors declare no conflict of interest.

## References

1. Sharma, S.; Zapatero-Rodríguez, J.; Estrela, P.; O’Kennedy, R. Point-of-Care diagnostics in low resource settings: Present status and future role of microfluidics. *Biosensors* **2015**, *5*, 577–601. [[CrossRef](#)] [[PubMed](#)]
2. Nayak, S.; Blumenfeld, N.R.; Laksanasopin, T.; Sia, S.K. Point-of-Care Diagnostics: Recent Developments in a Connected Age. *Anal. Chem.* **2017**, *89*, 102–123. [[CrossRef](#)] [[PubMed](#)]
3. St John, A.; Price, C.P. Existing and Emerging Technologies for Point-of-Care Testing. *Clin. Biochem. Rev.* **2014**, *35*, 155–167. [[PubMed](#)]
4. Lillehoj, P.B.; Huang, M.C.; Truong, N.; Ho, C.M. Rapid electrochemical detection on a mobile phone. *Lab Chip* **2013**, *13*, 2950–2955. [[CrossRef](#)] [[PubMed](#)]
5. Zhao, G.; Si, Y.; Wang, H.; Liu, G. A Portable Electrochemical Detection System based on Graphene/Ionic Liquid Modified Screen-printed Electrode for the Detection of Cadmium in Soil by Square Wave Anodic Stripping Voltammetry. *Int. J. Electrochem. Sci.* **2016**, *11*, 54–64.
6. Martín, A.; Kim, J.; Kurniawan, J.F.; Sempionatto, J.R.; Moreto, J.R.; Tang, G.; Campbell, A.S.; Shin, A.; Lee, M.Y.; Liu, X.; et al. Epidermal Microfluidic Electrochemical Detection System: Enhanced Sweat Sampling and Metabolite Detection. *ACS Sens.* **2017**, *2*, 1860–1868. [[CrossRef](#)]
7. Yoo, E.H.; Lee, S.Y. Glucose biosensors: An overview of use in clinical practice. *Sensors* **2010**, *10*, 4558–4576. [[CrossRef](#)]
8. Teengam, P.; Siangproh, W.; Tuantranont, A.; Henry, C.S.; Vilaivan, T.; Chailapakul, O. Electrochemical paper-based peptide nucleic acid biosensor for detecting human papillomavirus. *Anal. Chim. Acta* **2017**, *952*, 32–40. [[CrossRef](#)]
9. Bettazzi, F.; Voccia, D.; Martellini, T.; Cincinelli, A.; Palchetti, I. Different enzyme-based strategies for the development of disposable electrochemical biosensors: Application to environmental pollutant monitoring. In Proceedings of the 2015 XVIII AISEM Annual Conference, Trento, Italy, 3–5 February 2015; pp. 1–3.
10. Jia, W.; Bandodkar, A.J.; Valdés-Ramírez, G.; Windmiller, J.R.; Yang, Z.; Ramírez, J.; Chan, G.; Wang, J. Electrochemical tattoo biosensors for real-time noninvasive lactate monitoring in human perspiration. *Anal. Chem.* **2013**, *85*, 6553–6560. [[CrossRef](#)]
11. Zuo, L.; Islam, S.K.; Mahbub, I.; Quaiyum, F. A low-power 1-V potentiostat for glucose sensors. *IEEE Trans. Circuits Syst. II Express Briefs* **2015**, *62*, 204–208. [[CrossRef](#)]
12. Colomer-Farrarons, J.; Miribel-Català, P.L. *A CMOS Self-Powered Front-End Architecture for Subcutaneous Event-Detector Devices: Three-Electrodes Amperometric Biosensor Approach*; Springer: Dordrecht, The Netherlands, 2011; ISBN 9789400706859.
13. Steinberg, M.D. A micropower amperometric potentiostat. *Sens. Actuators B Chem.* **2004**, *97*, 284–289. [[CrossRef](#)]
14. Montes-Cebrián, Y.; del Torno-de Román, L.; Álvarez-Carulla, A.; Colomer-Farrarons, J.; Minter, S.D.; Sabaté, N.; Miribel-Català, P.L.; Esquivel, J.P. ‘Plug-and-Power’ Point-of-Care diagnostics: A novel approach for self-powered electronic reader-based portable analytical devices. *Biosens. Bioelectron.* **2018**, *118*, 88–96. [[CrossRef](#)] [[PubMed](#)]
15. Dryden, M.D.M.; Wheeler, A.R. DStat: A versatile, open-source potentiostat for electroanalysis and integration. *PLoS ONE* **2015**, *10*, e0140349. [[CrossRef](#)] [[PubMed](#)]
16. Erickson, J.S.; Shriver-Lake, L.C.; Zabetakis, D.; Stenger, D.A.; Trammell, S.A. A simple and inexpensive electrochemical assay for the identification of nitrogen containing explosives in the field. *Sensors* **2017**, *17*, 1769. [[CrossRef](#)] [[PubMed](#)]
17. Serafín, V.; Martínez-García, G.; Aznar-Poveda, J.; Lopez-Pastor, J.A.; Garcia-Sanchez, A.J.; Garcia-Haro, J.; Campuzano, S.; Yáñez-Sedeño, P.; Pingarrón, J.M. Determination of progesterone in saliva using an electrochemical immunosensor and a COTS-based portable potentiostat. *Anal. Chim. Acta* **2019**, *1049*, 65–73. [[CrossRef](#)] [[PubMed](#)]
18. Aznar-Poveda, J.; Lopez-Pastor, J.A.; Garcia-Sanchez, A.J.; Garcia-Haro, J.; Otero, T.F. A cots-based portable system to conduct accurate substance concentration measurements. *Sensors* **2018**, *18*, 539. [[CrossRef](#)]
19. Jung, J.; Lee, J.; Shin, S.; Tae Kim, Y. Development of a telemetric, miniaturized electrochemical amperometric analyzer. *Sensors* **2017**, *17*, 2416. [[CrossRef](#)]
20. Cruz, A.F.D.; Norena, N.; Kaushik, A.; Bhansali, S. A low-cost miniaturized potentiostat for point-of-care diagnosis. *Biosens. Bioelectron.* **2014**, *62*, 249–254. [[CrossRef](#)]

21. Muñoz-Martínez, A.I.; Peña, O.I.G.; Colomer-Farrarons, J.; Rodríguez-Delgado, J.M.; Ávila-Ortega, A.; Dieck-Assad, G. Electrochemical instrumentation of an embedded potentiostat system (Eps) for a programmable-system-on-a-chip. *Sensors* **2018**, *18*, 4490. [[CrossRef](#)]
22. Sun, A.C.; Yao, C.; Ag, V.; Hall, D.A. An efficient power harvesting mobile phone-based electrochemical biosensor for point-of-care health monitoring. *Sens. Actuators B Chem.* **2016**, *235*, 126–135. [[CrossRef](#)]
23. Aymerich, J.; Márquez, A.; Terés, L.; Muñoz-Berbel, X.; Jiménez, C.; Domínguez, C.; Serra-Graells, F.; Dei, M. Cost-effective smartphone-based reconfigurable electrochemical instrument for alcohol determination in whole blood samples. *Biosens. Bioelectron.* **2018**, *117*, 736–742. [[CrossRef](#)] [[PubMed](#)]
24. Montes-Cebrián, Y.; Álvarez-Carulla, A.; Colomer-Farrarons, J.; Puig-Vidal, M.; Miribel-Català, P.L. Self-Powered Portable Electronic Reader for Point-of-Care Amperometric Measurements. *Sensors* **2019**, *19*, 3715. [[CrossRef](#)] [[PubMed](#)]
25. Sun, A.C.; Hall, D.A. Point-of-Care Smartphone-based Electrochemical Biosensing. *Electroanalysis* **2019**, *31*, 2–16. [[CrossRef](#)]
26. Cao, Z.; Chen, P.; Ma, Z.; Li, S.; Gao, X.; Wu, R.; Pan, L.; Shi, Y. Near-Field Communication Sensors. *Sensors* **2019**, *19*, 3947. [[CrossRef](#)]
27. Krainer, F.W.; Glieder, A. An updated view on horseradish peroxidases: Recombinant production and biotechnological applications. *Appl. Microbiol. Biotechnol.* **2015**, *99*, 1611–1625. [[CrossRef](#)]
28. Khanmohammadi, M.; Dastjerdi, M.B.; Ai, A.; Ahmadi, A.; Godarzi, A.; Rahimi, A.; Ai, J. Horseradish peroxidase-catalyzed hydrogelation for biomedical applications. *Biomater. Sci.* **2018**, *6*, 1286–1298. [[CrossRef](#)]
29. Hong, T.; Liu, W.; Li, M.; Chen, C. Recent advances in the fabrication and application of nanomaterial-based enzymatic microsystems in chemical and biological sciences. *Anal. Chim. Acta* **2019**, *1067*, 31–47. [[CrossRef](#)]
30. Maduraiveeran, G.; Sasidharan, M.; Ganesan, V. Electrochemical sensor and biosensor platforms based on advanced nanomaterials for biological and biomedical applications. *Biosens. Bioelectron.* **2018**, *103*, 113–129. [[CrossRef](#)]
31. Nguyen, H.H.; Lee, S.H.; Lee, U.J.; Fermin, C.D.; Kim, M. Immobilized enzymes in biosensor applications. *Materials* **2019**, *12*, 121. [[CrossRef](#)]
32. Ainla, A.; Mousavi, M.P.S.; Tsaloglou, M.N.; Redston, J.; Bell, J.G.; Fernández-Abedul, M.T.; Whitesides, G.M. Open-Source Potentiostat for Wireless Electrochemical Detection with Smartphones. *Anal. Chem.* **2018**, *90*, 6240–6246. [[CrossRef](#)]
33. Steinberg, M.D.; Kassal, P.; Kereković, I.; Steinberg, I.M. A wireless potentiostat for mobile chemical sensing and biosensing. *Talanta* **2015**, *143*, 178–183. [[CrossRef](#)] [[PubMed](#)]
34. Arevalo-Ramirez, T.; Torres, C.C.; Rosero, A.C.; Espinoza-Montero, P. Low cost potentiostat: Criteria and considerations for its design and construction. In Proceedings of the Proceedings of the 2016 IEEE ANDESCON, Arequipa, Peru, 19–21 October 2016; pp. 1–4.





# Chapter 3

## Summary and discussion of the results

In this section are summarized the results that fulfill the expected objectives behind the conception of low-power e-reader platforms for electrochemical detections defined as Plug-and-Power solutions.

An innovative solution in terms of power requirements was developed, creating the Plug-and-Power concept in which the energy required to perform a test is always available. The proposed self-powered Point-of-Care electronic reader (e-reader) ran the test and showed a quantitative result, while external disposable test-strip, acted as a sensor and a power source.

The e-reader comprises a Printed Circuit Board (PCB) and an outer case (Figure 3.1). The doubled-sided printed circuit had a size of 77.5 mm x 32.5 mm x 2mm, and it was made in glass-reinforced epoxy laminate material (FR4) with silver-finish. The outer case was made of a photosensitive epoxy resin called Accura®25, and it was created with the solid-state stereolithography (SLA®) 3-D printing technology. It has a total size of 85 mm x 42 mm x 21 mm.

The proposed system was characterized and validated before the integration with test units. First, it was characterized through a Source Measurement Unit (SMU). The SMU was used to generate different current signals, emulating the behavior of test strips. The results showed that the reader had a maximum relative uncertainty of 1.8%, which depended on the Analog-to-Digital (ADC) quantification error and the passive component tolerances.

Then, it was calculated the best moment to perform the measurement that depends mainly on the electronics' resolution and the measurement uncertainty.



### CHAPTER 3. SUMMARY AND DISCUSSION OF THE RESULTS

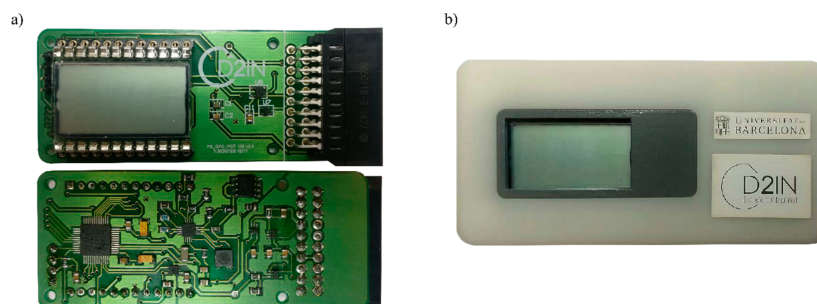


Figure 3.1: Picture of the (a) printed circuit board, and (b) the whole self-powered electronic reader (printed circuit board and outer case). Reprinted from [163] with permission.

On the one hand, the resolution of the e-reader is defined by the ADC resolution, which was 13 nA for the developed device. On the other hand, the measurement uncertainty depends on the current change rate. In a chronoamperometry, a redox reaction occurs when a potential step is applied to the electrode. At this moment, the current decays  $t^{1/2}$ , obeying the Cottrell equation. Consequently, during the initial time, a small deviation at the time to extract the measurement is translated into a large current uncertainty. Whereas in the final region, it is difficult to distinguish between concentrations because they have a similar value. For these reasons, neither the initial nor the final region were used to extract the measurement. The time chosen to extract the measurement for each sensor was the one that presented the lower uncertainty value for the worst case of detection, that is the lowest level of concentration. When the ideal moment to perform the measurement was calculated, the e-reader was programmed to take the measurement at this time.

Additionally, the power consumption of the system was measured in order to assure that the developed electronic was able to work with the proposed power sources. When the external test unit was inserted into the e-reader, electronics started to collect the energy. When enough energy was recollected, the system was started-up. At the start-up phase, a typical inrush current peak took place, reaching a power demand of up to 5 mW. Then, the e-reader entered into a low-power mode of operation, consuming only 900  $\mu$ W. The applicability of the proposed e-reader was demonstrated in the first publication with the development of a self-powered portable blood glucometer. A disposable test strip used was composed of a glucose battery, which supplied the device, and a glucose Fuel Cell (FC), which monitored the glucose concentration.

First, the electronic reader was characterized through the SMU, which simulated the behavior of the disposable test strips. The reader was adjusted to measure currents up to 30  $\mu$ A with a resolution of 13 nA. Then, the whole system was assembled, programmed, and calibrated to work with real test strips. The

## CHAPTER 3. SUMMARY AND DISCUSSION OF THE RESULTS

full-custom reader was characterized and validated using real test strips fed with 50  $\mu\text{L}$  of serum at glucose concentrations between 5 and 30 mmol/L.

Sensor characterization revealed that the best potential for this application was 0.45 V. Moreover, calibration tests showed that the best time to carry out the measurement was 12 s. At that time, the uncertainty of the device was lower than 5% for the lowest glucose concentration, and it had a maximum uncertainty of 1.8% (Figure 3.2a, Figure 3.2b, and Figure 3.2c).

Chronoamperometries obtained with the e-reader were compared against a commercial potentiostat (Autolab PGSTAT2014). The results showed that currents measured by the e-reader virtually matched with the commercial equipment. As expected, the main difference between both systems was obtained at currents higher than 30  $\mu\text{A}$ , which is the current detection limit of the developed reader. Moreover, it was represented the relationship between the current measurement and the glucose concentration captured by the electronic reader, and it was compared against the one measured with the commercial potentiostat. (Figure 3.2d). Data obtained with both systems were proportional, although the results showed a slight shift between the curves, which was corrected in the final device by the software.

As is stated before, the e-reader presented an inrush current peak of 5 mW and a consumption of 900  $\mu\text{W}$  in low-power mode (Figure 3.2e). On the other side, the paper-based power source could provide more than 10 mW of power. Consequently, the power consumption of the full-custom reader was much lower than provided by the power source, allowing show the numerical results on the screen until the disposable component ran out of power (after few hours) or when it was removed.

The second publication showed the e-reader's capability of adaptation to different electrochemical scenarios. In this study, the e-reader was validated by using a commercial ethanol FC and emulating three FCs (urine, ethanol, and methanol) and a sensor (methanol). Two approaches were followed, using FC as a power element or as a dual power/sensor element.

With the energy extracted from the FC, the self-powered platform supplied all the electronic modules, which perform the measurement, process data, and show the qualitative result on the numerical display. In order to verify the energy extraction capacity of the system, and its capability of adaptation to countless scenarios, a commercial methanol FC, and two emulated FC of methanol and urine were used. The e-reader's startup voltages are shown in Figure 3.3. To obtain these signals, the platform was fed by the commercial FC of ethanol. The upper curve ( $V_{\text{FC}}$ ) shows the voltage provided by the ethanol FC ( $V_{\text{FC}}$ ), and the middle graph shows the boost converter voltage ( $V_{\text{BOOST}}$ ). This voltage supplied the circuits

## CHAPTER 3. SUMMARY AND DISCUSSION OF THE RESULTS

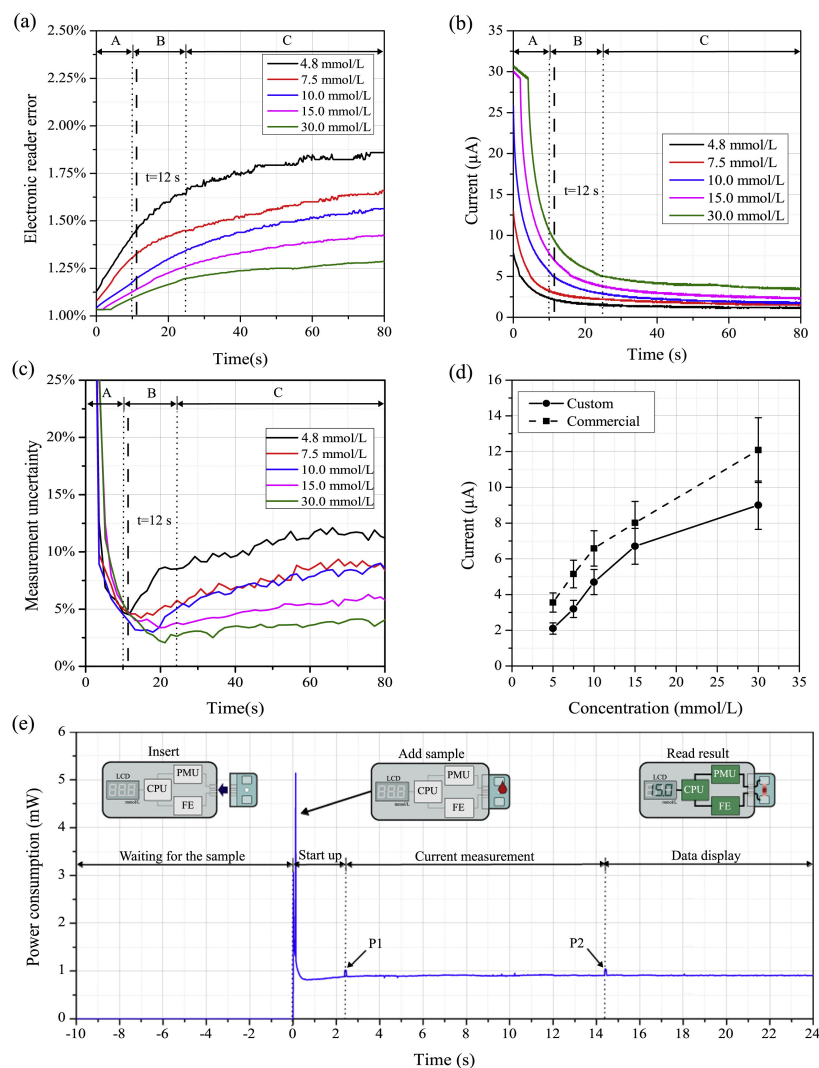


Figure 3.2: a) Electronic reader current error. b) Chronoamperometry curves done with the electronic reader. c) Uncertainty in current measurement produced by the e-reader. d) Transfer function that relates the current captured by the e-reader with the glucose concentration and comparison against a commercial potentiostat (Autolab PGSTAT204). e) Temporal evolution of the electronic reader power consumption. Reprinted from [164] with permission.

that process the signal and display the result. The bottom graph shows the low-dropout regulator voltage ( $V_{\text{LDO}}$ ), used to feed the analog circuit, which performs the measurement. The ethanol FC was connected to the e-reader, and it started to collect energy. When enough energy was harvested, the system was beginning to operate, changing the state of the  $V_{\text{LDO}}$  signal. The  $V_{\text{FC}}$  peaks correspond to the Maximum Power Point Tracking system, which optimized the energy extraction.

## CHAPTER 3. SUMMARY AND DISCUSSION OF THE RESULTS

The DC/DC boost converter ( $V_{\text{BOOST}}$ ) reduced the voltage peaks, and the linear low-dropout regulator stabilized and regulated the signal, even more, to supply the measurement module. This sensitive module needed the most stable voltage possible because it carried out the measurement. The experiments confirmed the self-powered performance of the system, which could operate with a minimum voltage of 330 mV and supplied all the low-powered electronic modules.

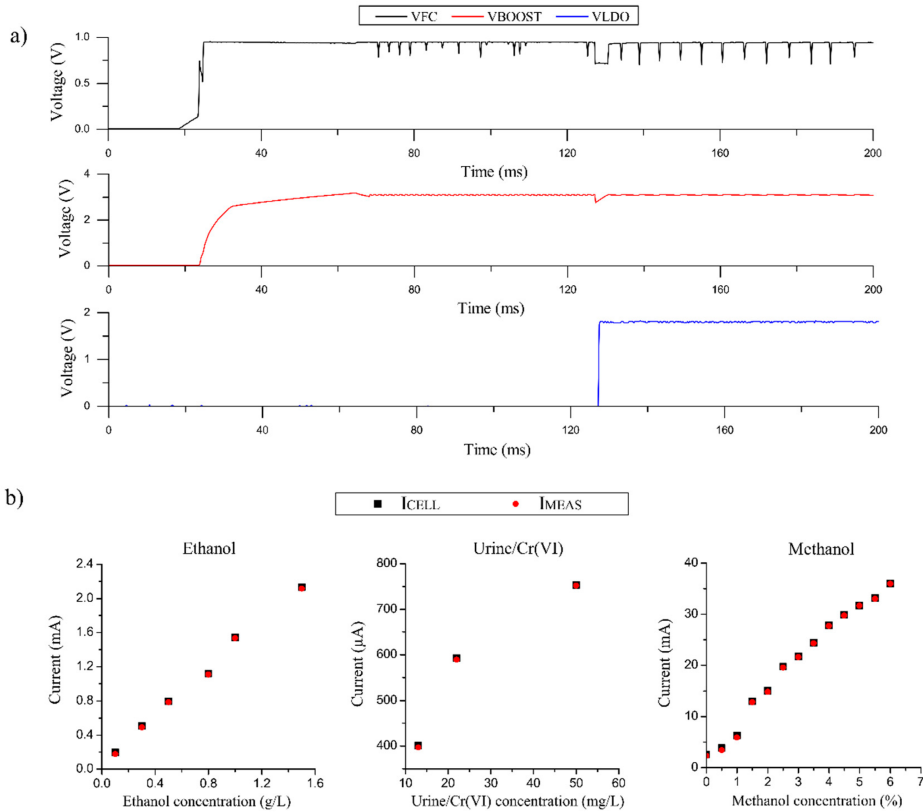


Figure 3.3: (a) Start-up curves of the e-reader powered by ethanol FC. (b) Transfer function that relates the measured current by the e-reader with different emulated sensors and fuel cell concentrations (ethanol, urine and methanol), and the comparison against the current produced by the sensor. Reprinted from [163] with permission.

Besides, it was validated the capability of the reader to measure multiple ranges of current. The results showed that the currents measured by the e-reader were practically the same as the nominal current injected by emulated FCs, with a maximum deviation of 1.8% (Figure 3.3). The system had a minimum resolution of 13 nA and could measure a maximum current of 3 mA. The validation has been carried out with three different FCs, although it could operate with other FCs, measuring a wide range of analytes.

This thesis has also demonstrated experimentally the performance of a full-

### CHAPTER 3. SUMMARY AND DISCUSSION OF THE RESULTS

Resolution	13 nA
Maximum deviation of the measurement	1.8 %
Maximum current measurement	3 mA
Peak of power consumption	5 mW
Stationary power consumption	900 $\mu$ W
Electronics operating voltage	1.8 V
Minimum supply voltage	330 mV

Table 3.1: Summary of the electronic characteristics of the self-powered portable electronic reader for Point-of-Care testing.

custom, and customizable POC system able to perform fast and sensitive amperometric detection. The low-cost and portable e-reader, called AmpStat, was designed, fabricated, characterized, and tested against three high-cost commercial potentiostats.

The hand-held device had a final size of 10.5 x 5.8 x 2.5 cm, a weight of 41 g, and an approximate manufacturing cost of \$85. It was composed of a connector that houses the disposable amperometric sensor, an USB-powered electronic platform for measurement acquisition, and a custom LabVIEW-based graphic user interface called Ampview (Figure 3.4). This custom software displayed and stored results, making the plug-and-play and easy-to-use system able to operate on any computer.

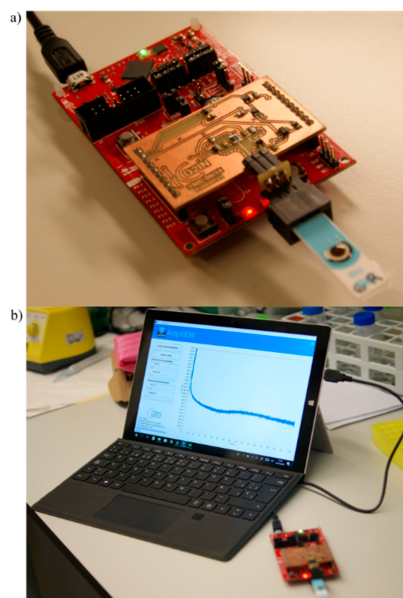


Figure 3.4: Picture of the prototype developed. (a) AmpStat potentiostat composed of the full-custom PCB (copper board) and the MCU board (red board). (b) AmpVIEW software registering an amperometry in real-time. Reprinted from [165] with permission.

## CHAPTER 3. SUMMARY AND DISCUSSION OF THE RESULTS

The low-cost platform was composed of a full-custom PCB and a microcontroller board, which operated at 5V and consumed 6.45 mA. However, the high-performance instrumentation circuit, placed on the full-custom PCB, operated at 3.6V and consumed a maximum current of 235  $\mu\text{A}$ . The developed prototype was powered and controlled by USB. It registered currents ranging from 5 nA to 11  $\mu\text{A}$  in real-time, with a resolution of 0.13 nA. However, it could be adapted to measure currents up to 3 mA and to drive the sensor electrodes to voltages up to 3.6 V. Moreover, it had a maximum measurement deviation of 4.26%.

The efficacy of the AmpStat prototype was validated by detecting horseradish peroxidase (HRP) concentrations ranging from 0.01  $\text{ng}\cdot\text{mL}^{-1}$  to 1  $\mu\text{g}\cdot\text{mL}^{-1}$ . For detections, it was used screen-printed carbon electrodes and a ready-to-use commercial substrate solution. The sensor characterization showed that the best potential for this application was 0 V. The chronoamperometry obtained for 500  $\text{ng}\cdot\text{mL}^{-1}$  of HRP, and the procedure followed to perform each detection are shown in Figure 3.5.

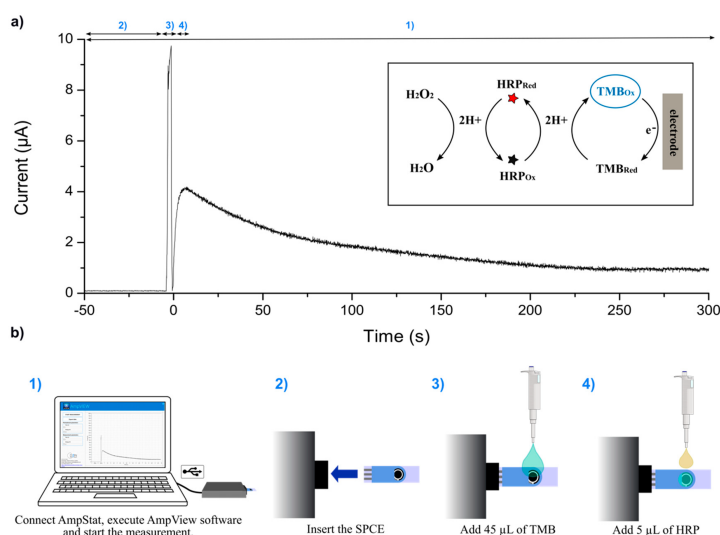


Figure 3.5: (a) Example of a chronoamperometry registered for 500  $\text{ng}\cdot\text{mL}^{-1}$  of HRP. (b)

The procedure followed for current measurement: (1) First, the AmpStat potentiostat was connected via USB to the computer, the AmpView software executed, and the “Start” button clicked on; (2) the SPCE was plugged to the connector, and (3) 45  $\mu\text{L}$  of TMB were added; then, to begin the enzymatic reaction, (4) 5  $\mu\text{L}$  of HRP were pipetted on the electrodes, and the current was registered during 300 s; finally, the “Stop” button was pressed and the data saved. Reprinted from [165] with permission.

AmpStat device was compared with three commercial potentiostats used in parallel as reference standards. A histogram summarizing the currents registered over time for increasing HRP concentrations is shown in Figure 3.6. As is shown in the histogram, the results obtained with AmpStat were comparable to those

## CHAPTER 3. SUMMARY AND DISCUSSION OF THE RESULTS

obtained using three commercial systems, which were significantly more expensive. For the blanks, the four systems provided currents ranging from 20 to 50 nA. These currents increased proportionally to HRP concentrations up to  $100 \text{ ng}\cdot\text{mL}^{-1}$ , for higher concentrations currents increased a lesser extent or plateaued when the reaction was substrate limited.

All the systems displayed the highest reproducibility at 300 s that it when current stabilization had been reached. The potentiostat-3 had the smallest data dispersion, although it registered the lowest currents for all HRP concentrations. On the other side, the potentiostat-2 presented the most stable and reproducible background noise in the blanks and measured the highest currents. The potentiostat-2 and the Ampstat measured similar currents and had a comparable dispersion, both systems had a variation coefficient from 4.7% to 21%. However, the AmpStat displayed more variable blank measures affecting the SNR assay (Figure 3.7.).

A summary of the figures of merit calculated for the HRP detection assay carried out with the four electrochemical systems is shown in Table 3.2. The designed potentiostat displayed Limit of Detection (LOD) of  $0.83 \text{ ng}\cdot\text{mL}^{-1}$ , a Limit of Quantification (LOQ) of  $1.52 \text{ ng}\cdot\text{mL}^{-1}$ , and sensitivity of  $0.0305 \mu\text{A}\cdot\text{mL}\cdot\text{ng}^{-1}$ . The four potentiostats displayed comparable LOD and LOQ, although potentiostat-3 had higher and worse values. The LOD and LOQ values were slightly higher than those provided by the potentiostat-1 and the potentiostat-2. Furthermore, assay sensitivity was comparable for all three equipment.

Table 3.3 shows a summary of the electronic specifications of the competitive portable potentiostat for POC applications presented in this thesis.

## CHAPTER 3. SUMMARY AND DISCUSSION OF THE RESULTS

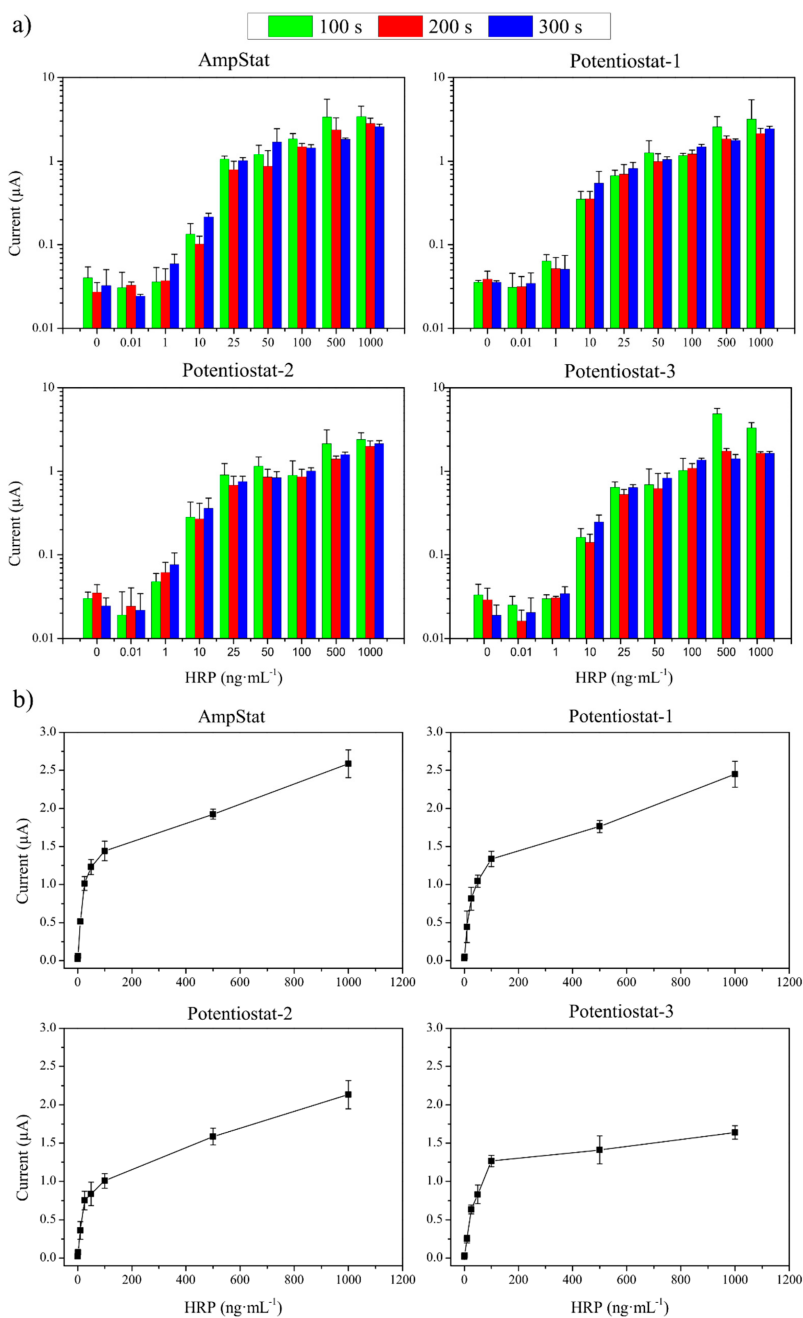


Figure 3.6: (a) Currents recorded by the four potentiostats used for HRP concentrations ranging from 0 to 1000  $\text{ng}\cdot\text{mL}^{-1}$  after 100 s, 200 s and 300 s of reaction with the substrate. (b) Currents registered after 300 s of reaction with the substrate ( $n = 3$ ). Reprinted from [165] with permission.



### CHAPTER 3. SUMMARY AND DISCUSSION OF THE RESULTS

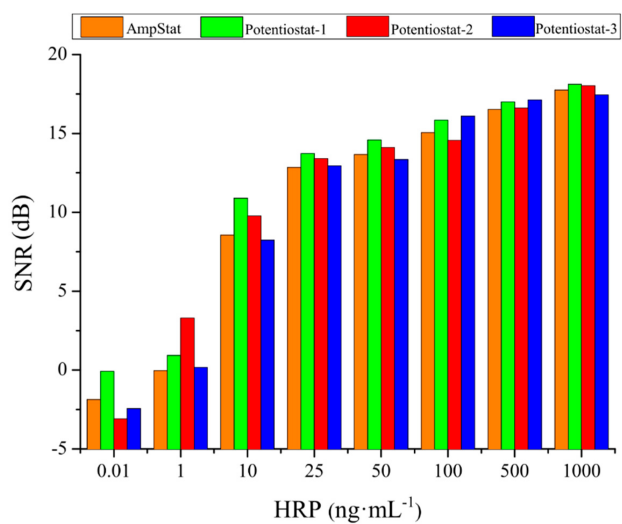


Figure 3.7: SNR of the four potentiostats for HRP concentrations ranging from 0.1 to  $1000 \text{ ng mL}^{-1}$ . Reprinted from [165] with permission.

CHAPTER 3. SUMMARY AND DISCUSSION OF THE RESULTS

	AmpStat	Potentiostat-1	Potentiostat-2	Potentiostat-3
<b>LOD</b>				
Current ( $\mu\text{A}$ )	0.05	0.05	0.04	0.04
Concentration ( $\text{ng}\cdot\text{mL}^{-1}$ )	0.83	0.53	0.56	1.27
<b>LOQ</b>				
Current ( $\mu\text{A}$ )	0.07	0.08	0.07	0.06
Concentration ( $\text{ng}\cdot\text{mL}^{-1}$ )	1.52	1.16	1.61	2.89
Sensitivity ( $\text{ng}\cdot\text{mL}^{-1}\cdot\mu\text{A}^{-1}$ )	0.0328	0.0326	0.0305	0.0219
Weight (g)	41	1600	480	5433
Weight (g)	41	1600	480	5433
Dimensions (cm)	10.5 x 5.8 x 2.5	22.2 x 20.5 x 7.5	13.2 x 10.0 x 3.6	360.7 x 233.7 x 116.9
Cost (USD)	85	11,013	4087	16,000

Table 3.2: Comparison of the figures of merit of the HRP detection assay, carried out with the four tested potentiostats. Reprinted from [165] with permission.

### CHAPTER 3. SUMMARY AND DISCUSSION OF THE RESULTS

Resolution	0.13 nA	
Maximum deviation of the measurement	4.26 %	
Maximum current measurement	3 mA	
Power consumption	AmpStat	6.45 mA
	Custom electronics	235 $\mu$ A
Operating voltage	AmpStat	5 V
	Custom electronics	3.6 V
Minimum sensor bias voltage	3.6 V	
Cost	85 USD	

Table 3.3: Summary of the electronic characteristics of the USB-powered Handheld potentiostat for Point-of-Care applications.

# Chapter 4

## Conclusions

In this chapter, the main conclusions of this doctoral thesis are gathered, and the feasibility of the developed Plug-and-Power systems for electrochemical Point-of-Care applications is evaluated.

First, some general conclusions are presented to provide an overall approach to the whole research. Then, it is drawn the specific conclusions for each study proposed in this thesis. Finally, future steps towards portable POC devices for biomonitoring applications are exposed.

### 4.1 General conclusions

- Different electronic instrumentation circuits have been proposed to trigger the electrochemical reaction and measure the response of the sensing element. These low-power consumption systems are capable of working with electrochemical sensors and Fuel Cells and can adapt to a wide variety of measurement ranges.
- Electronic solutions have been developed that enable display results of a qualitative way. Besides, a discrete approach has been proposed capable of showing the results with minimal power consumption.
- New approaches based on potentiostats have been presented. These e-readers were able to perform electrochemical detections, resulting in miniaturized, versatile, and low-cost devices for Point-of-Care applications that require minimal user interaction. The main advantages of the developed platforms were: portability, easy-to-use; quantitative data; adaptability to a wide range of cases; rapidity, and accuracy of results.

## CHAPTER 4. CONCLUSIONS

- The feasibility of a Self-powered Point-of-Care concept was validated, which can extract energy from the sample to supply the electronic circuits and perform electrochemical detections.
- Low-power and high-performance instrumentation circuits based on current sense circuits were designed, implemented, and tested. The results gathered that these electronic circuits are able to provide accurate and high-resolution data with minimum power consumption.
- Other studies were carried out in parallel with the researches presented in this thesis. An ultra-low-power instrumentation circuit for self-powered applications was designed and presented in a conference. In addition, I participated in the design of the electronic instrumentation of the patent EP19382604.7 entitled “Self-powered system and method for power extraction and measurement of energy-generator units”. Furthermore, a multimodal and portable biosensing system was designed and implemented to help in investigations about Dystonia disorder, within the framework of a predoctoral stay at the Trinity Center for Biomedical Engineering and Trinity College Institute of Neuroscience of the Trinity College Dublin (Ireland).

### 4.2 Self-powered portable electronic system for POC applications

An electronic reader for self-powered POC solutions based on the use of Fuel Cells (FC) as a power source and as a sensor was developed and successfully employed in different cases, showing its capability of adaptation to a wide range of scenarios.

The plug-and-play system performed amperometric detections automatically and in just a few seconds, providing quantitative results on the display without the need for external laboratory equipment. Moreover, it did not need external power sources because the sample sensed was also used to power the electronics. The system can operate with conventional lithium batteries or with the sample to sense. It is a valuable feature for developing areas with a lack of good electricity grids and batteries. Besides, it can provide environmental benefits related to battery usage and disposal, as uncontrolled battery disposal leads to severe environmental pollution. Furthermore, this portable system can be adapted to a wide range of cases, providing rapid and accurate results.

The platform operated with a minimum voltage of 330 mV and consumed 900  $\mu$ W in the low power mode. The device provided reliable, robust, and effective results. It had a maximum measurement uncertainty of 1.8 % and a minimum

## CHAPTER 4. CONCLUSIONS

resolution of 13 nA. In addition, it can be adapted to measure different current ranges, measuring a maximum current of 3 mA.

The applicability of the platform was demonstrated with the development of a self-powered portable blood glucometer. A disposable test strip was employed, which included a paper-based power source, and a paper-based biofuel cell used as a glucose sensor. The device was tested with human serum samples with glucose concentrations between 5 and 30 mM. The results showed that the test strip provided enough power to supply the electronic system and perform the test. Moreover, the proposed electronic platform supplied the necessary energy to trigger the reaction, acquire the sensor response, process data, and show glucose concentrations numerically on a display, providing quantitative results in good agreement with commercial measuring instruments.

Furthermore, the electronic reader was validated in other cases, following two approaches, using the FC as a power element or as a dual power and sense element. The platform was validated using a commercial ethanol FC, three emulated FCs (urine, ethanol, and methanol) and a sensor (methanol), showing its capability of adaptation to different scenarios.

As shown, the system is fully customizable. Consequently, the applicability of the concept can be extended to other kinds of electrochemical sensors to detect other analytes or biological matrices, developing portable electronic analytical platforms for veterinary or environmental fields.

The platform reach could be extended, for example, adding an adjustable signal generator to perform cyclic voltammeteries or including a wireless communication module to show the results on a smartphone or a laptop. A big challenge would be to integrate the electronic system into an Application-Specific Integrated Circuit (ASIC) with the aim of a flexible and completely disposable device.

### 4.3 Portable USB-powered potentiostat for POC amperometric detections

A low-cost and portable e-reader for electrochemical analysis was designed and characterized, which was powered and supplied by USB. Also, it was tested against three high-cost commercial systems. The developed platform included user-friendly and full-custom software, which controlled the system, represented the chronoamperometry in real-time on a computer display, and saved the data in different file formats, making it plug-and-play and easy-to-use.

The USB-powered system operated at 5 V and consumed 6.45 mA. However,

## CHAPTER 4. CONCLUSIONS

the high-performance instrumentation circuit developed only consumed 235  $\mu\text{A}$  at 3.6 V. It measured currents from 5 nA to 11  $\mu\text{A}$  in real-time, although it can be adjusted to measure currents up to 3 mA. The proposed platform had a resolution of 0.13 nA, with a maximum measurement deviation of 4.26 %. Moreover, the potentiostat was able to drive the sensor electrodes to voltages up to 3.6 V. The portable platform had a final size of 10.5 x 5.8 x 2.5 cm, a weight of 42g, and an approximate manufacturing cost of 85 USD.

The viability of the USB-powered platform was demonstrated by detecting horseradish peroxidase in a concentration range from 0.01  $\text{ng}\cdot\text{mL}^{-1}$  to 1  $\mu\text{g}\cdot\text{mL}^{-1}$ . The results obtained with the developed system were comparable to those obtained using three commercial electrochemical systems, considerably more expensive. Furthermore, the results showed that designed potentiostat had a Limit of Detection of 0.83  $\text{ng}\cdot\text{mL}^{-1}$ , a Limit of Quantification of 1.52  $\text{ng}\cdot\text{mL}^{-1}$ , and a sensitivity of 0.0305  $\mu\text{A}\cdot\text{mL}\cdot\text{ng}^{-1}$ .

In the future, the size of the platform could be optimized by integrating a microcontroller module on the full-custom board. It also could be enhanced by including additional functionalities based on mobile resources, such as a Bluetooth module to connect the system to a smartphone. Besides, a rechargeable battery would improve the portability of the POC system. Even, it could be adapted to operate as a self-powered system, extracting the power from the sample to detect, generating a more flexible electrochemical detection solution.

### 4.4 Future steps towards low-powered devices for biosensing POC applications

The development of low-powered POC platforms for amperometric detections based on a potentiostat has been shown to be a feasible option. The use of this portable and low-power technology makes that the next generation of devices for healthcare a step closer to a real implementation. However, the developed platforms address some challenges.

As was discussed in the Introduction chapter, despite the substantial progress of the POC testing, there are still substantial problems that must be addressed. One way to address these issues is fomenting and incorporating new technologies that research contributions offer. The proposed technologies enable a paradigm shift from the traditional hospital-centered model towards a patient-centered model. Furthermore, these technologies allow addressing the challenges of POC diagnostic systems, establishing the basis of the next generation of POC biosensing platforms which must accomplish the following premises:

## CHAPTER 4. CONCLUSIONS

- Portability. They must allow to acquire, process, and represent biological parameters (such as biochemical markers, vital signals, environmental parameters, among others) near to patient.
- Usability is a key factor. It is important to make sure that the individuals perform tests accurately. For this reason, the systems must require the minimum steps to obtain a result and make data easy to interpret.
- Active feedback. Provide rapid diagnosis and response, and help to the disease prevention as well as the treatment, and rehabilitation.
- Durability and simplicity to improve the effectiveness of the systems in areas where systems must travel across a long supply chain and are used in facilities with very different requirements.

These premises are a good reference point to identify the different elements that must be improved in technology, with the aim of enhance the health of the patient while reducing the costs of the healthcare system.





# Appendix A

## List of publications

### A.1 Journals

**Authors:** Yaiza Montes-Cebrián, Albert Álvarez-Carulla, Gisela Ruiz-Vega, Jordi Colomer-Farrarons, Manel Puig-Vidal, Eva Baldrich, and, Pere Ll. Miribel-Catalá.

**Title:** Competitive USB-Powered Hand-Held Potentiostat for POC Applications: An HRP Detection Case

**Journal:** Sensors. Volume: 19 Issue: 24 Pages: 5388 Year: 2019 ISSN: 1424-8220

---

**Authors:** Yaiza Montes-Cebrián, Albert Álvarez-Carulla, Jordi Colomer-Farrarons, Manel Puig-Vidal and, Pere Ll. Miribel-Catalá.

**Title:** Self-Powered Portable Electronic Reader for Point-of-Care Amperometric Measurements

**Journal:** Sensors. Volume: 19 Issue: 17 Pages: 3715 Year: 2019 ISSN: 1424-8220

---

**Authors:** Yaiza Montes-Cebrián, Lorena del Torno-de Román, Albert Álvarez-Carulla, Jordi Colomer-Farrarons, Shelley D. Minter, Neus Sabaté, Pere Ll. Miribel-Catalá and, Juan Pablo Esquivel.

**Title:** ‘Plug-and-Power’ Point-of-Care diagnostics: A novel approach for self-powered electronic reader-based portable analytical devices

**Journal:** Biosensors and Bioelectronics. Volume: 118 Pages: 88-96 Year: 2018 ISSN: 0956-5663

---

## APPENDIX A. LIST OF PUBLICATIONS

### A.2 Patents

**Authors:** Albert Álvarez-Carulla, Pere Ll. Miribel-Catalá., **Yaiza Montes-Cebrián** and, Jordi Colomer-Farrarons

**Title:** Self-powered system and method for power extraction and measurement of energy-generator units

**Number:** EP19382604.7

**Date:** 17th July 2019

### A.3 Conferences

**Authors:** **Y. Montes-Cebrián**, A. Álvarez-Carulla, J. Colomer-Farrarons, E. O’rourke, I. Ndukwe, S. O’riordan, M. Hutchinson, P.L. Miribel-Catalá and, R.B. Reilly

**Title:** A Portable System for Measuring the Tactile Temporal Discrimination Threshold in Cervical Dystonia

**Conference:** NanoBioMed 2018. Place: Barcelona, Spain.

**Date:** 20th-22nd November 2018.

---

**Authors:** **Y. Montes-Cebrián**, A. Álvarez-Carulla, J. Colomer-Farrarons, M. Puig-Vidal, J. López-Sánchez, P. Miribel-Catalá

**Title:** A Fuel Cell-based adaptable Self-Powered Event Detection platform enhanced for biosampling applications

**Conference:** DCIS 2018: 33th Conference on Design of Circuits and Integrated Systems. Place: Lyon, France.

**Date:** 14th-16th November 2018.

---

**Authors:** A. Álvarez-Carulla, **Y. Montes-Cebrián**, M. Puig-Vidal, J. López-Sánchez, J. Colomer-Farrarons and, P. Miribel-Catalá

**Title:** Energy-Aware Adaptative Supercapacitor Storage System for Multi-Harvesting Solutions

**Conference:** DCIS 2018: 33th Conference on Design of Circuits and Integrated Systems. Place: Lyon, France.

**Date:** 14th-16th November 2018.

## APPENDIX A. LIST OF PUBLICATIONS

---

**Authors:** M. Genovart-Coll, **Y. Montes-Cebrián**, J. Colomer-Farrarons and, P. Miribel-Catalá

**Title:** Design of an Ultra-Portable Wearable Electrocardiograph

**Conference:** CASEIB 2017: 35th Congreso de la Sociedad Espanola de Ingenieria Biomédica (CASEIB). Place: Bilbao, Spain.

**Date:** 29th November - 1st December 2017.

---



# Appendix B

## Multimodal TDT system for biosensing Dystonia disorder

The author of this doctoral dissertation developed a portable biosensing device with the collaboration of the members of Reilly lab, within the framework of a pre-doctoral stay at the Trinity Center for Biomedical Engineering and Trinity College Institute of Neuroscience of the Trinity College Dublin (Ireland) [126]. During this stay, the author developed a tool to investigate the underlying neuropathology of the movement disorder Dystonia. Dystonia is the third most common neurological movement disorder, after Parkinson's disease and Essential Tremor [166]. This disease causes sustained or intermittent muscle contractions that produce abnormal movements or postures. Temporal discrimination is defined as the shortest time interval at which an individual can discriminate two sequential stimuli as being asynchronous. There is a hypothesis that both abnormal temporal discrimination and cervical dystonia are related, and they are caused by a disorder of the midbrain network for covert attentional orienting [167]. A study had evaluated that visually temporal discrimination thresholds (TDT) were abnormal in cervical dystonia patients [168], and it was tested with a portable system previously developed [169, 170].

In the study carried out as a part of this thesis, it is developed a multimodal portable platform that generated visual and tactile stimuli for measuring TDT. This system combined two main elements: a) the electronic hardware that contains the actuators that produce the stimuli, and the circuit for control these actuators, and b) the software that controls the system, shows visual stimuli and records the data. It had three operational modes: vibrotactile, visual, and multimodal (a combination of visual and vibrotactile stimuli) and allowed producing staircase or random stimuli. The device generated two vibrotactile stimuli of 5 ms of duration

## APPENDIX B. MULTIMODAL TDT SYSTEM FOR BIOSENSING DYSTONIA DISORDER

with precise inter-stimulus intervals (ISI). In the staircase mode, the ISI starts in 0 ms, and it increases in steps of 5ms. After each stimulus, the individual is requested to indicate if they perceive a single stimulus (or synchronous), or two stimuli separated in time (asynchronous). The staircase mode test finishes when the individual responds "asynchronous" for three consecutive increasing ISIs. In the random mode, the ISI is randomized between 0 to 100 ms, and the experiment ends after a set duration or when the user presses the stop button. A Printed Circuit Board (PCB) was connected to an Arduino Mega board. This PCB generated the signals to control the haptic motors and communicate with the smartphone through a Bluetooth Low Energy (BLE) module. The Arduino microcontroller and the Android App controlled the signals that generated the stimuli presented to the participant's fingers. To generate the tactile stimuli, two vibration motors were employed, since vibrotactile stimulation generation is more power-efficient than electrotactile stimulation systems [171]. Microcontrollers can only provide a small amount of current from their output, as these are intended to send control signals, not to act as power sources. In order to control a high-current DC load, such as a DC motor, it is necessary to use a motor driver. In this device, two MOSFETs were employed as a switch for high-current loads. Furthermore, a BLE module was used to connect the vibrotactile board with the smartphone. The device also integrated a touchscreen because it is wanted to include more functionalities in the future.

The biosensing system was controlled by an Android application called TD-TApp installed on an Android smartphone. The TDTApp allowed a) registering the experimenter's name and date of the test, b) selecting the experiment mode (staircase or random) and the type of stimuli (visual, tactile and multimodal), c) connecting and controlling the electronic hardware, d) registering the experiment data, and e) sending the data via email. Currently, the TDT system is being validated by members of the Trinity College of Dublin and St Vincent's University Hospital (Dublin, Ireland), and it is expected publication of the results in the next months.

## APPENDIX B. MULTIMODAL TDT SYSTEM FOR BIOSENSING DYSTONIA DISORDER

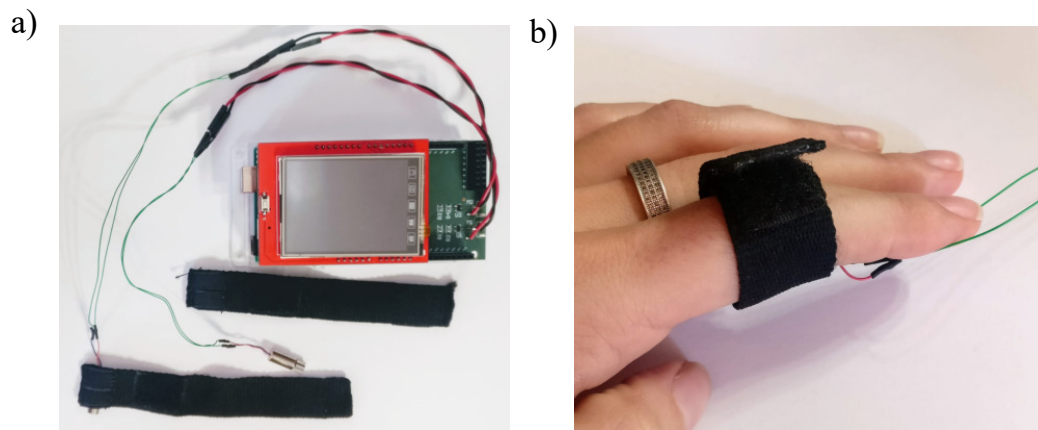


Figure B.1: a) Multimodal portable platform for measuring Temporal Discrimination Thresholds in Dystonia patients. b) The two vibration motors were inserted in a textile-black band to generate the vibrotactile stimulation in the fingers.



## APPENDIX B. MULTIMODAL TDT SYSTEM FOR BIOSENSING DYSTONIA DISORDER

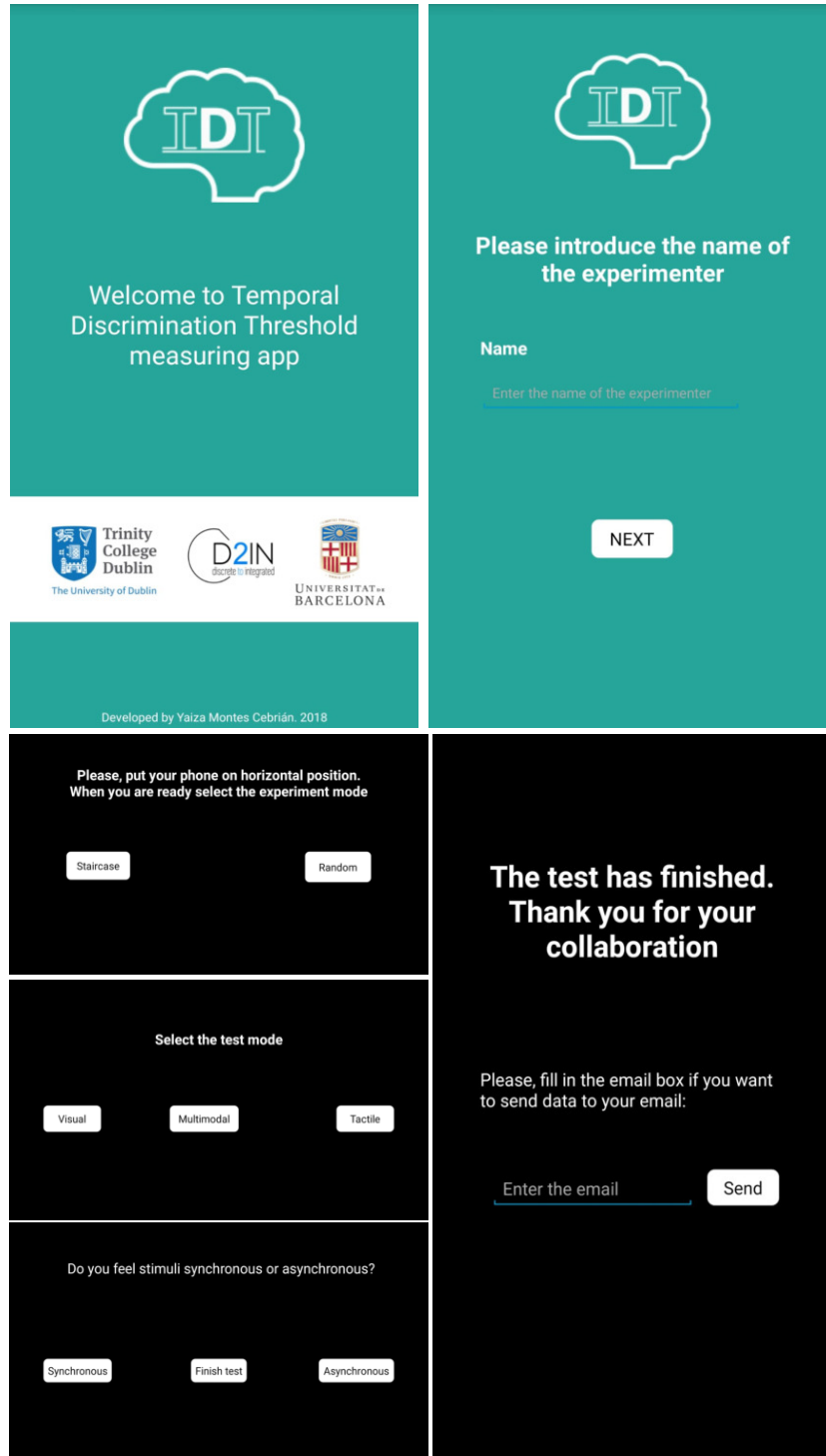


Figure B.2: Screenshots of the TDT App developed for generating visual and tactile stimuli to measure Temporal Discrimination Thresholds.

# Appendix C

## Resumen en castellano

Las pruebas de punto de atención (de sus siglas en inglés, POC) son una tecnología emergente aplicable a una amplia variedad de aplicaciones [63]. Al igual que otras tecnologías, los POC mejoran constantemente gracias a los diferentes avances en las tecnologías electrónicas y al desarrollo de nuevas aplicaciones.

Convencionalmente, las pruebas de diagnóstico se realizan con grandes analizadores en laboratorios centrales. Por lo general, esto implica que los pacientes deben esperar durante largos períodos antes de recibir sus resultados. Esta situación se agrava en las zonas rurales y los países en desarrollo, donde hay escasez de personal capacitado y el equipo de diagnóstico es básico [41, 48]. Las pruebas POC permiten monitorear las condiciones de salud y obtener resultados rápidos cerca del paciente. Permiten reducir los costes médicos y controlar los brotes infecciosos sin la necesidad de equipos de laboratorio dedicados. Además, los sistemas POC eliminan muchas de las limitaciones, ya que no requieren grandes infraestructuras de atención médica, equipos médicos complejos y técnicos especializados.

En los últimos años, ha aumentado el interés por desarrollar dispositivos POC, como se ha señalado en el capítulo de introducción de esta tesis. Según el sitio web Dimensions.ai, en los últimos 5 años, se han publicado más de 1.7 millones de artículos y 325,000 patentes sobre pruebas POC. Esto indica que existe una creciente necesidad de desarrollar dispositivos POC de bajo costo, portátiles y fáciles de usar con el fin de diagnosticar enfermedades en etapas tempranas.

El detector de glucosa en sangre es el dispositivo POC por excelencia. Este dispositivo se basa en el concepto de inmunoensayo de flujo lateral [24], y permite detectar la presencia de cierto analito, en este caso, glucosa. Sin embargo, la detección por flujo lateral no siempre es una técnica válida. Existen multitud de analitos que requieren de métodos basados en sistemas electrónicos más comple-

## APPENDIX C. RESUMEN EN CASTELLANO

jos, capaces de suministrar la energía necesaria para desencadenar una reacción, detectar la respuesta del sensor y mostrar el resultado al usuario. Por esta razón, se necesitan circuitos electrónicos miniaturizados, de alto rendimiento e integrables en sistemas POC.

Por lo general, los sistemas POC portátiles usan baterías como fuente de energía eléctrica. Estas baterías deben reemplazarse o recargarse periódicamente y tienen una autonomía limitada. Esta simple tarea es un desafío en entornos de bajos recursos, que es donde más se necesitan estos sistemas.

El objetivo principal de esta tesis doctoral es el desarrollo de lectores electrónicos Plug-and-Power para detecciones electroquímicas y la demostración de sus posibilidades en estudios biomédicos como pruebas de diagnóstico POC. Estos sistemas pueden alimentarse desde un puerto USB o batería o ser sistemas autoalimentados, que extraen la energía de fuentes de energía alternativas como las celdas de combustible.

Los diversos enfoques de detección electroquímica propuestos en esta tesis permiten adquirir señales de baja corriente, procesarlas y mostrar un resultado cuantitativo, consumiendo una potencia mínima. Gracias a su reducido consumo de energía, ha sido posible desarrollar plataformas autoalimentadas capaces de operar solo con la energía extraída de la muestra biológica. Las plataformas propuestas también se pueden alimentar a través de dispositivos externos, como puertos USB y baterías recargables o desechables. Estos dispositivos son fáciles de usar y plug-and-play, y permiten a las personas no calificadas realizar pruebas después de un entrenamiento mínimo. Debido a su interfaz fácil de usar, los resultados son claros y fáciles de interpretar. Las soluciones propuestas en esta tesis doctoral permiten mejorar las pruebas de POC, cuyas premisas son la descentralización de laboratorio, la medicina personalizada, el diagnóstico rápido y la mejora de la atención al paciente [16].

El capítulo introductorio de esta tesis analiza el estado del arte de los sistemas de diagnósticos POC con el objetivo de estudiar sus fortalezas y debilidades, y determinar las mejoras necesarias. Se da una descripción general del impacto de las pruebas de POC en la atención médica en países de bajos ingresos, enfocándose en las barreras, las pautas normativas y políticas, la ubicación geográfica, las características del sistema de infraestructura de salud y la gestión de la cadena de suministro. Además, se realiza una clasificación de las pruebas de diagnóstico de POC según el biosensor utilizado, destacando los sensores y las técnicas de detección basadas en sensores electroquímicos. El desarrollo de tecnologías y dispositivos POC conlleva la integración de tecnologías electrónicas y biosensores. Por este motivo, el capítulo introductorio proporciona una visión general de posibles arquitecturas aplicables a las tecnologías POC, analizando los últimos avances y describiendo diferentes soluciones.

## APPENDIX C. RESUMEN EN CASTELLANO

El tercer capítulo muestra los resultados de esta tesis doctoral, que se presenta como un compendio de artículos. Según el sitio web Dimensions.ai, en los últimos 5 años, se han publicado más de 13,000 artículos y 4,000 patentes sobre sistemas POC portátiles y de baja potencia para detecciones electroquímicas.

Las publicaciones se presentan en la tesis en orden cronológico. Sin embargo, los estudios se llevaron a cabo en secuencia inversa a la publicación de las investigaciones. Los primeros desarrollos fueron dispositivos electrónicos discretos alimentados por USB y baterías. Estos complejos sistemas electrónicos condujeron a dispositivos simplificados que impulsaron el desarrollo de plataformas autoalimentadas. Aunque, debido a los intereses estratégicos de los grupos de investigación, las publicaciones se publicaron en orden cronológico inverso.

La publicación titulada “‘Plug-and-Power’ Point-of-Care diagnostics: A novel approach for self-powered electronic reader-based portable analytical devices” se publicó en la revista Biosensors and Bioelectronics de la editorial Elsevier. Todas las categorías de la revista están clasificadas en el primer cuartil (Q1). Además, tiene un CiteScore de 17.6 y un Factor de impacto de 10.257 en 2019. Las otras dos publicaciones que componen esta tesis se publicaron en la revista Sensors (editorial MDPI). Sensors es una revista Open Source clasificada en el primer cuartil (Q1) en la categoría de Instrumentación. Tiene un CiteScore de 5.0 y un Factor de Impacto de 3.275 en 2019. El manuscrito titulado “Self-Powered Portable Electronic Reader for Point-of-Care Amperometric Measurements” tiene más de 775 vistas del resumen y 750 vistas de texto completo, y el artículo “Competitive USB-Powered Hand-Held Potentiostat for POC Applications: An HRP Detection Case” tiene más de 600 vistas del resumen y 785 vistas de texto completo. Uno de los desafíos de esta tesis es desarrollar sistemas de detección electroquímica autoalimentados y fáciles de usar, capaces de mostrar datos cualitativos y medir amplios rangos de corriente con alta resolución. El artículo titulado “‘Plug-and-Power’ Point-of-Care diagnostics: A novel approach for self-powered electronic reader-based portable analytical devices” describe un dispositivo POC portátil e innovador capaz de proporcionar un resultado cuantitativo de la concentración de glucosa de un muestra. El sistema propuesto combina un lector plug-and-play y un sensor de papel desechable. El lector electrónico sin batería extrae la energía de la unidad desechable, adquiere la señal, la procesa y muestra la concentración de glucosa en una pantalla. Debido al bajo consumo de energía de los circuitos de instrumentación y procesamiento, todo el sistema electrónico puede funcionar solo con la energía extraída del elemento desechable que actúa como sensor y fuente de energía. Además, el proceso de recolección de energía, medición y procesamiento de datos lo realiza el dispositivo de forma automática, sin necesidad de ninguna acción externa. El dispositivo inteligente minimiza la interacción del usuario, que solo debe depositar la muestra en la tira de papel y esperar unos segundos para ver el resultado de la prueba. Además, el dispositivo de alto rendimiento proporciona resultados precisos y de alta resolución, pudiendo medir corrientes de hasta  $30 \mu$

## APPENDIX C. RESUMEN EN CASTELLANO

A con una resolución de 13 nA y un error inferior al 1.8 %.

La segunda publicación titulada “Self-Powered Portable Electronic Reader for Point-of-Care Amperometric Measurements” presenta en detalle la concepción, diseño, implementación y caracterización de los circuitos electrónicos que componen el lector electrónico sin batería. Este concepto versátil detecta de forma amperométrica una amplia variedad de analitos, además de procesar y mostrar los resultados sin necesidad de baterías comerciales, ya que la energía necesaria para llevar a cabo la prueba se extrae de una pila de combustible (o fuel cell, FC de sus siglas en inglés). El lector electrónico fue validado siguiendo diferentes enfoques, utilizando las FC como elementos de potencia y como elementos duales de alimentación y detección. El dispositivo se probó con FCs y sensores de glucosa, orina, metanol y etanol, mostrando la adaptabilidad del sistema a diferentes escenarios, y validando la posibilidad de extrapolar el sistema a una amplia variedad de campos más allá del diagnóstico clínico, como el ámbito veterinario o ambiental.

El tercer artículo presenta el estudio titulado “Competitive USB-Powered Hand-Held Potentiostat for POC Applications: An HRP Detection Case”, en el que se desarrolló el sistema AmpStat. Este es sistema de bajo coste, miniaturizado y personalizable está compuesto por un potencióstato alimentado por USB y permite realizar detecciones amperométricas. El dispositivo portátil combina un conector que aloja el sensor amperométrico desechable, un sistema electrónico totalmente personalizado para la adquisición de señal y un software llamado AmpView, que representa, muestra y guarda los resultados. El dispositivo personalizable fue diseñado para medir corrientes de hasta  $11.2 \mu A$ , aunque puede adaptarse fácilmente para detectar corrientes de hasta 3 mA. La eficacia del prototipo AmpStat se evaluó midiendo amperométricamente peroxidasa de rábano picante en un rango de concentración de  $0.01 \text{ ng} \cdot \text{mL}^{-1}$  a  $1 \mu \text{g} \cdot \text{mL}^{-1}$ . En este estudio, el rendimiento del dispositivo se comparó con tres potencióstatos comerciales. Estos se probaron en paralelo con el dispositivo propuesto, obteniendo el límite de detección, el límite de cuantificación y la sensibilidad de los cuatro equipos. El potencióstato desarrollado proporcionó una detección razonablemente precisa con resultados comparables a los obtenidos con tres sistemas comerciales significativamente más costosos. Como prueba de concepto, el sistema fue validado con muestras de peroxidasa de rábano picante, aunque podría ampliarse fácilmente su alcance y medir otros tipos de analitos o matrices biológicas. El dispositivo fue alimentado externamente a través del puerto USB de un ordenador. Sin embargo, en el futuro, se quiere actualizar el dispositivo con el fin de adaptarlo para que sea autoalimentado y envíe los datos a través de un módulo inalámbrico a un ordenador o teléfono inteligente.

En el contexto de esta tesis, se han llevado a cabo otras investigaciones, cuyos resultados se presentan en la sección de Anexos.

Algunos de estos estudios se han presentado en conferencias. Estos se basan en

## APPENDIX C. RESUMEN EN CASTELLANO

circuitos de instrumentación de ultra baja potencia aplicables a sistemas autoalimentados y en circuitos de instrumentación electrónica para diferentes aplicaciones de biosensores.

En el marco de esta tesis, también se ha participado en el diseño del circuito de instrumentación electrónica de la patente EP19382604.7 titulada “Self-powered system and method for power extraction and measurement of energy-generator units”.

Además, se desarrolló un sistema de biodetección portátil para investigar el trastorno de distonía con la colaboración de los miembros del laboratorio Reilly lab, en el marco de una estancia predoctoral en el Trinity Center for Biomedical Engineering y el Trinity College Institute of Neuroscience del Trinity College of Dublin (Irlanda) . La distonía es un trastorno del movimiento neurológico que causa contracciones musculares involuntarias que producen movimientos o posturas anormales, a veces dolorosas. La discriminación temporal es el intervalo de tiempo más corto en el que un sujeto puede discriminar dos estímulos secuenciales como asíncronos. Algunos estudios asocian la distonía cervical con una discriminación temporal anormal. Durante la estancia en Dublín, se desarrolló una plataforma electrónica multimodal y un software personalizado para medir los intervalos de discriminación temporal a través de estímulos visuales, táctiles, y una combinación de ambos. Este dispositivo portátil estaba alimentado a través de un puerto USB y conectado a un teléfono inteligente Android a través de un módulo de comunicación Bluetooth Low Energy. La aplicación personalizada desarrollada para este dispositivo, permitía al usuario controlar los estímulos, registrar los datos y enviarlos por correo electrónico, con la ventaja de poder ser utilizados por personas no calificadas después de un entrenamiento mínimo gracias a su interfaz fácil de usar.

Finalmente, en los capítulos quinto y sexto de esta tesis, se resumen y discuten los resultados, y se presentan las conclusiones de las investigaciones realizadas, recomendando desarrollos futuros para crear la próxima generación de dispositivos POC de baja potencia y autoalimentados.



# Bibliography

- [1] R. L. White and J. D. Meindl, “The impact of integrated electronics in medicine,” *Science*, vol. 195, pp. 1119–1124, mar 1977.
- [2] E. Ozdalga, A. Ozdalga, and N. Ahuja, “The smartphone in medicine: A review of current and potential use among physicians and students,” *Journal of Medical Internet Research*, vol. 14, p. e128, sep 2012.
- [3] M. R. Neuman, G. D. Baura, S. Meldrum, O. Soykan, M. E. Valentinuzzi, R. S. Leder, S. Micera, and Y. T. Zhang, “Advances in medical devices and medical electronics,” in *Proceedings of the IEEE*, vol. 100, pp. 1537–1550, Institute of Electrical and Electronics Engineers Inc., may 2012.
- [4] F. Tasnim, A. Sadraei, B. Datta, M. Khan, K. Y. Choi, A. Sahasrabudhe, T. A. Vega Gálvez, I. Wicaksono, O. Rosello, C. Nunez-Lopez, and C. Dagdeviren, “Towards personalized medicine: the evolution of imperceptible health-care technologies,” *Foresight*, vol. 20, no. 6, pp. 589–601, 2018.
- [5] D. M. Berwick, “Disseminating Innovations in Health Care,” *Journal of the American Medical Association*, vol. 289, pp. 1969–1975, apr 2003.
- [6] R. Hawkins, “Managing the pre- and post-analytical phases of the total testing process,” *Annals of Laboratory Medicine*, vol. 32, pp. 5–16, jan 2012.
- [7] S. Shrivastava, T. Q. Trung, and N. E. Lee, “Recent progress, challenges, and prospects of fully integrated mobile and wearable point-of-care testing systems for self-testing,” *Chemical Society Reviews*, vol. 49, pp. 1812–1866, mar 2020.
- [8] W. V. Gonzales, A. T. Mobashsher, and A. Abbosh, “The progress of glucose monitoring—A review of invasive to minimally and non-invasive techniques, devices and sensors,” *Sensors*, vol. 19, p. 800, feb 2019.
- [9] N. A. B. A. Salam, W. H. B. M. Saad, Z. B. Manap, and F. Bte Salehuddin, “The evolution of non-invasive blood glucose monitoring system for personal application,” *Journal of Telecommunication, Electronic and Computer Engineering*, vol. 8, no. 1, pp. 59–65, 2016.



## BIBLIOGRAPHY

- [10] D. Bruen, C. Delaney, L. Florea, and D. Diamond, “Glucose sensing for diabetes monitoring: Recent developments,” *Sensors*, vol. 17, p. 1866, aug 2017.
- [11] World Health Organization, “World Health Organization — Innovation,” 2016.
- [12] R. Hillestad, J. Bigelow, A. Bower, F. Girosi, R. Meili, R. Scoville, and R. Taylor, “Can electronic medical record systems transform health care? Potential health benefits, savings, and costs,” *Health Affairs*, vol. 24, pp. 1103–1117, sep 2005.
- [13] Lucintel, “Construction Aggregate Market Report: Trends, Forecast and Competitive Analysis,” tech. rep., 2019.
- [14] S. Nam, H. R. Han, H. J. Song, Y. Song, K. B. Kim, and M. T. Kim, “Utility of a point-of-care device in recruiting ethnic minorities for diabetes research with community partners,” *Journal of Health Care for the Poor and Underserved*, vol. 22, no. 4, pp. 1253–1263, 2011.
- [15] W. W. Weston, “Patient-centered medicine: A guide to the biopsychosocial model,” *Families, Systems and Health*, vol. 23, pp. 387–392, dec 2005.
- [16] A. M. R. Schols, G.-J. Dinant, R. Hopstaken, C. P. Price, R. Kusters, and J. W. L. Cals, “International definition of a point-of-care test in family practice: a modified e-Delphi procedure,” *Family Practice*, vol. 35, pp. 475–480, jul 2018.
- [17] G. Wu and M. H. Zaman, “Low-cost tools for diagnosing and monitoring HIV infection in low-resource settings,” *Bulletin of the World Health Organization*, vol. 90, no. 12, pp. 914–920, 2012.
- [18] N. Engel, K. Wachter, M. Pai, J. Gallarda, C. Boehme, I. Celentano, and R. Weintraub, “Addressing the challenges of diagnostics demand and supply: insights from an online global health discussion platform.,” *BMJ global health*, vol. 1, no. 4, p. e000132, 2016.
- [19] C. Páez Avilés, *Innovation on Nanoscience: Processes and Ecosystems of Innovation with a multi-KET approach to foster Technology Transfer and Commercialization of Nanotechnologies in the Field of Healthcare*. PhD thesis, feb 2017.
- [20] D. Grieshaber, R. MacKenzie, J. Vörös, and E. Reimhult, “Electrochemical Biosensors - Sensor Principles and Architectures,” *Sensors*, vol. 8, pp. 1400–1458, mar 2008.
- [21] N. Bhalla, P. Jolly, N. Formisano, and P. Estrela, “Introduction to biosensors,” *Essays in Biochemistry*, vol. 60, pp. 1–8, jun 2016.

## BIBLIOGRAPHY

- [22] R. J. Narayan, *Medical Biosensors for Point of Care (POC) Applications*. 2016.
- [23] S. F. Cheung, S. K. L. Cheng, and D. T. Kamei, "Paper-Based Systems for Point-of-Care Biosensing," *Journal of Laboratory Automation*, vol. 20, pp. 316–333, aug 2015.
- [24] Y. Huang, T. Xu, W. Wang, Y. Wen, K. Li, L. Qian, X. Zhang, and G. Liu, "Lateral flow biosensors based on the use of micro- and nanomaterials: a review on recent developments," *Microchimica Acta*, vol. 187, pp. 1–25, jan 2020.
- [25] S. Q. Wang, T. Chinnasamy, M. A. Lifson, F. Inci, and U. Demirci, "Flexible Substrate-Based Devices for Point-of-Care Diagnostics," *Trends in Biotechnology*, vol. 34, pp. 909–921, nov 2016.
- [26] A. J. Bandonkar, W. Jia, C. Yardimci, X. Wang, J. Ramirez, and J. Wang, "Tattoo-based noninvasive glucose monitoring: A proof-of-concept study," *Analytical Chemistry*, vol. 87, pp. 394–398, jan 2015.
- [27] W. Jung, J. Han, J. W. Choi, and C. H. Ahn, "Point-of-care testing (POCT) diagnostic systems using microfluidic lab-on-a-chip technologies," *Microelectronic Engineering*, vol. 132, pp. 46–57, jan 2015.
- [28] P. N. Nge, C. I. Rogers, and A. T. Woolley, "Advances in microfluidic materials, functions, integration, and applications," *Chemical Reviews*, vol. 113, pp. 2550–2583, apr 2013.
- [29] P. K. Das and A. B. Hasan, "Mechanical micropumps and their applications: A review," in *AIP Conference Proceedings*, vol. 1851, p. 020110, AIP Publishing LLC, jun 2017.
- [30] J. P. Laffleur, A. Jönsson, S. Senkbeil, and J. P. Kutter, "Recent advances in lab-on-a-chip for biosensing applications," *Biosensors and Bioelectronics*, vol. 76, pp. 213–233, feb 2016.
- [31] G. Alfian, M. Syafrudin, M. F. Ijaz, M. A. Syaekhoni, N. L. Fitriyani, and J. Rhee, "A personalized healthcare monitoring system for diabetic patients by utilizing BLE-based sensors and real-time data processing," *Sensors*, vol. 18, p. 2183, jul 2018.
- [32] K. M. Palamountain, J. Baker, E. P. Cowan, S. Essajee, L. T. Mazzola, M. Metzler, M. Schito, W. S. Stevens, G. J. Young, and G. J. Domingo, "Perspectives on introduction and implementation of new point-of-care diagnostic tests.," *The Journal of infectious diseases*, vol. 205 Suppl, pp. S181–90, may 2012.

## BIBLIOGRAPHY

- [33] A. Amira, N. Agoulmine, F. Bensaali, A. Bermak, and G. Dimitrakopoulos, “Special issue: Empowering eHealth with smart internet of things (IoT) medical devices,” *Journal of Sensor and Actuator Networks*, vol. 8, p. 33, jun 2019.
- [34] A. F. Subahi, “Edge-Based IoT Medical Record System: Requirements, Recommendations and Conceptual Design,” *IEEE Access*, vol. 7, pp. 94150–94159, 2019.
- [35] I. Hernández-Neuta, F. Neumann, J. Brightmeyer, T. Ba Tis, N. Madaboosi, Q. Wei, A. Ozcan, and M. Nilsson, “Smartphone-based clinical diagnostics: towards democratization of evidence-based health care,” *Journal of Internal Medicine*, vol. 285, pp. 19–39, jan 2019.
- [36] C. Chan, J. A. Inskip, A. R. Kirkham, J. M. Ansermino, G. Dumont, L. C. Li, K. Ho, H. Novak Lauscher, C. J. Ryerson, A. M. Hoens, T. Chen, A. Garde, J. D. Road, and P. G. Camp, “A smartphone oximeter with a fingertip probe for use during exercise training: usability, validity and reliability in individuals with chronic lung disease and healthy controls,” *Physiotherapy (United Kingdom)*, oct 2019.
- [37] H. Zhu, I. Sencan, J. Wong, S. Dimitrov, D. Tseng, K. Nagashima, and A. Ozcan, “Cost-effective and rapid blood analysis on a cell-phone.,” *Lab on a chip*, vol. 13, pp. 1282–8, apr 2013.
- [38] S. Choi, “Powering point-of-care diagnostic devices,” *Biotechnology Advances*, vol. 34, no. 3, pp. 321–330, 2016.
- [39] Q. Xu, F. Zhang, L. Xu, P. Leung, C. Yang, and H. Li, “The applications and prospect of fuel cells in medical field: A review,” *Renewable and Sustainable Energy Reviews*, vol. 67, pp. 574–580, jan 2017.
- [40] European Commission, “2018 reform of EU data protection rules European Commission,” 2018.
- [41] R. Peeling and D. Mabey, “Point-of-care tests for diagnosing infections in the developing world,” *Clinical Microbiology and Infection*, vol. 16, pp. 1062–1069, aug 2010.
- [42] UN Department of Economics and Social Affairs, “World Population Prospects - Population Division - United Nations,” 2015.
- [43] D. Vidyasagar, “Global notes: the 10/90 gap disparities in global health research,” *Journal of Perinatology*, vol. 26, pp. 55–56, jan 2006.
- [44] World Health Organisation, *The world health report 2013: Research for universal health coverage*. 2013.

## BIBLIOGRAPHY

- [45] T. P. Mashamba-Thompson, R. L. Morgan, B. Sartorius, B. Dennis, P. K. Drain, and L. Thabane, “Effect of Point-of-Care Diagnostics on Maternal Outcomes in Human Immunodeficiency Virus–Infected Women,” *Point of Care: The Journal of Near-Patient Testing & Technology*, vol. 16, pp. 67–77, jun 2017.
- [46] D. Watson-Jones, J. Changalucha, B. Gumodoka, H. Weiss, M. Rusizoka, L. Ndeki, A. Whitehouse, R. Balira, J. Todd, D. Ngeleja, D. Ross, A. Buvé, R. Hayes, and D. Mabey, “Syphilis in Pregnancy in Tanzania. I. Impact of Maternal Syphilis on Outcome of Pregnancy,” *The Journal of Infectious Diseases*, vol. 186, pp. 940–947, oct 2002.
- [47] N. S. Wijesooriya, R. W. Rochat, M. L. Kamb, P. Turlapati, M. Temmerman, N. Broutet, and L. M. Newman, “Global burden of maternal and congenital syphilis in 2008 and 2012: a health systems modelling study.,” *The Lancet. Global health*, vol. 4, pp. e525–33, aug 2016.
- [48] M. Marks and D. C. Mabey, “The introduction of syphilis point of care tests in resource limited settings,” *Expert Review of Molecular Diagnostics*, vol. 17, no. 4, pp. 321–325, 2017.
- [49] N. P. Pai, C. Vadnais, C. Denkinger, N. Engel, and M. Pai, “Point-of-care testing for infectious diseases: diversity, complexity, and barriers in low- and middle-income countries.,” *PLoS medicine*, vol. 9, no. 9, p. e1001306, 2012.
- [50] C. D. Chin, T. Laksanasopin, Y. K. Cheung, D. Steinmiller, V. Linder, H. Parsa, J. Wang, H. Moore, R. Rouse, G. Umvilighozo, E. Karita, L. Mwambarangwe, S. L. Braunstein, J. van de Wijgert, R. Sahabo, J. E. Justman, W. El-Sadr, and S. K. Sia, “Microfluidics-based diagnostics of infectious diseases in the developing world,” *Nature Medicine*, vol. 17, pp. 1015–1019, aug 2011.
- [51] L. Bissonnette and M. G. Bergeron, “Portable devices and mobile instruments for infectious diseases point-of-care testing,” *Expert Review of Molecular Diagnostics*, vol. 17, pp. 471–494, may 2017.
- [52] T. Kujinga, “Access to HIV diagnostics in Sub-Sahara Africa. In WHO Meeting with Diagnostics Manufacturers and Stakeholders Global Forecast of Diagnostics Demand for 2014–2018,” tech. rep., 2014.
- [53] P. W. Gething, F. A. Johnson, F. Frempong-Ainguah, P. Nyarko, A. Baschieri, P. Aboagye, J. Falkingham, Z. Matthews, and P. M. Atkinson, “Geographical access to care at birth in Ghana: a barrier to safe motherhood,” *BMC Public Health*, vol. 12, p. 991, dec 2012.
- [54] G. Alemnji, J. N. Nkengasong, and B. S. Parekh, “HIV testing in developing countries: What is required?,” *Indian Journal of Medical Research*, vol. 134, pp. 779–786, dec 2011.

## BIBLIOGRAPHY

- [55] A. Biza, I. Jille-Traas, M. Colomar, M. Belizan, J. Requejo Harris, B. Crahay, M. Merialdi, M. H. Nguyen, F. Althabe, A. Aleman, E. Bergel, A. Carbonell, L. Chavane, T. Delvaux, D. Geelhoed, M. Gülmezoglu, C. R. Malapende, A. Melo, N. B. Osman, M. Widmer, M. Temmerman, and A. P. Betrán, “Challenges and opportunities for implementing evidence-based antenatal care in Mozambique: a qualitative study,” *BMC Pregnancy and Childbirth*, vol. 15, p. 200, dec 2015.
- [56] C. Wang, P. W. Horby, F. G. Hayden, and G. F. Gao, “A novel coronavirus outbreak of global health concern,” *The Lancet*, vol. 395, pp. 470–473, feb 2020.
- [57] T. Nguyen, D. D. Bang, and A. Wolff, “2019 Novel coronavirus disease (COVID-19): Paving the road for rapid detection and point-of-care diagnostics,” *Micromachines*, vol. 11, pp. 1–7, mar 2020.
- [58] Z. Khurshid, F. Y. I. Asiri, and H. Al Wadaani, “Human saliva: Non-invasive fluid for detecting novel coronavirus (2019-nCoV),” *International Journal of Environmental Research and Public Health*, vol. 17, p. 2225, mar 2020.
- [59] A. St John and C. P. Price, “Existing and Emerging Technologies for Point-of-Care Testing,” *The Clinical biochemist. Reviews*, vol. 35, pp. 155–67, aug 2014.
- [60] International Diabetes Federation, “IDF Diabetes Atlas, 8th ed.,” tech. rep., International Diabetes Federation, Brussels, Belgium, 2017.
- [61] Grand View Research, “Point of care diagnostics market analysis by product,” 2015.
- [62] G. Foundation, “Foundation and Grand Challenges Canada Announce over \$31 Million for Point-of-Care Diagnostics,” tech. rep.
- [63] S. Nayak, N. R. Blumenfeld, T. Laksanasopin, and S. K. Sia, “Point-of-Care Diagnostics: Recent Developments in a Connected Age,” *Analytical Chemistry*, vol. 89, no. 1, pp. 102–123, 2017.
- [64] “Afinion CRP Test.”
- [65] “Alere q — Fully automated nucleic acid testing platform.”
- [66] “Pima CD4 Cartridge.”
- [67] “Analizador Cholestech LDX.”
- [68] J. Colomer-Farrarons, P. Ll., A. Ivon, and J. Samitier, “Portable Bio-Devices: Design of electrochemical instruments from miniaturized to implantable devices,” in *New Perspectives in Biosensors Technology and Applications*, InTech, jul 2011.

## BIBLIOGRAPHY

- [69] A. Syahir, K. Usui, K.-Y. Tomizaki, K. Kajikawa, and H. Mihara, "Label and Label-Free Detection Techniques for Protein Microarrays," *Microarrays*, vol. 4, pp. 228–244, apr 2015.
- [70] J. G. Lijmer and P. M. M. Bossuyt, "Various randomized designs can be used to evaluate medical tests.," *Journal of clinical epidemiology*, vol. 62, pp. 364–73, apr 2009.
- [71] E. Kim, M. D. Baaske, and F. Vollmer, "Towards next-generation label-free biosensors: recent advances in whispering gallery mode sensors," *Lab on a Chip*, vol. 17, pp. 1190–1205, mar 2017.
- [72] U. Anik, "Electrochemical medical biosensors for POC applications," in *Medical Biosensors for Point of Care (POC) Applications*, pp. 275–292, Elsevier Inc., jan 2017.
- [73] J. L. Hammond, N. Formisano, P. Estrela, S. Carrara, and J. Tkac, "Electrochemical biosensors and nanobiosensors," *Essays in Biochemistry*, vol. 60, pp. 69–80, jun 2016.
- [74] P. Arora, A. Sindhu, N. Dilbaghi, and A. Chaudhury, "Biosensors as innovative tools for the detection of food borne pathogens," *Biosensors and Bioelectronics*, vol. 28, pp. 1–12, oct 2011.
- [75] C. Chen, Q. Xie, D. Yang, H. Xiao, Y. Fu, Y. Tan, and S. Yao, "Recent advances in electrochemical glucose biosensors: A review," *RSC Advances*, vol. 3, pp. 4473–4491, mar 2013.
- [76] L. Rotariu, F. Lagarde, N. Jaffrezic-Renault, and C. Bala, "Electrochemical biosensors for fast detection of food contaminants - trends and perspective," *TrAC - Trends in Analytical Chemistry*, vol. 79, pp. 80–87, may 2016.
- [77] F. Arduini, L. Micheli, D. Moscone, G. Palleschi, S. Piermarini, F. Ricci, and G. Volpe, "Electrochemical biosensors based on nanomodified screen-printed electrodes: Recent applications in clinical analysis," *TrAC - Trends in Analytical Chemistry*, vol. 79, pp. 114–126, may 2016.
- [78] "Metrohm DropSens . Screen-printed electrodes."
- [79] X. Zhu and L. Shi, "Electrochemistry," in *Nano-inspired Biosensors for Protein Assay with Clinical Applications*, pp. 209–236, Elsevier, jan 2018.
- [80] S. Yunus, A. M. Jonas, and B. Lakard, "Potentiometric Biosensors," in *Encyclopedia of Biophysics*, pp. 1941–1946, Berlin, Heidelberg: Springer Berlin Heidelberg, 2013.
- [81] N. Jaffrezic-Renault, S. Dzyadevych, N. Jaffrezic-Renault, and S. V. Dzyadevych, "Conductometric Microbiosensors for Environmental Monitoring," *Sensors*, vol. 8, pp. 2569–2588, apr 2008.

## BIBLIOGRAPHY

- [82] P. D’Orazio, “Biosensors in clinical chemistry,” *Clinica Chimica Acta*, vol. 334, pp. 41–69, aug 2003.
- [83] V. Encinas-Sánchez, M. de Miguel, M. Lasanta, G. García-Martín, and F. Pérez, “Electrochemical impedance spectroscopy (EIS): An efficient technique for monitoring corrosion processes in molten salt environments in CSP applications,” *Solar Energy Materials and Solar Cells*, vol. 191, pp. 157–163, mar 2019.
- [84] M. Islam, K. A. Wahid, A. V. Dinh, and P. Bhowmik, “Model of dehydration and assessment of moisture content on onion using EIS,” *Journal of Food Science and Technology*, vol. 56, pp. 2814–2824, jun 2019.
- [85] F. Clemente, M. Romano, P. Bifulco, and M. Cesarelli, “EIS measurements for characterization of muscular tissue by means of equivalent electrical parameters,” *Measurement: Journal of the International Measurement Confederation*, vol. 58, pp. 476–482, dec 2014.
- [86] M. Piliarik, H. Vaisocherová, and J. Homola, “Surface plasmon resonance biosensing,” *Methods in molecular biology (Clifton, N.J.)*, vol. 503, pp. 65–88, 2009.
- [87] P. Damborský, J. Švitel, and J. Katrlík, “Optical biosensors,” *Essays in biochemistry*, vol. 60, no. 1, pp. 91–100, 2016.
- [88] S. Firdous, S. Anwar, and R. Rafya, “Development of surface plasmon resonance (SPR) biosensors for use in the diagnostics of malignant and infectious diseases,” *Laser Physics Letters*, vol. 15, p. 065602, jun 2018.
- [89] D. Harpaz, B. Koh, R. S. Marks, R. C. Seet, I. Abdulhalim, and A. I. Tok, “Point-of-Care Surface Plasmon Resonance Biosensor for Stroke Biomarkers NT-proBNP and S100 $\beta$  Using a Functionalized Gold Chip with Specific Antibody,” *Sensors*, 2019.
- [90] J. Homola, “Present and future of surface plasmon resonance biosensors,” *Analytical and Bioanalytical Chemistry*, vol. 377, pp. 528–539, oct 2003.
- [91] P. Kozma, F. Kehl, E. Ehrentreich-Förster, C. Stamm, and F. F. Bier, “Integrated planar optical waveguide interferometer biosensors: A comparative review,” *Biosensors and Bioelectronics*, vol. 58, pp. 287–307, aug 2014.
- [92] N. Zaytseva, W. Miller, V. Goral, J. Hepburn, and Y. Fang, “Microfluidic resonant waveguide grating biosensor system for whole cell sensing,” *Applied Physics Letters*, vol. 98, p. 163703, apr 2011.
- [93] J. Xu, D. Suarez, and D. S. Gottfried, “Detection of avian influenza virus using an interferometric biosensor,” *Analytical and Bioanalytical Chemistry*, vol. 389, pp. 1193–1199, sep 2007.

## BIBLIOGRAPHY

- [94] H. N. Daghestani and B. W. Day, "Theory and Applications of Surface Plasmon Resonance, Resonant Mirror, Resonant Waveguide Grating, and Dual Polarization Interferometry Biosensors," *Sensors*, vol. 10, pp. 9630–9646, 2010.
- [95] A. Sai Sarathi Vasani, "Point-of-care biosensor system," *Frontiers in Bioscience*, vol. S5, no. 1, p. 39, 2013.
- [96] S. Satyanarayana, D. T. McCormick, and A. Majumdar, "Parylene micro membrane capacitive sensor array for chemical and biological sensing," *Sensors and Actuators B*, vol. 115, pp. 494–502, 2006.
- [97] K. W. Wee, G. Y. Kang, J. Park, J. Y. Kang, D. S. Yoon, J. H. Park, and T. S. Kim, "Novel electrical detection of label-free disease marker proteins using piezoresistive self-sensing micro-cantilevers," in *Biosensors and Bioelectronics*, vol. 20, pp. 1932–1938, Elsevier, apr 2005.
- [98] P. Rasmussen, J. Thaysen, O. Hansen, S. Eriksen, and A. Boisen, "Optimised cantilever biosensor with piezoresistive read-out," *Ultramicroscopy*, vol. 97, pp. 371–376, oct 2003.
- [99] V. K. T. Ngo, D. G. Nguyen, H. P. U. Nguyen, V. M. Tran, T. K. M. Nguyen, T. P. Huynh, Q. V. Lam, T. D. Huynh, and T. N. L. Truong, "Quartz crystal microbalance (QCM) as biosensor for the detecting of Escherichia coli O157:H7," *Advances in Natural Sciences: Nanoscience and Nanotechnology*, vol. 5, p. 045004, oct 2014.
- [100] S. Atay, K. Pişkin, F. Yılmaz, C. Çakır, H. Yavuz, and A. Denizli, "Quartz crystal microbalance based biosensors for detecting highly metastatic breast cancer cells via their transferrin receptors," *Analytical Methods*, vol. 8, pp. 153–161, dec 2016.
- [101] M. R. Kierny, T. D. Cunningham, and B. K. Kay, "Detection of biomarkers using recombinant antibodies coupled to nanostructured platforms," *Nano reviews*, vol. 3, 2012.
- [102] A. J. Bard and L. R. Faulkner, *Electrochemical Methods: Fundamentals and Applications*. 2nd ed., 2001.
- [103] P. Kumar, V. Narwal, R. Jaiwal, and C. S. Pundir, "Construction and application of amperometric sarcosine biosensor based on SOxNPs/AuE for determination of prostate cancer," *Biosensors and Bioelectronics*, vol. 122, pp. 140–146, dec 2018.
- [104] X. Luo, J. Pan, K. Pan, Y. Yu, A. Zhong, S. Wei, J. Li, J. Shi, and X. Li, "An electrochemical sensor for hydrazine and nitrite based on graphene-cobalt hexacyanoferrate nanocomposite: Toward environment and food detection," *Journal of Electroanalytical Chemistry*, vol. 745, pp. 80–87, may 2015.



## BIBLIOGRAPHY

- [105] F. T. Moreira, M. G. F. Sale, and M. Di Lorenzo, "Towards timely Alzheimer diagnosis: A self-powered amperometric biosensor for the neurotransmitter acetylcholine," *Biosensors and Bioelectronics*, vol. 87, pp. 607–614, jan 2017.
- [106] J. Colomer-Farrarons and P. L. Miribel-Català, *A CMOS self-powered front-end architecture for subcutaneous event-detector devices: Three-electrodes amperometric biosensor approach*. Springer Netherlands, 2011.
- [107] S. S. Ghoreishizadeh, I. Taurino, G. De Micheli, S. Carrara, and P. Georgiou, "A Differential Electrochemical Readout ASIC with Heterogeneous Integration of Bio-Nano Sensors for Amperometric Sensing," *IEEE Transactions on Biomedical Circuits and Systems*, vol. 11, pp. 1148–1159, oct 2017.
- [108] K. Hanley, A. Murphy, N. Creedon, A. O. Riordan, D. O. Hare, and I. O. Connell, "Current readout circuit for point-of-care infectious disease diagnostics in animal health," in *2018 IEEE Nordic Circuits and Systems Conference, NORCAS 2018: NORCHIP and International Symposium of System-on-Chip, SoC 2018 - Proceedings*, pp. 1–5, IEEE, oct 2018.
- [109] J. Punter, J. Colomer-Farrarons, and P. Ll., "Bioelectronics for Amperometric Biosensors," in *State of the Art in Biosensors - General Aspects*, InTech, mar 2013.
- [110] C. Loncaric, Y. Tang, C. Ho, M. A. Parameswaran, and H. Z. Yu, "A USB-based electrochemical biosensor prototype for point-of-care diagnosis," *Sensors and Actuators, B: Chemical*, vol. 161, pp. 908–913, jan 2012.
- [111] J. Punter-Villagrasa, J. Cid, C. Páez-Avilés, I. Rodríguez-Villarreal, E. Juanola-Feliu, J. Colomer-Farrarons, and P. L. Miribel-Català, "An instantaneous low-cost point-of-care anemia detection device," *Sensors*, vol. 15, pp. 4564–4577, feb 2015.
- [112] Y. Fan, J. Liu, Y. Wang, J. Luo, H. Xu, S. Xu, and X. Cai, "A wireless point-of-care testing system for the detection of neuron-specific enolase with microfluidic paper-based analytical devices," *Biosensors and Bioelectronics*, vol. 95, pp. 60–66, sep 2017.
- [113] A. C. Sun, C. Yao, V. Ag, and D. A. Hall, "An efficient power harvesting mobile phone-based electrochemical biosensor for point-of-care health monitoring," *Sensors and Actuators, B: Chemical*, vol. 235, pp. 126–135, nov 2016.
- [114] D. Ji, L. Liu, S. Li, C. Chen, Y. Lu, J. Wu, and Q. Liu, "Smartphone-based cyclic voltammetry system with graphene modified screen printed electrodes for glucose detection," *Biosensors and Bioelectronics*, vol. 98, pp. 449–456, dec 2017.

## BIBLIOGRAPHY

- [115] E. Ghodsevali, B. Gosselin, M. Boukadoum, and A. Miled, “High accuracy and sensitivity differential potentiostat with amplifier-based error cancellation feedback loop,” in *IEEE Biomedical Circuits and Systems Conference: Engineering for Healthy Minds and Able Bodies, BioCAS 2015 - Proceedings*, pp. 1–4, IEEE, oct 2015.
- [116] W. Jett, “Maximize dynamic range with micropower rail-to-rail op amp,” in *Analog Circuit Design*, pp. 931–932, Elsevier, jan 2015.
- [117] “High-Side Current Sensing — Analog Devices.”
- [118] Y. Montes-Cebrián, A. Álvarez-Carulla, J. Colomer-Farrarons, M. Puig-Vidal, J. López-Sánchez, and P. Miribel-Català, “A Fuel Cell-based adaptable Self-Powered Event Detection platform enhanced for biosampling applications,” in *Proceedings - 33rd Conference on Design of Circuits and Integrated Systems, DCIS 2018*, pp. 1–6, IEEE, nov 2019.
- [119] G. Niezen, P. Eslambolchilar, and H. Thimbleby, “Open-source hardware for medical devices,” *BMJ Innovations*, vol. 2, pp. 78–83, apr 2016.
- [120] J. Ferretti, L. Di Pietro, and C. De Maria, “Open-source automated external defibrillator,” *HardwareX*, vol. 2, pp. 61–70, oct 2017.
- [121] J. M. Pearce, “Maximizing returns for public funding of medical research with open-source hardware,” *Health Policy and Technology*, vol. 6, pp. 381–382, dec 2017.
- [122] K. Pardee, A. A. Green, M. K. Takahashi, D. Braff, G. Lambert, J. W. Lee, T. Ferrante, D. Ma, N. Donghia, M. Fan, N. M. Daringer, I. Bosch, D. M. Dudley, D. H. O’Connor, L. Gehrke, and J. J. Collins, “Rapid, Low-Cost Detection of Zika Virus Using Programmable Biomolecular Components,” *Cell*, vol. 165, pp. 1255–1266, may 2016.
- [123] B. G. Gahan, R. M. Sumir, N. Thomas, P. Umesh, L. Priyanka, U. Rahul, J. Chaturvedi, R. Drsouza, and A. Tauheed, “A Portable Color Sensor Based Urine Analysis System to Detect Chronic Kidney Disease,” in *2019 11th International Conference on Communication Systems and Networks, COM-SNETS 2019*, pp. 876–881, Institute of Electrical and Electronics Engineers Inc., may 2019.
- [124] J. Kim and C. Koo, “A highly sensitive and portable fluorescence detector for small volumes of biosamples,” in *International Conference on Electronics, Information and Communication, ICEIC 2018*, vol. 2018-Janua, pp. 1–2, Institute of Electrical and Electronics Engineers Inc., apr 2018.
- [125] Libelium, “MySignals - eHealth e Medical IoT Development Platform,” 2019.

## BIBLIOGRAPHY

- [126] Y. Montes-Cebrián, A. Álvarez-Carulla, J. Colomer-Farrarons, E. O’rourke, I. Ndukwe, S. O’riordan, M. Hutchinson, P. L. Miribel-Català, and R. B. Reilly, “A Portable System for Measuring the Tactile Temporal Discrimination Threshold in Cervical Dystonia,” in *NanoBio&Med 2018*, pp. 1–2, 2018.
- [127] S. Kanchi, M. I. Sabela, P. S. Mdluli, Inamuddin, and K. Bisetty, “Smartphone based bioanalytical and diagnosis applications: A review,” *Biosensors and Bioelectronics*, vol. 102, pp. 136–149, apr 2018.
- [128] X. Huang, D. Xu, J. Chen, J. Liu, Y. Li, J. Song, X. Ma, and J. Guo, “Smartphone-based analytical biosensors,” *Analyst*, vol. 143, pp. 5339–5351, nov 2018.
- [129] J. Guo, “Uric acid monitoring with a smartphone as the electrochemical analyzer,” *Analytical Chemistry*, vol. 88, no. 24, pp. 11986–11989, 2016.
- [130] O. Hosu, A. Ravalli, G. M. Lo Piccolo, C. Cristea, R. Sandulescu, and G. Marrazza, “Smartphone-based immunosensor for CA125 detection,” *Talanta*, vol. 166, pp. 234–240, may 2017.
- [131] H. Im, C. M. Castro, H. Shao, M. Liong, J. Song, D. Pathania, L. Fexon, C. Min, M. Avila-Wallace, O. Zurkiya, J. Rho, B. Magaoay, R. H. Tambouret, M. Pivovarov, R. Weissleder, and H. Lee, “Digital diffraction analysis enables low-cost molecular diagnostics on a smartphone,” *Proceedings of the National Academy of Sciences of the United States of America*, vol. 112, pp. 5613–5618, may 2015.
- [132] L. Ortega, A. Llorella, J. P. Esquivel, and N. Sabaté, “Self-powered smart patch for sweat conductivity monitoring,” *Microsystems and Nanoengineering*, vol. 5, pp. 1–10, dec 2019.
- [133] H. C. Moon, C. H. Kim, T. P. Lodge, and C. D. Frisbie, “Multicolored, Low-Power, Flexible Electrochromic Devices Based on Ion Gels,” *ACS Applied Materials and Interfaces*, vol. 8, pp. 6252–6260, mar 2016.
- [134] K. W. Oh and C. H. Ahn, “A review of microvalves,” *Journal of Micromechanics and Microengineering*, vol. 16, pp. R13–R39, may 2006.
- [135] M. Azarmanesh, M. Dejam, P. Azizian, G. Yesiloz, A. A. Mohamad, and A. Sanati-Nezhad, “Passive microinjection within high-throughput microfluidics for controlled actuation of droplets and cells,” *Scientific Reports*, vol. 9, p. 6723, dec 2019.
- [136] T. Salafi, K. K. Zeming, and Y. Zhang, “Advancements in microfluidics for nanoparticle separation,” *Lab on a Chip*, vol. 17, pp. 11–33, dec 2017.

## BIBLIOGRAPHY

- [137] G. Kaur and N. Verma, “Colorimetric determination of Cu<sup>2+</sup> ions in water and milk by apo-tyrosinase disc,” *Sensors and Actuators, B: Chemical*, vol. 263, pp. 524–532, jun 2018.
- [138] L. J. Wang, Y. C. Chang, R. Sun, and L. Li, “A multichannel smartphone optical biosensor for high-throughput point-of-care diagnostics,” *Biosensors and Bioelectronics*, vol. 87, pp. 686–692, jan 2017.
- [139] B. B. Rajeeva, Z. Wu, A. Briggs, P. V. Acharya, S. B. Walker, X. Peng, V. Bahadur, S. R. Bank, and Y. Zheng, ““Point-and-Shoot” Synthesis of Metallic Ring Arrays and Surface-Enhanced Optical Spectroscopy,” *Advanced Optical Materials*, vol. 6, p. 1701213, may 2018.
- [140] J. Punter-Villagrasa, C. Paez-Aviles, J. Colomer-Farrarons, J. Lopez-Sanchez, E. Juanola-Feliu, P. Miribel-Catala, M. Kitsara, M. Aller-Pellitero, and F. J. Del Campo, “A low-power electronic instrumentation for multiparametric diabetes mellitus analysis,” in *IECON Proceedings (Industrial Electronics Conference)*, pp. 5211–5215, IEEE, oct 2016.
- [141] J. Song, M. G. Mauk, B. A. Hackett, S. Cherry, H. H. Bau, and C. Liu, “Instrument-Free Point-of-Care Molecular Detection of Zika Virus,” *Analytical Chemistry*, vol. 88, pp. 7289–7294, jul 2016.
- [142] A. A. Weaver, H. Reiser, T. Barstis, M. Benvenuti, D. Ghosh, M. Hunckler, B. Joy, L. Koenig, K. Raddell, and M. Lieberman, “Paper analytical devices for fast field screening of beta lactam antibiotics and antituberculosis pharmaceuticals,” *Analytical Chemistry*, vol. 85, pp. 6453–6460, jul 2013.
- [143] B. Castro, M. Sala de Medeiros, B. Sadri, and R. V. Martinez, “Portable and power-free serodiagnosis of Chagas disease using magnetic levitating microbeads,” *Analyst*, vol. 143, pp. 4379–4386, sep 2018.
- [144] Y. Li, J. Xuan, Y. Song, P. Wang, and L. Qin, “A microfluidic platform with digital readout and ultra-low detection limit for quantitative point-of-care diagnostics,” *Lab on a Chip*, vol. 15, pp. 3300–3306, jul 2015.
- [145] V. Tran, B. Walkenfort, M. König, M. Salehi, and S. Schlücker, “Rapid, Quantitative, and Ultrasensitive Point-of-Care Testing: A Portable SERS Reader for Lateral Flow Assays in Clinical Chemistry,” *Angewandte Chemie - International Edition*, vol. 58, pp. 442–446, jan 2019.
- [146] S. T. Phillips and G. G. Lewis, “Advances in materials that enable quantitative point-of-care assays,” *MRS Bulletin*, vol. 38, pp. 315–319, apr 2013.
- [147] C. D. Ahrberg, B. R. Ilic, A. Manz, and P. Neuzil, “Handheld real-time PCR device,” *Lab on a Chip*, vol. 16, pp. 586–592, feb 2016.

## BIBLIOGRAPHY

- [148] C. D. Ahrberg, A. Manz, and P. Neuzil, “Palm-Sized Device for Point-of-Care Ebola Detection,” *Analytical Chemistry*, vol. 88, pp. 4803–4807, may 2016.
- [149] M. Dou, J. Lopez, M. Rios, O. Garcia, C. Xiao, M. Eastman, and X. J. Li, “A fully battery-powered inexpensive spectrophotometric system for high-sensitivity point-of-care analysis on a microfluidic chip,” *Analyst*, vol. 141, pp. 3898–3903, jun 2016.
- [150] B. Shu, C. Zhang, and D. Xing, “A handheld flow genetic analysis system (FGAS): Towards rapid, sensitive, quantitative and multiplex molecular diagnosis at the point-of-care level,” *Lab on a Chip*, vol. 15, pp. 2597–2605, jun 2015.
- [151] D. Larcher and J. M. Tarascon, “Towards greener and more sustainable batteries for electrical energy storage,” *Nature Chemistry*, vol. 7, pp. 19–29, jan 2015.
- [152] M. H. Cho, J. Trottier, C. Gagnon, P. Hovington, D. Clément, A. Vijh, C. S. Kim, A. Guerfi, R. Black, L. Nazar, and K. Zaghbi, “The effects of moisture contamination in the Li-O<sub>2</sub> battery,” *Journal of Power Sources*, vol. 268, pp. 565–574, dec 2014.
- [153] X. Chen, L. Yin, J. Lv, A. J. Gross, M. Le, N. G. Gutierrez, Y. Li, I. Jeerapan, F. Giroud, A. Berezovska, R. K. O’Reilly, S. Xu, S. Cosnier, and J. Wang, “Stretchable and Flexible Buckypaper-Based Lactate Biofuel Cell for Wearable Electronics,” *Advanced Functional Materials*, vol. 29, p. 1905785, nov 2019.
- [154] A. Nozariasbmarz, H. Collins, K. Dsouza, M. H. Polash, M. Hosseini, M. Hyland, J. Liu, A. Malhotra, F. M. Ortiz, F. Mohaddes, V. P. Ramesh, Y. Sargolzaeiaval, N. Snouwaert, M. C. Öztürk, and D. Vashaee, “Review of wearable thermoelectric energy harvesting: From body temperature to electronic systems,” *Applied Energy*, vol. 258, p. 114069, jan 2020.
- [155] G. T. Hwang, H. Park, J. H. Lee, S. Oh, K. I. Park, M. Byun, H. Park, G. Ahn, C. K. Jeong, K. No, H. Kwon, S. G. Lee, B. Joung, and K. J. Lee, “Self-powered cardiac pacemaker enabled by flexible single crystalline PMN-PT piezoelectric energy harvester,” *Advanced Materials*, vol. 26, pp. 4880–4887, jul 2014.
- [156] M. Q. Hasan, R. Kuis, J. S. Narayanan, and G. Slaughter, “Fabrication of highly effective hybrid biofuel cell based on integral colloidal platinum and bilirubin oxidase on gold support,” *Scientific Reports*, vol. 8, pp. 1–10, dec 2018.

## BIBLIOGRAPHY

- [157] L. del Torno-de Román, M. Navarro, G. Hughes, J. P. Esquivel, R. D. Milton, S. D. Minter, and N. Sabaté, “Improved performance of a paper-based glucose fuel cell by capillary induced flow,” *Electrochimica Acta*, vol. 282, pp. 336–342, aug 2018.
- [158] C. W. Narvaez Villarrubia, F. Soavi, C. Santoro, C. Arbizzani, A. Serov, S. Rojas-Carbonell, G. Gupta, and P. Atanassov, “Self-feeding paper based biofuel cell/self-powered hybrid  $\mu$ -supercapacitor integrated system,” *Biosensors and Bioelectronics*, vol. 86, pp. 459–465, dec 2016.
- [159] G. Slaughter and T. Kulkarni, “Highly Selective and Sensitive Self-Powered Glucose Sensor Based on Capacitor Circuit,” *Scientific Reports*, vol. 7, pp. 1–9, dec 2017.
- [160] I. Lee, T. Sode, N. Loew, W. Tsugawa, C. R. Lowe, and K. Sode, “Continuous operation of an ultra-low-power microcontroller using glucose as the sole energy source,” *Biosensors and Bioelectronics*, vol. 93, pp. 335–339, jul 2017.
- [161] C. Fischer, A. Fraiwan, and S. Choi, “A 3D paper-based enzymatic fuel cell for self-powered, low-cost glucose monitoring,” *Biosensors and Bioelectronics*, vol. 79, pp. 193–197, may 2016.
- [162] E. Cho, M. Mohammadifar, and S. Choi, “A single-use, self-powered, paper-based sensor patch for detection of exercise-induced hypoglycemia,” *Micro-machines*, vol. 8, p. 265, aug 2017.
- [163] Y. Montes-Cebrián, A. Álvarez-Carulla, J. Colomer-Farrarons, M. Puig-Vidal, and P. L. Miribel-Català, “Self-Powered Portable Electronic Reader for Point-of-Care Amperometric Measurements,” *Sensors*, vol. 19, p. 3715, aug 2019.
- [164] Y. Montes-Cebrián, L. del Torno-de Román, A. Álvarez-Carulla, J. Colomer-Farrarons, S. D. Minter, N. Sabaté, P. L. Miribel-Català, and J. P. Esquivel, “‘Plug-and-Power’ Point-of-Care diagnostics: A novel approach for self-powered electronic reader-based portable analytical devices,” *Biosensors and Bioelectronics*, vol. 118, pp. 88–96, oct 2018.
- [165] Y. Montes-Cebrián, A. Álvarez-Carulla, G. Ruiz-Vega, J. Colomer-Farrarons, M. Puig-Vidal, E. Baldrich, and P. L. Miribel-Català, “Competitive USB-Powered Hand-Held Potentiostat for POC Applications: An HRP Detection Case,” *Sensors*, vol. 19, p. 5388, dec 2019.
- [166] S. Fahn, “Concept and classification of dystonia.,” *Advances in neurology*, vol. 50, pp. 1–8, 1988.

## BIBLIOGRAPHY

- [167] M. Hutchinson, T. Isa, A. Molloy, O. Kimmich, L. Williams, F. Molloy, H. Moore, D. G. Healy, T. Lynch, C. Walsh, J. Butler, R. B. Reilly, R. Walsh, and S. O’Riordan, “Cervical dystonia: A disorder of the midbrain network for covert attentional orienting,” *Frontiers in Neurology*, vol. 5 APR, p. 54, 2014.
- [168] D. Bradley, R. Whelan, O. Kimmich, S. O’Riordan, N. Mulrooney, P. Brady, R. Walsh, R. B. Reilly, S. Hutchinson, F. Molloy, and M. Hutchinson, “Temporal discrimination thresholds in adult-onset primary torsion dystonia: An analysis by task type and by dystonia phenotype,” *Journal of Neurology*, vol. 259, pp. 77–82, jan 2012.
- [169] A. Molloy, O. Kimmich, L. Williams, B. Quinlivan, A. Dabacan, A. Fanning, J. S. Butler, S. O’Riordan, R. B. Reilly, and M. Hutchinson, “A headset method for measuring the visual temporal discrimination threshold in cervical dystonia.,” *Tremor and other hyperkinetic movements (New York, N.Y.)*, vol. 4, p. 249, 2014.
- [170] R. B. Beck, E. M. McGovern, J. S. Butler, D. Birsanu, B. Quinlivan, I. Beiser, S. Narasimham, S. O’Riordan, M. Hutchinson, and R. B. Reilly, “Measurement & Analysis of the Temporal Discrimination Threshold Applied to Cervical Dystonia,” *Journal of Visualized Experiments*, pp. e56310–e56310, jan 2018.
- [171] V. Yem and H. Kajimoto, “Comparative Evaluation of Tactile Sensation by Electrical and Mechanical Stimulation,” *IEEE Transactions on Haptics*, vol. 10, pp. 130–134, jan 2017.

# Abbreviations

**WHO** World Health Organization

**CAGR** Compound Annual Growth Rate

**POC** Point-of-Care

**STI** Sexually Transmitted Infections

**KET** Key Enabling Technologies

**LOC** Lab-On-a-Chip

**IoT** Internet-of-Things

**BLE** Bluetooth Low Energy

**FC** Fuel cell

**BFC** Biological Fuel cell

**GDPR** General Data Protection Regulation

**HIV** Human Immunodeficiency Virus

**ARI** Acute Respiratory Infection

**NGO** Non-Governmental Organization

**2019-nCoV** 2019-novel Coronavirus

**DNA** Deoxyribonucleic Acid

**ELISA** Enzyme-linked immune-absorbent assay

**FRET** Frequency Resonance Energy Transfer

**SPR** Surface Plasmon Resonance

**RWG** Resonant Waveguide Grating



## Abbreviations

**MEMS** Microelectromechanical systems

**NEMS** Nanoelectromechanical systems

**QCM** Quartz crystal microbalances

**RE** Reference Electrode

**CE** Counter Electrode

**WE** Working Electrode

**CV** Cyclic voltammetry

**CA** Chronoamperometry

**EIS** Electrochemical Impedance Spectroscopy

**DAC** Digital-to-Analog Converter

**IA** Instrumentation Amplifier

**TIA** Transimpedance Amplifier

**ASIC** Application-Specific Integrated Circuit

**CMOS** Complimentary Metal Oxide Semiconductor

**BJT** Bipolar Junction Transistor

**MOSFET** Metal-oxide-semiconductor field-effect transistor

**IC** Integrated Circuits

**LED** Light Emitting Diode

**PCR** Polymerase Chain Reaction

**OPAMP** Operational Amplifier

# List of Figures

1.1	Main fields that compose Point-of-Care Diagnostics. . . . .	5
1.2	Challenges to overcome for implementing POC diagnostic devices in developing countries. . . . .	10
1.3	Block diagram of the structure of a biosensor. . . . .	14
1.4	Classification of biosensors based on the detection method [22]. . .	14
1.5	Electrochemical biosensor based on screen-printed electrode [78]. Reprinted from Metrohm-DropSens website. . . . .	17
1.6	Typical cyclic voltammetry input (a) and output (b) waveforms. .	19
1.7	Typical chronoamperometry input (a) and output waveforms (b). .	19
1.8	a) An oscillating perturbation in the cell produces an oscillating current response. b) Schematic of a Nyquist plot. Top-right points are at lower frequencies, while bottom-left points are at higher frequencies. . . . .	21
1.9	Schematic of a resonant grating waveguide biosensor. Reprinted from [94] with permission. . . . .	24
1.10	Schematic of cantilever biosensors response: (A) initial state and (B) sensing state. Reprinted from [95] with permission. . . . .	24
1.11	Schematic of quartz crystal microbalance biosensor: when analyte binding occurs, the resonance frequency varies. Reprinted from [101] with permission. . . . .	26
1.12	Block diagram of an electronic system to make electrochemical measurements. . . . .	27

## LIST OF FIGURES

1.13	Basic schematic of (a) two-electrode and (b) three-electrode configuration. . . . .	28
1.14	Example of a potentiostat circuit comprised of the Control Amplifier, and the Current-to-Voltage Converter. . . . .	29
1.15	Schematic of a) a basic control amplifier circuit; and b) a Control Amplifier circuit using voltage followers to isolate it and the RE. . . . .	30
1.16	Potentiostat circuit formed by a basic Control Amplifier configuration with an Instrumentation Amplifier as a Current-to-Voltage converter. . . . .	31
1.17	Potentiostat circuit which combines a basic Control Amplifier configuration with a Transimpedance Amplifier as a Current-to-Voltage converter. . . . .	32
1.18	Potentiostat circuit composed of a basic Control Amplifier configuration with a Switching Capacitor as a Current-to-Voltage converter. . . . .	33
1.19	Principle of a) low-side current configuration, and b) high-side current configuration. . . . .	36
1.20	High-side current monitoring amplifier . . . . .	37
1.21	a) Photograph of the proposed device; b) Smartphone with the sensor pre-buried; c) Diagram of the electrometer; d) Capture of the electrochemical module integrated into the PCB of the smartphone. Reproduced from [129] with permission from American Chemical Society. . . . .	40
1.22	a) Photograph of the hand-held detector. b) Schematic of the potentiostat based on a transimpedance amplifier. c) Block diagram of the smartphone-based CV system. Reproduced from Ref. [114] with permission from Biosensors and Bioelectronics Journal. . . . .	41
1.23	a) Capture of the chemically heated cup for POC diagnostics of the Zika virus and microfluidic cassette for nucleic acid extraction. b) Capture of the PAD colorimetric testing in which the sample was “swiped” to deposit material for analysis in several lanes. Reprinted from [141] and [142] with all permissions. . . . .	44
1.24	A) Schematic of the circuit formed by a charge pump based on an amplifier circuit, B) capture of the system, and (C) power curve of glucose BFC. Reprinted from [156] with permission. . . . .	46

## LIST OF FIGURES

1.25	a) Diagram of the self-powered, wearable, and disposable patch for monitoring glucose in sweat to detect hypoglycemia-related to the exercise. b) Power output profile during an on-body experiment, schematics used by the authors to power an LED with the BFC, capture of experiment setup, and the LED switched on and off. Reprinted from [162] and [153] with permission. . . . .	47
3.1	Picture of the (a) printed circuit board, and (b) the whole self-powered electronic reader (printed circuit board and outer case). Reprinted from [163] with permission. . . . .	102
3.2	a) Electronic reader current error. b) Chronoamperometry curves done with the electronic reader. c) Uncertainty in current measurement produced by the e-reader. d) Transfer function that relates the current captured by the e-reader with the glucose concentration and comparison against a commercial potentiostat (Autolab PG-STAT204). e) Temporal evolution of the electronic reader power consumption. Reprinted from [164] with permission. . . . .	104
3.3	(a) Start-up curves of the e-reader powered by ethanol FC. (b) Transfer function that relates the measured current by the e-reader with different emulated sensors and fuel cell concentrations (ethanol, urine and methanol), and the comparison against the current produced by the sensor. Reprinted from [163] with permission. . . . .	105
3.4	Picture of the prototype developed. (a) AmpStat potentiostat composed of the full-custom PCB (copper board) and the MCU board (red board). (b) AmpVIEW software registering an amperometry in real-time. Reprinted from [165] with permission. . . . .	106
3.5	(a) Example of a chronoamperometry registered for $500 \text{ ng}\cdot\text{mL}^{-1}$ of HRP. (b) The procedure followed for current measurement: (1) First, the AmpStat potentiostat was connected via USB to the computer, the AmpView software executed, and the “Start” button clicked on; (2) the SPCE was plugged to the connector, and (3) $45 \mu\text{L}$ of TMB were added; then, to begin the enzymatic reaction, (4) $5 \mu\text{L}$ of HRP were pipetted on the electrodes, and the current was registered during 300 s; finally, the “Stop” button was pressed and the data saved. Reprinted from [165] with permission. . . . .	107

## LIST OF FIGURES

3.6	(a) Currents recorded by the four potentiostats used for HRP concentrations ranging from 0 to 1000 ng·mL <sup>-1</sup> after 100 s, 200 s and 300 s of reaction with the substrate. (b) Currents registered after 300 s of reaction with the substrate (n = 3). Reprinted from [165] with permission. . . . .	109
3.7	SNR of the four potentiostats for HRP concentrations ranging from 0.1 to 1000 ng mL <sup>-1</sup> . Reprinted from [165] with permission. . . . .	110
B.1	a) Multimodal portable platform for measuring Temporal Discrimination Thresholds in Dystonia patients. b) The two vibration motors were inserted in a textile-black band to generate the vibrotactile stimulation in the fingers. . . . .	125
B.2	Screenshots of the TDT App developed for generating visual and tactile stimuli to measure Temporal Discrimination Thresholds. . . . .	126

# List of Tables

1.1	The ASSURED criteria that indicate the attributes that should have a POC device. . . . .	4
1.2	Summary of front-end solutions based on potentiostat architecture [109]. . . . .	34
3.1	Summary of the electronic characteristics of the self-powered portable electronic reader for Point-of-Care testing. . . . .	106
3.2	Comparison of the figures of merit of the HRP detection assay, carried out with the four tested potentiostats. Reprinted from [165] with permission. . . . .	111
3.3	Summary of the electronic characteristics of the USB-powered Hand-held potentiostat for Point-of-Care applications. . . . .	112



